

ADDIS ABABA UNIVERSITY
COLLEGE OF HEALTH SCIENCES
SCHOOL OF PHARMACY

DEPARTMENT OF PHARMACEUTICS AND SOCIAL PHARMACY

FORMULATION AND OPTIMIZATION OF SUSTAINED RELEASE FLOATING, BIOADHESIVE AND SWELLABLE MATRIX TABLETS OF RANITIDINE HYDROCHLORIDE

BY
BIRHANU NIGUSSE (BSC, B.PHARM)

MARCH, 2018
ADDIS ABABA, ETHIOPIA

ADDIS ABABA UNIVERSITY

COLLEGE OF HEALTH SCIENCES

SCHOOL OF PHARMACY

DEPARTMENT OF PHARMACEUTICS AND SOCIAL PHARMACY

FORMULATION AND OPTIMIZATION OF SUSTAINED RELEASE FLOATING, BIOADHESIVE AND SWELLABLE MATRIX TABLETS OF RANITIDINE HYDROCHLORIDE

BY

BIRHANU NIGUSSE (BSC, B.PHARM)

MARCH, 2018

ADDIS ABABA, ETHIOPIA

Formulation and Optimization of Sustained Release Floating, Bioadhesive and Swellable Matrix Tablets of Ranitidine Hydrochloride

By

Birhanu Nigusse (BSc, B. Pharm)

A Thesis Submitted to the Department of Pharmaceutics and Social Pharmacy, School of Pharmacy, College of Health Sciences, Addis Ababa University, in Partial Fulfillment of the Requirements for the Degree of Master of Science in Pharmaceutics

Under the Supervision of Professor Tsige Gebre-Mariam and Dr. Anteneh Belete, Department of Pharmaceutics and Social Pharmacy, School of Pharmacy, Addis Ababa University

March, 2018
Addis Ababa, Ethiopia

ADDIS ABABA UNIVERSITY

COLLEGE OF HEALTH SCIENCES, SCHOOL OF PHARMACY

DEPARTMENT OF PHARMACEUTICS AND SOCIAL PHARMACY

This is to certify that the thesis studied by Birhanu Nigusse Kahsay, entitled: "Formulation and Optimization of Sustained Release Floating, Bioadhesive and Swellable Matrix Tablets of Ranitidine Hydrochloride" and submitted in partial fulfillment of the requirements for the Degree of Master of Science in Pharmaceutics complies with the regulations of the University and meets the accepted standards with respect to originality and quality.

Approved by:

Name	**Signature**	**Date**
Professor Tsige Gebre-Mariam (Advisor)	.....	08 March 2018
Dr. Anteneh Belete (Advisor)	.....	08 March 2018
Professor Kaleab Asres (External Examiner)	.....	08 March 2018
Dr. Nisha Mary Joseph (Internal Examiner)	.....	08 March 2018

…….

Head of Department

ACKNOWLEDGEMENTS

Above all, I offer my adoration to Almighty God and His mother Virgin Saint Mary who gave me the strength and courage to complete my thesis, and the opportunity to thank all those people who contribute their unreserved support for the completion of the work.

I take it as a privilege to sincerely express my deep sense of gratitude and thank to my advisors Prof. Tsige Gebre-Mariam and Dr. Anteneh Belete for their valuable advice, comments and follow-up throughout the course of this work.

I extend my heartfelt thanks to the Regional Bioeqivalence Center (RBEC) for sponsoring my postgraduate study and Addis Ababa University for sponsoring my thesis research.

I thank all the academic and administrative staff of the School of Pharmacy, Addis Ababa University for providing me with the necessary materials during my study.

I would like to thank Cadila Pharmaceutical Factory PLC for donating ranitidine HCl; and Ethiopian Pharmaceutical Manufacturing Sh.Co. (EPHARM) for allowing me to use their FTIR.

I would also like to thank my family (especially my sister, Sindu Nigusse), friends and others who were directly or indirectly involved in motivating, encouraging and supporting me throughout my entire career.

Finally, this thesis is dedicated to the memory of my beloved mother, Mebrahte Nigusse, who had been an inspiration in my life; and who advised me to work hard without waiting for tomorrow, to have a solution oriented mindset in challenging situations; and to become the best version of me. There isn't a day that she didn't cross my mind; and I will be ever grateful for the impact she made in my life.

Table of Contents

ACKNOWLEDGEMENTS i
LIST OF TABLES v
LIST OF FIGURES vii
ACRONYMS x
ABSTRACT xi
1. INTRODUCTION 1
1.1 Gastroretentive drug delivery systems (GRDDS) 1
1.1.1 Overview of GRDDS 1
1.1.2 Anatomy and physiology of the stomach 1
1.1.2.1 Structural organization 2
1.1.2.2 Gastric pH 2
1.1.2.3 Gastric motility patterns 2
1.1.2.4 Gastric emptying process 3
1.1.3 Drug candidates for gastroretentive delivery approach 6
1.1.4 Approaches to gastric retention 7
1.1.4.1 Co-administration of pharmacological agents that slow gastric motility ... 7
1.1.4.2 Size increasing systems 7
1.1.4.2.1 Expanding, swellable systems 7
1.1.4.2.2 Unfolding and modified-shape systems 8
1.1.4.3 Bioadhesive and mucoadhesive systems 8
1.1.4.4 Density-Controlled Systems 8
1.1.4.4.1 High Density Systems 8
1.1.4.4.2 Floating Systems 9
1.1.4.5 Magnetic systems 9
1.1.4.6 Combination systems 10
1.2 Gastroretentive matrix tablets (matrices) 10
1.3 Hydrophilic polymers used in gastroretentive drug delivery system 11
1.3.1 Hydroxypropylmethylcellulose 11
1.3.2 Sodium carboxymethylcellulose 12

1.4 Ranitidine hydrochloride 12
1.5 Optimization studies in gastroretentive drug delivery system 13
1.6 Rationale of the present study 14
1.7 Research questions 15
1.8 Objectives 16
1.8.1 General objective 16
1.8.2 Specific objectives 16
2. EXPERIMENTAL 17
2.1 Materials 17
2.2 Methods 17
2.2.1 Preparation of powder blends 17
2.2.2 Characterization of powder blends: 18
2.2.3 Preparation of floating, bioadhesive and swellable matrix tablets 19
2.2.4 Evaluation of the matrix tablets 19
2.2.5 Analysis of kinetics and mechanism of drug release 24
2.2.6 Formulation optimization by RSM 25
2.2.6.1 Experimental design 25
2.2.6.2 Validation of the experimental design 25
2.3 Drug-excipient interaction study 27
2.4 Statistical analysis 27
3. RESULTS & DISCUSSION 28
3.1 Preliminary studies 28
3.1.1 Density and related properties 28
3.1.2 Evaluation of prepared tablets in the preliminary studies 29
3.1.2.1 Physicochemical properties of the tablets 29
3.1.2.2 Effect of viscosity grade of HPMC on different response variables 31
3.1.2.3 Effect of HPMC/NaCMC ratio on different response variables 31
3.1.2.4 Effect of polymer concentration on different response variables 33
3.1.2.5 Effect of concentration of $NaHCO_3$ on different response variables 34
3.1.2.6 Effect of hardness on different response variables 37

3.2 Optimization 38
3.2.1 Powder characteristics 38
3.2.2 Characteristics of tablets 39
3.2.2.1 Physicochemical properties of the tablets 39
3.2.2.2 *In vitro* drug release 41
3.2.3 Drug release kinetics 43
3.2.4 Selection of response variables 45
3.2.5 Selection of mathematical model 45
3.2.6 Model adequacy checking 47
3.2.7 Contour plot and surface response analysis 54
3.2.8 Simultaneous optimization of response variables 59
3.2.8.1 Numerical optimization 60
3.2.8.2 Graphical optimization 60
3.2.9 Evaluation and validation of the optimized formulation 62
3.2.9.1 Evaluation of optimized formulation 62
3.2.9.2 Validation of the optimized formulation 64
3.3 Drug-excipient compatibility studies 64
4. CONCLUSION 69
5. SUGGESTIONS FOR FURTHER WORK 70
REFERENCES 71

LIST OF TABLES

Table 1.1: Transit times of various dosage forms across the GIT 4

Table 1.2: Rationale for gastro-retention of drugs..... 6

Table 1.3: Main drawbacks of different types of gastroretentive systems. 10

Table 2.1: Composition of ranitidine HCl (150mg) matrix tablets in the preliminary studies. .. 17

Table 2.2: Factor combination for formulation of ranitidine HCl (150mg) tablets as per CCD 26

Table 2.3: Formulae for the preparation of ranitidine HCl (150mg) matrix tablets as per CCD.26

Table 3.1: Density and related properties of ranitidine HCl (150mg) formulations in the preliminary study 28

Table 3.2: Properties of different formulations of ranitidine HCl (150 mg) matrix tablets in the preliminary study..... 29

Table 3.3: Summary of effects of formulation and process variables on different response variables of ranitidine HCl (150 mg) matrix tablets in the preliminary studies..... 30

Table 3.4: Powder characteristics of 13 formulations of ranitidine HCl prepared as per CCD . 38

Table 3.5: Tablet characteristics of the 13 formulations of ranitidine HCl (150) matrix tables prepared as per CCD 40

Table 3.6: Drug release properties for the 13 formulations of ranitidine HCl (150mg) matrix tablets prepared as per CCD..... 42

Table 3.7: Rate constants and correlation coefficient fits of different kinetic equations for the 13 formulations of ranitidine HCl (150mg) matrix tablets prepared as per CCD..... 44

Table 3.8: Summary of experimental responses of the 13 formulations of ranitidine HCl (150mg) matrix tablets prepared as per CCD..... 45

Table 3.9: Fit summary statistics for response variables of the 13 formulations of ranitidine HCl (150mg) matrix tablets prepared as per CCD..... 46

Table 3.10: Summary of ANOVA results for dependent variables of the 13 formulations of ranitidine HCl (150mg) matrix tablets prepared as per CCD..... 48

Table 3.11: Numerical test results of model adequacy checking for the 13 formulations of ranitidine HCl (150mg) matrix tablets prepared as per CCD..... 49

Table 3.12: Estimated model term regression coefficients for the responses of the 13 formulations of ranitidine HCl (150mg) prepared as per CCD..... 54

Table 3.13: Constraints for factors & responses used during numerical & graphical optimization for the 13 formulations of ranitidine HCl (150mg) prepared as per CCD. 59
Table 3.14: Numerical optimization results of predicted optimum values for the 13 formulations of ranitidine HCl (150mg) prepared as per CCD. 60
Table 3.15: Density and related properties of the optimized powder blend and tablet formulation of Ranitidine HCl (15 mg)..... 662
Table 3.16: Release kinetics and release mechanism results for the optimized formulation of ranitidine HCl (150) mg matrix tablets. 63
Table 3.17: Response values of predicted, experimental and percentage error obtained at optimal levels of the factors..... 64

LIST OF FIGURES

Fig 1.1: Overview of the phases of the MMC 3

Fig 1.2: Chemical structure of ranitidine hydrochloride..... 13

Fig 2.1: The experimental setup for the determination of bioadhesive strength 21

Fig 2.2: Modified tablet disintegration tester for ex vivo mucoadhesion time measurement.... 22

Fig 2.3: UV absorption calibration curve of ranitidine HCl reference standard in 0.1N HCl at 314 nm with 95% confidence interval..... 23

Fig. 3.1: Effect of viscosity grade of HPMC on swelling index of ranitidine HCl (150 mg) matrix tablets at (a) 28.7% and (b) 50% polymer concentration..... 32

Fig. 3.2: Effect of viscosity grade of HPMC on drug release profile of ranitidine HCl (150 mg) matrix tablets at a) 28.7% and b) 47.8% polymer concentration 32

Fig. 3.3: Effect of HPMC/NaCMC ratio at (a) 28.7% (b) 47.8 % polymer concentration on swelling index of ranitidine (150 mg) matrix tablet..... 35

Fig. 3.4: Effect of HPMC/NaCMC ratio at a) 28.7% and b) 47.8% polymer concentration on drug release profile of ranitidine (150 mg) matrix tablet 35

Fig. 3.5: Effect of polymer concentration on swelling index of ranitidine HCl (150 mg) matrix tablet 36

Fig. 3.6: Effect of polymer concentration on release profile of ranitidine from ranitidine HCl (150 mg) matrix tablet..... 36

Fig. 3.7: Effect of concentration of $NaHCO_3$ on swelling index of ranitidine HCl (150 mg) matrix tablet..... 37

Fig. 3.8: Effect of concentration of $NaHCO_3$ on drug release profile of ranitidine from ranitidine HCl (150 mg) matrix tablet..... 37

Fig. 3.9: Effect of hardness on swelling index of ranitidine HCl (150 mg) matrix tablets 37

Fig. 3.10: Effect of hardness on release profile of ranitidine from ranitidine HCl (150 mg) matrix tablets..... 37

Fig 3.11: Swelling index of the 13 formulations of ranitidine HCl (150mg) matrix tablets prepared as per CCD 41

Fig 3.12: In vitro release profiles of the 13 formulations of ranitidine HCl (150mg) matrix tablets prepared as per CCD..... 43

Fig 3.13: a) Normal probability plot of residuals b) plots of the residuals against predicted response for Y_1 (floating lag time) results of the 13 formulations of ranitidine HCl (150mg) prepared as per CCD..... 50
Fig 3.14: a) Normal probability plot of residuals b) plots of the residuals against predicted response for Y_2 (bioadhesive strength) results of the 13 formulations of ranitidine HCl (150mg) prepared as per CCD..... 50
Fig. 3.15: a) Normal probability plot of residuals b) plots of the residuals against predicted response for Y_3 (swelling index) results of the 13 formulations of ranitidine HCl (150mg) prepared as per CCD..... 51
Fig 3.16: a) Normal probability plot of residuals b) plots of the residuals against predicted response for Y_4 (drug release at 1h) results of the 13 formulations of ranitidine HCl (150mg) prepared as per CCD..... 51
Fig 3.17: a) Normal probability plot of residuals b) plots of the residuals against predicted response for Y_5 (t50%) for results of the 13 formulations of ranitidine HCl (150mg) prepared as per CCD 52
Fig 3.18: a) Normal probability plot of residuals b) plots of the residuals against predicted response for Y_6 (drug release at 12 h) results of the 13 formulations of ranitidine HCl (150mg) prepared as per CCD..... 52
Fig 3.19: a) Contour plot and b) response surface plot showing the effect of X_1 (amount of polymer) and X_2 (amount of sodium bicarbonate) on Y_1 (floating lag time) for the 13 formulations of ranitidine HCl (150mg) prepared as per CCD. 56
Fig 3.20: a) Contour plot b) response surface plot showing the effect of X_1 (amount of polymer) and X_2 (amount of sodium bicarbonate) on Y_2 (bioadhesive strength) for the 13 formulations of ranitidine HCl (150mg) prepared as per CCD. 56
Fig 3.21: a) Contour plot b) response surface plot showing the effect of X_1 (amount of polymer) and X_2 (amount of sodium bicarbonate) on Y_3 (maximum swelling index) for the 13 formulations of ranitidine HCl (150mg) prepared as per CCD..... 57
Fig 3.22: a) Contour plot b) response surface plot showing the effect of X_1 (amount of polymer) and X_2 (amount of sodium bicarbonate) on Y_4 (drug release at 1 h) for the 13 formulations of ranitidine HCl (150mg) prepared as per CCD. 57

Fig 3.23: a) Contour plot b) response surface plot showing the effect of X_1 (amount of polymer) and X_2 (amount of sodium bicarbonate) on Y_5 (time to 50% drug release) for the 13 formulations of ranitidine HCl (150mg) prepared as per CCD. 58
Fig 3.24: a) Contour plot b) response surface plot showing the effect of X_1 (amount of polymer) and X_2 (amount of sodium bicarbonate) on Y_6 (drug release at 12 h) for the 13 formulations of ranitidine HCl (150mg) prepared as per CCD. 58
Fig 3.25: 3D plot of the overall desirability function. 61
Fig 3.26: Overlay plot of the six responses as functions of dependent variables for the 13 formulations of ranitidine HCl (150mg) prepared as per CCD. 61
Fig 3.27: Release profile of optimized formulation of ranitidine HCl (150mg) matrix tablets... 63
Fig 3.28: FTIR spectrum of excipients. 65
Fig 3.29: FTIR spectrum of pure ranitidine HCl 66
Fig 3.30: FTIR spectrum of optimized formulation of ranitidine HCl (150) matrix tablets..... 67
Fig 3.31: FTIR spectrum overlay of A) ranitidine HCl and B) optimized formulation of ranitidine HCl (150mg) matrix tablets showing characterstic bands of ranitidine HCl at the same wavenumber. 68

ACRONYMS

APIs:	Active Pharmaceutical Ingredients
CCD:	Central Composite Design
CMC:	Carboxymethylcellulose
DDS:	Drug Delivery System
FDDS:	Floating Drug Delivery System
FTIR:	Fourier Transform Infrared
GIT:	Gastrointestinal Tract
GRDDS:	Gastro Retentive Drug Delivery System
GRT:	Gastric Residence Time
HBS:`	Hydrodynamically Balanced Systems
HPMC:	Hydroxypropylmethylcellulose
MMC:	Migrating Motor Complex
NaCMC:	Sodium Carboxymethylcellulose
$NaHCO_3$:	Sodium bicarbonate
HCl:	Hydrochloride
SI:	Swelling Index

ABSTRACT

Ranitidine HCl is an ideal candidate for gastrortentive drug delivery system (GRDDS) because of its short biological half-life (~2.5-3.0 h), low bioavailability (50 % absolute bioavailability), site specific absorption (in the proximal part of small intestine), and susceptibility to colonic degradation. Designing the drug as an immediate release dosage form may result in bioavailability variation due to factors associated with GIT. The conventional controlled delivery approach may not improve its bioavailability because of the inherent characteristics of the drug and shorter gastric emptying nature of this delivery approach. Furthermore, designing the drug using any single GRDDS (e.g. floating or bioadhesive or swelling, etc) may not be effective due to the limitations associated with each system (for example, floating systems need sufficient gastric fluid, bioadhesive systems may not be effective due to high mucus turnover, and swelling systems may not have the desired mechanical strength); and this may lead to variation in bioavailability among individuals. Recently, use of combination systems have been effective strategies to overcome the limitations associated with the individual systems.

The aim of the present study was therefore, to prepare and optimize floating, bioadhesive, and swellable matrix tablets of ranitidine HCl (150mg) using hydroxypropylmethylcellulose (HPMC) and sodium carboxymethylcellulose (NaCMC) (as release retarding polymers) and sodium bicarbonate ($NaHCO_3$) (as gas generating agent) to increase the mean residence time in the stomach, thereby increasing bioavailability and reducing *in vivo* variability among individuals.

The polymer powder blends were evaluated for density and related properties. The matrix tablets were prepared by direct compression method (EK0 Korsch, 8410- 68, Berlin, Germany) and their physicochemcial properties were evaluated. Compatibility study was done using FTIR. Origin 8 software and one way analysis of variance (ANOVA) were applied for analysis and comparison of results. Response surface methodology (RSM) based on central composite design (CCD) (design expert version 10.0.7.0) was employed to optimize the formulation.

Results from preliminary studies indicated that viscosity grade of HPMC, concentration of polymer, HPMC/NaCMC ratio and the concentration of $NaHCO_3$ significantly affect the floating, bioadhesive, swelling and drug release characteristics of the matrix tablets. Hardness of tablets significantly affected the floating lag time, while its effect on the other properties was not

significant. The two polymers exhibited synergistic effect on prolonging the drug release; and the polymer blend containing HPMC/NaCMC (3:1) showed better matrix characteristics.

From preliminary studies, concentration of HPMC/NaCMC (3:1) (X_1) and $NaHCO_3$ (X_2) were selected as independent variables; and floating lag time (Y_1), bioadhesive strength (Y_2), swelling index (Y_3), cumulative drug release at 1 h (Y_4), time to 50% drug release ($t_{50\%}$) (Y_5) and cumulative drug release at 12 h (Y_6) were taken as the response variables during optimization.

By comparing several statistical parameters, linear model was selected as best fit for bioadhesive strength, swelling index, cumulative drug release at 1 h and 12 h; and the quadratic model was selected as best fit for floating lag time and $t_{50\%}$. The adequacy of the models as per ANOVA revealed that both models have significant values indicating the terms in the models have significant effect ($P < 0.05$) on the responses.

An optimum region of 5.12 sec, 29.27 g, 313.37 %, 23.48%, 3.89 h and 90.00% was obtained for floating lag time, bioadhesive strength, maximum swelling index, cumulative drug release in the first 1 h, $t_{50\%}$ and cumulative release at 12 h, respectively at corresponding level of 214.55 mg/tab (45.65 %) of HPMC/NaCMC and 61.22 mg/tab (13.02 %) of $NaHCO_3$ with desirability of 0.856. Analysis of three batches formulated at the optimum region confirmed the effectiveness of optimization. The experimental values were found to be in close agreement with the predicted values confirming the predictability and validity of the model. The kinetic study of the optimized formulation followed Higuchi square root model with non Fickian diffusion release mechanism. The FT-IR spectra showed no incompatibility between ranitidine HCl and the excipients.

In conclusion, this study has come up with an optimum formulation of floating, bioadhesive and swellable matrix tablets of ranitidine HCl that could remain buoyant for > 12 h with shorter lag time, swellable with sufficient matrix integrity, bioadhesive to gastric mucus with *ex vivo* retention time of > 12 h, and that release the drug over a period of 12 h in a sustained manner. Hence, from *in vitro* perspective, this formulation may overcome the low bioavailability of oral ranitidine HCl and the associated variability among individuals.

Keywords: Ranitidine hydrochloride, gastroretentive drug delivery systems, floating, bioadhesive, swelling, HPMC, NaCMC, central composite design

1. INTRODUCTION

1.1 Gastroretentive drug delivery systems (GRDDS)

1.1.1 Overview of GRDDS

Oral delivery accounts for the largest proportion of administered pharmaceuticals due to the ease of administration, patient compliance, and flexibility in formulation. However, the bioavailability of drugs delivered by this route can vary greatly due to many constraints, especially, if the therapeutic agents are delivered using conventional or immediate-release dosage forms, and this led to the development of controlled drug delivery systems. The real challenge in the development of sustained-release drug delivery system is not just to sustain the drug release but to prolong the presence of the dosage form within the gastrointestinal tract (GIT) until all the drug is completely released at the desired period of time in the desired region. Conventional controlled drug delivery systems have shown some limitations related to fast gastric-emptying time. Because the transit time for solid particles through the small intestine is reported to be relatively constant, the time that a dosage form remains in the stomach becomes the most significant factor in the overall GIT transit time [Davis *et al.,* 1986] and this led to the development of gastroretentive drug delivery system (GRDDS).

GRDDS are dosage forms that have prolonged residence time in the stomach thereby delivering drugs for extended periods of time. This results in reduced fluctuations in plasma drug levels, higher bioavailability [Kotreka & Adeyeye, 2011; Lopes *et al*., 2016], an improvement in therapeutic effectiveness, a reduction in drug loss, reduction in drug administration frequency and benefits due to the delivery of drugs that act locally in the stomach and duodenum (Talukder and Fassihi, 2004).

1.1.2 Anatomy and physiology of the stomach

The human stomach is “J”-shaped organ which is positioned in the left upper part of the abdomen, behind the liver, part of the diaphragm, and the anterior abdominal wall. The position, shape, and size of the stomach may vary depending on the extent of the gastric contents. The empty stomach has a volume of approx. 50 ml; in the filled state, the stomach volume increases up to a maximum of 1500 ml.

1.1.2.1 Structural organization

The human stomach is dividable into different anatomical regions, these include the fundus, the body/corpus, and the pylorus. The proximal part of the stomach, which is composed of the fundus and the upper one-third of the body, functions as a reservoir for ingested food and liquids. The distal stomach, consisting of the remaining body and the pyloric portion, is the main region responsible for mixing motions, grinding, and homogenization of gastric contents. In addition, the gastric emptying of ingested material is regulated in this part by contraction and propelling.

1.1.2.2 Gastric pH

In general, the gastric pH for the fasted state is reported to range from 1.5 to 2.0 [Charman *et al*. 1997]. It is not uniform within the different regions of the human stomach due to variations in the distribution of the gastric acid-producing parietal cells and due to gastric motility. Dressman *et al*. [1990] measured a median gastric pH of 1.7 in the case of young, healthy men and women. In the fed state, following the ingestion of a standard solid and liquid meal, the gastric pH increased to a median value of 6.7 [Dressman *et al*. 1990]. Several parameters, including gender and age [Russell et al., 1993], diseases [McConnell *et al*, 2008], drugs [Charman *et al*., 1997], and composition of meals, were investigated regarding their effect on the gastric pH.

1.1.2.3 Gastric motility patterns

Two distinct patterns of GI motility, based on fed or fasted state, are distinguished [Fell, 1996]. The gastric emptying process occurs in both conditions [Davis *et al*., 1986].

A. Fasted state

The fasted state is characterized by an interdigestive series of events: the migrating myoelectric complex or migrating motor complex (MMC) [Luiking *et al*., 1998]. The contraction pattern cycles through the stomach and the small intestine in 2 to 3 h [Fell, 1996]. Within an individual and between individuals, the MCC activity varies significantly [Dooley *et al*., 1992]. Differences are observed in the total MMC cycle length, the duration of the individual phases, and the amplitude of the contractions [Kellow *et al*., 1986]. Figure 1.1 displays the four consecutive phases of the MMC which are discriminated by different contractile activities.

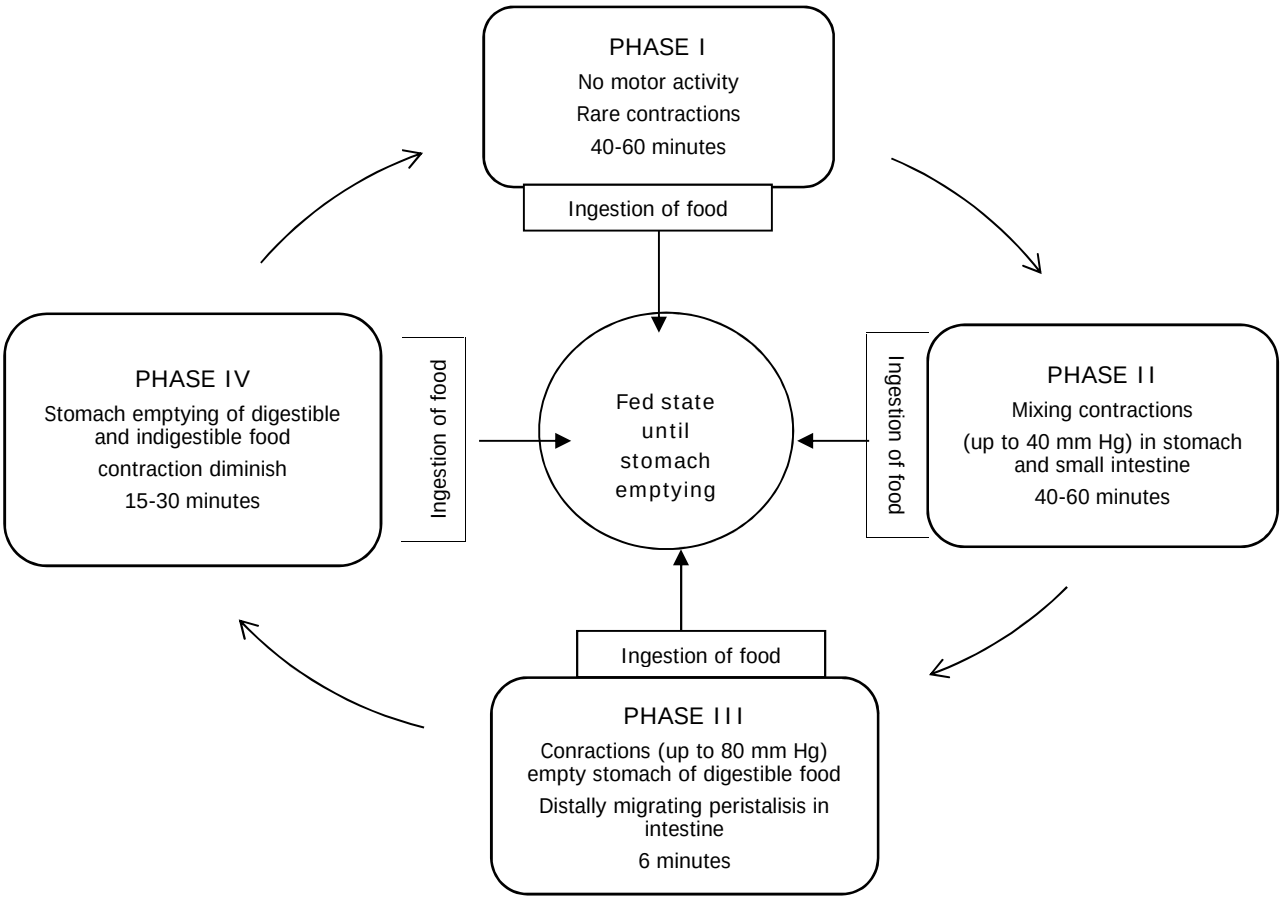


Fig 1.1. Overview of the phases of the MMC [Kong and Singh, 2008]

B. Fed state

In the fed state, the motility pattern of the stomach walls is characterized by two types of contractions. The first type of motor activity is slow and weak, volume-reducing contractions that arise in the upper part of the stomach. The second type of muscle contractions are series of peristaltic waves which originate in the corpus and spread distally towards the duodenum with continuously increasing intensity. The gastric emptying of meal components (liquids, digestible and indigestible solids) occurs at different rates and not in form of a homogeneous mass [Camilleri *et al*., 1985; Kong and Singh, 2008].

1.1.2.4 Gastric emptying process

Gastric emptying is a motility-driven process whereby a dosage form is emptied from the stomach into the small intestine. In drug delivery, gastric emptying determines the length of time that the

dosage form remains in the stomach. Numerous factors influence the gastric emptying process and, consequently, the gastric residence time (GRT) of orally-administered drug delivery systems. These factors are discussed below:

i) Properties of dosage forms

Gastric emptying is dependent on type, density and size of dosage form. The transit time of various dosage forms is shown in Table 1.1. In most cases, the larger the size of the system the longer the GRT. Disintegrated tablets are emptied with the digestible phase of a meal; whereas, tablets that remained in shape are emptied with the indigestible material.

Table 1.1: Transit times of various dosage forms across the GIT [Pawar *et al.*, 2011]

Dosage form	Transit time (h)		
	Stomach	Small intestine	Total
Tablets	2.7±1.5	3.1±0.4	5.8
Pellets	1.2±1.3	3.4±1.0	4.6
Capsules	0.8±1.2	3.2±0.8	4.0
Solutions	0.3±0.07	4.1±0.5	4.4

ii) Pharmaceutical agents

The GI motility is slowed down by anticholinergic agents (e.g. atropin), propantheline, opioids, and tricyclic antidepressants [Rashid and Bateman, 1990; Murphy *et al.*, 1997]. In contrast, prokinetic drugs (e.g. benzamides, cholinergic agonists, dopamine antagonists, macrolide antibiotics, opiate antagonists, somatostatin analogs) enhance the gastric motility and promote the transit through the GIT [Tack, 2008; Longo and Vernava, 1993]. *ß*-Adrenergic agonists (e.g. isoprenaline) retard, whereas, *ß*-adrenergic antagonists (e.g. propanolol) accelerate the gastric emptying process [Mcintyre *et al*., 1992].

iii) Food

The stomach empties liquids more rapid than solid material. The gastric emptying of digestible solid meal components occurs faster than indigestible solids [Feldman *et al.*, 1984]. The larger the amount of ingested liquid or solid material, the longer the time period which the stomach remains in the fed motility pattern. There is only little evidence provided to support the hypothesis that the meal consistency has an impact [Houghton *et al*., 1987]. However, the nutritive density and the

food composition (carbohydrates, proteins, fat) are reported to influence the gastric emptying rate [Velchik *et al*., 1989]. The frequency of the intake significantly increases the GRT because of lower MCC overall activity.

iv) The pylorus limitation

The size of the pylorus is about 2- 3 mm and 12.8 ± 7.0 mm during digestion and inter-digestive phases respectively [Dressman *et al*., 1990]. Therefore, all particles which have a diameter inferior to 5 mm can pass through the pylorus to duodenum [Hwang *et al.*, 1998]. The gastric peristalsis exerts forces which are able to disintegrate dosage forms of sufficient size having hardness inferior or equal to 1.89 Newton [Prinderre *et al*., 2011]

v) Physiological factors

The gastric emptying follows the circadian rhythm. The emptying of solids occurs in the morning faster than in the afternoon and evening. In the case of liquids, no differences in the gastric emptying depending on the time of day are observed [Goo *et al*., 1987]. It was reported by Mangoni and Jackson [2004] that the gastric emptying is not affected by age; although, the secretion of HCl and pepsin decreases in elderly people. Healthy women exhibit significantly prolonged GRT of solid material compared to men; but, no significant difference is observed in the gastric emptying of liquid meals [Bennink *et al.*, 1998]. In contrast, Datz *et al*. [1987] discovered that females empty both, solids and liquids, slower than men. The menstrual cycle and pregnancy are known to alter the gastric motility patterns [Brennan *et al*., 2009]. Obesity is associated with increased gastric emptying rates [Johansson and Ekelund, 1976]. However, obese subjects were also found to exhibit similar or depressed stomach emptying rates compared to normal weight subjects [Verdich *et al.*, 2000]. The lying body position delays the gastric emptying process in comparison to the sitting, standing, and combined sitting-standing postures [Moore *et al.*, 1988].

vi) Diseases

Diseases which alter the stomach emptying process and the gastric motility are primarily disorders of the GI tract. Gastric ulcerations reduce the antral motility; therefore, the stomach emptying is delayed [Miller *et al.*, 1980]. In contrast, ulcerations in the duodenum are reported to promote the gastric motility [Lam *et al*., 1982]. Patients suffering from diseases, such as atrophic gastritis [Davies *et al.*, 1971], Crohn's disease [Nóbrega *et al.*, 2012], and pernicious anaemia [Lahner and

Annibale, 2009] show delayed gastric emptying. In some patients, gastro-esophageal reflux slowed down the gastric emptying, whereas, in a number of patients the gastric motility patterns remained unaffected [McCallum *et al*., 1981]. Diabetic patients are known to exhibit altered GI motility patterns and drastically delayed gastric emptying rates [Horowitz *et al.*, 2002]. Anorexia nervosa is associated with delayed stomach emptying of liquid and solid meal components [Devlin *et al*., 2012]. The gastric emptying process is depressed in patients with migraine attack [Boyle *et al*., 1990].

1.1.3 Drug candidates for gastroretentive delivery approach

The gastroretentive delivery approach offers new and important therapeutic options for numerous active principle ingredients (APIs). The rationale for the selection of APIs for fabrication as a GRDDS is described in Table 1.2. On the other hand, it has to be kept in mind that a prolonged retention in the stomach is not appropriate for drugs which may cause gastric lesions (e.g. non-steroidal anti-inflammatory drugs). It is also not convenient for APIs that are unstable in the acidic stomach environment.

Table 1.2: Rationale for gastro-retention of drugs [Srikanth et al., 2011]

S/N	Rationale for gastro-retention	Examples of drugs
1	Narrow absorption window at upper part of GIT	Levodopa (Klausner *et al*., 2003b); Acyclovir (Gröning *et al*., 1998)
2	pH dependent absorption from stomach (acidic drugs)	Furosemide (Ozdemir et al., 2000)
3	Drugs for local action – antacids, anti-ulcer drugs, antibacterial for *H. pylori* infection	Amoxicillin (Rajinikanth *et al*., 2007, Clarithromycin (Nama *et al*., 2008), Metronidazole (Ishak *et al*., 2007); Ranitidine (Rohith *et al*., 2009)
4	Degradation at higher pH (higher stability at lower pH)	Captopril (Jiménez-Martínez *et al*., 2008)
5	Poor solubility at an alkaline pH (higher solubility at lower pH or weakly basic drugs)	Verapamil (Sawicki, 2002), Ofloxacin (Chavanpatil *et al*., 2006)
6	Degradation in intestine or colon	Ranitidine hydrochloride (Basit, 2001)
7	Drugs with short biological half life	Metformin (Ali *et al*., 2007)

1.1.4 Approaches to gastric retention

Various approaches have been pursued to increase the retention of oral dosage forms in the stomach. These include a) co-administration of the drug delivery system with pharmacological agents that slow gastric motility b) bioadhesive systems, c) size increasing systems, which are either due to expansion and shape modification or swelling, d) density controlled systems which are either, high density systems or floating systems, e) magnetic systems, and f) combination systems.

1.1.4.1 Co-administration of pharmacological agents that slow gastric motility

There are two approaches for this strategy. The first approach involves the ingestion of indigestible polymers (Russell and Bass, 1985), or fatty acid salts (Keinke and Ehrlein, 1983) which change the motility pattern of the stomach to a fed state, thereby decreasing the gastric emptying rate and accordingly permitting prolongation of drug release (Deshpande *et al*., 1996). The other approach is modulating the GI transit time by the administration of other drug substance. For example, an *in vivo* study has demonstrated that pre-treatment with metoclopramide enhances; whereas, pre-treatment with propantheline delays the gastric emptying process (Murata *et al.,* 2000).

1.1.4.2 Size increasing systems

These systems are based on the principle of expansion of the pharmaceutical dosage form in the stomach to dimensions larger than the pyloric sphincter [Streubel *et al.*, 2006]. Due to significant inter-individual variations, the cutoff size cannot be given exactly, but the diameter of the pyloric sphincter was reported to be 12.8 ± 7.0 mm (Quigley, 1996). Researchers have suggested to set a minimum tablet size of 13 mm as cut-off value for being retained in the stomach (Streubel *et al*., 2006; Klausner *et al*., 2003a). The increase in the systems' size is based on two strategies, namely, expansion due to swellable excipients or unfolding and/ or shape modification (to complex geometric shapes) in the stomach [Lopes *et al*., 2016).

1.1.4.2.1 Expanding, swellable systems

The expansion of these systems is generally due to the presence of specific hydrogel formers or hydrophilic polymers, which after swallowing; drastically increase in size upon contact with gastric media. This increase in size prevents their exit from the stomach through the pylorus; and leads to longer retention of the dosage forms in the stomach. A certain mechanical strength is

required to make these systems resistant to gastric contractions, since the fully swollen superporous hydrogels are mechanically very fragile (Omidian *et al*., 2005).

1.1.4.2.2 Unfolding and modified-shape systems

These systems consist of at least one erodible polymer (e.g., Eudragit® E, hydroxypropyl cellulose (HPC)), one non-erodible polymer (e.g., polyamides, polyolefins, polyurethanes), and a drug dispersed within the polymer matrix. The carrier is degraded in the stomach [Lopes *et al.*, 2016]; allowing drug release in a controlled manner. These systems extend the gastric residence time depending on size, shape and flexural modulus of the drug delivery device (Kedzierewicz *et al.*, 1999).

1.1.4.3 Bioadhesive and mucoadhesive systems

Bioadhesive/mucoadhesive systems prolong the relatively short gastric retention time (GRT) of orally-administered drug delivery systems by adherence of the dosage form to the mucous membrane of the stomach or the epithelial surface of the remaining GI tract [Talukder and Fassihi, 2004]. Mucoadhesive systems increase the intimacy and duration of drug contact with biological membranes [Lopes *et al*., 2016]. Adhesion to the epithelial surface will not only lead to the proper location and mobilization of the drug but also favor a closer and more lasting association between the drug and the local microenvironment.

1.1.4.4 Density-controlled systems

1.1.4.4.1 High density systems

Dosage forms with a density higher than the density of the gastric contents (1.004-1.01 g/cm^3 [Prajapati *et al.*, 2013]) sink down to the bottom of the greater curvature of the stomach, in case the patient is in an upright position, and get entrapped in the folds of the antrum. These systems are prepared by the incorporation of heavy inert material, such as zinc oxide, titanium dioxide, iron powder and barium sulphate [Rouge *et al*., 1998; Bardonnet *et al*., 2006]. These materials increase density by up to 1.5–2.4 g/cm^3. Above a threshold value of 2.4-2.8 g/cm^3, the high-density delivery systems are reported to be retained in the rugae at the bottom of the stomach [Clarke *et al*., 1993; Devereux *et al*., 1990].

1.1.4.4.2 Floating systems

Floating drug delivery systems (FDDS) have a bulk density lower than the gastric fluids (1.004-1.01 g/cm^3) [Prajapati *et al*., 2013), and thus remain buoyant in the stomach without affecting the gastric emptying rate for a prolonged period of time. These systems are the most prominent systems among the GRDDS (Choi *et al*., 2002; Zhang *et al*., 2016). Based on the mechanism of buoyancy, floating systems can be classified into two distinct categories viz effervescent and non-effervescent systems [Streubel *et al*., 2006].

A. Effervescent systems

These systems utilize gas (CO_2) generating agents (e.g. sodium bicarbonate, citric acid or tartaric acid) or volatile liquid containing systems to achieve buoyancy [Michaels, 1975; Micheals, 1974]. Effervescent systems that utilize gas are prepared by mixing CO_2 generating agents with swellable polymers. Effervescent systems that utilize volatile liquid involves the use of matrices containing a gas with a boiling point below 37 ^{0}C (e.g. cyclopentane, diethyl ether) [Talukder and Fassihi, 2004]. The gas is incorporated in the device in solid or liquid form at ambient temperature. It evaporates at physiological temperature and inflates the dosage form.

B. Non-effervescent systems

The non-effervescent approach relies in two ways by which the systems float. One is floatation due to polymer swelling. These systems are also called hydrodynamically balanced systems (HBS) [Sheth and Tossounian, 1984) and contain one or more gel-forming hydrophilic polymers. Upon contact with the gastric fluids, hydration and swelling of the polymers occur and a buoyant mucus body with a density of less than unity is formed. The API release is controlled by diffusion and by erosion of the hydrated gel barrier. The other systems are non-effervescent floatation system with inherently low density (Singh and Kim, 2000). These systems are immediately floating on the gastric contents. An inherently low density may be achieved by the entrapment of air and/or the incorporation of low-density material such fatty components or oils [Spickett *et al*., 1994], porous material [Eberle *et al*., 2014], and foamed powders [Streubel *et al*., 2002].

1.1.4.5 Magnetic systems

These systems represent a strategy that is very different from all other gastroretentive delivery forms, as they are based on the attraction between two magnets (Lopes *et al*., 2016). These systems

are composed of a dosage form, containing a small internal magnet or a mass of magnetic material, and an extra-corporal magnet to control the GI transit of the dosage form [Fujimori *et al*., 1995; Gröning *et al*., 1998].

1.1.4.6 Combination systems

Each of the gastroretentive drug delivery systems stated above have some limitations; and the main limitations of each system are summarized in Table 1.3 (Pawar *et al*., 2012). The combination system allows to overcome the drawbacks of the individual systems. It is common to combine the working principles of flotation and bio/mucoadhesion [Jiménez-Castellanos et al., 1994; Varshosaz *et al.*, 2006; Zheng *et al.*, 2006]. The joint application of swelling and bio/mucoadhesion for gastroretentive drug delivery was also investigated [Chavanpatil *et al.*, 2006].

Table 1.3: Main drawbacks of different types of gastroretentive systems (Pawar *et al.*, 2012).

Technology	Drawbacks
Expandable systems	• Maintenance problems due to the use of hydrolyzable/ biodegradable polymers; • Difficult to hold mechanical shape; • Difficult to manufacture with high costs.
High density systems	• Cannot manufacture with large amount of drug due to technical problems; • To date, none is commercially available.
Magnetic systems	• May be uncomfortable, compromising patient compliance.
Bioadhesive systems	• Efficiency can be reduced by constant turnover of the mucus; • Ability to link to other epithelial mucosa such as the esophagus.
Floating systems	• Highly dependent on the presence of food and gastric contents; • Need for high levels of gastric fluid in the stomach; • Lag time until reaching fluctuation

1.2 Gastroretentive matrix tablets (matrices)

Matrices represent a popular and widely used approach for an oral extended release drug delivery due to economic, process development and scale-up reasons. These systems are designed to hydrate on swallowing, and form a ‘gel’ layer of hydrated polymer at the tablet surface to control the rate of drug release [Saeio *et al.*, 2007]. During gastrointestinal transit, the matrices are reduced

in size through surface erosion and dissolution. Hydrophilic matrices release their drug content slowly, and their therapeutic effect is prolonged. However, in order to ensure a reproducible action on the body it is imperative that (1) the matrix remains intact and (2) the drug is released at a controlled rate.

1.3 Hydrophilic polymers used in gastroretentive drug delivery system

Hydrophilic polymers are often used as matrices in GRDDS and controlled drug release is due to the formation of a viscous hydrated layer around the tablet that acts as a barrier to water intake and the free movement of solutes to the outside of the matrix (Sriamornsak *et al*., 2007). The nature of the matrix determines the degree of swelling and erosion as well as the degree of drug diffusion, which determines the mechanism and kinetics of drug release (Jiménez-Martínez *et al*., 2008). A wide variety of natural, semi-synthetic and synthetic water-swellable polymers has been considered as release control candidates in hydrophilic matrices. By far the most widely used polymers are cellulose ethers, in particular HPMC [Kumar *et al*., 2005]. NaCMC has also been used in sustained release formulations due to its thickening and diffusion barrier properties [Colombo *et al*., 1999].

1.3.1 Hydroxypropylmethylcellulose

Hydroxypropylmethylcellullose (HPMC), also known as hypromellose, is a semi synthetic, inert, viscoelastic polymer, used as an excipient and controlled-delivery component in oral medicaments, found in a variety of commercial products. It is a water-soluble, non-ionic cellulose ether that is enzyme resistant and chemically stable over the pH range 3.0–11.0 [Ford, 2014]. The structure of HPMC is a cellulose backbone with ether linked methoxyl and hydroxypropyl side group substituents attached through ether linkages to the cellulose chain hydroxyl groups. Polymer properties are strongly influenced by the ratio of methoxyl and hydroxypropyl substitution, and this is reflected in the United States Pharmacopeia (USP) designation of different HPMC substitution types (HPMC 2208, HPMC 2906 and HPMC 2910) in which the first two numbers designate the average methoxyl (2208) and the last two numbers, the average percent hydroxypropoxyl (2208) substitution. HPMC substitution type can significantly modulate drug release. The lowest percentage of the hydrophobic substituents (methoxyl group) and the highest amount of hydrophilic substitution (hydropropoxyl) impart Methocel K series with the fastest rate of hydration, as compared to the E and F series [Singh *et al*., 2010].

1.3.2 Sodium carboxymethylcellulose

Sodium carboxymethylcellulose (NaCMC) is a low-cost commercial soluble and polyanionic polysaccharide derivative of cellulose. It has been used for many applications in the pharmaceutical industry because of is wide range of functional properties like binding, thickening, stabilizing, emulsification, film forming, suspending aid, diffusion barrier, gelling agent. It has been used in sustained release formulations due to its thickening and diffusion barrier properties [Colombo *et al*., 1999].

1.4 Ranitidine hydrochloride

Ranitidine is a selective, competitive histamine H_2-receptor antagonist [Pahwa *et al*., 2016]. It is commonly employed in the management and treatment of acute duodenal ulcer disease, Zollinger-Ellison syndrome and systemic mastocytosis with gastric hypersecretion [Gaginella and Bauman, 1983; Chopra *et al.*, 2014]. It is the drug of choice in the treatment of the Zollinger-Ellison syndrome [Pahwa1 *et al*., 2016]. It is also indicated for gastroduodenal ulcer, gastroesophageal reflux and hypersecretory states [Aouam *et al*., 2011]. The WHO recommended dose for ranitidine tablets is 150 mg ranitidine base, given as the hydrochloride salt. Strengths currently having a marketing authorization are the equivalents of 75, 150, and 300 mg ranitidine base [Kortejarvi *et al*., 2005].

Chemically ranitidine hydrochloride is *N*-[2-[[[5-[(Dimethylamino)methyl]furan-2-yl] methyl]sulphanyl] ethyl]-*N*'-methyl-2-nitroethene-1, 1-diamine hydrochloride (Fig 1.2). It contains a furan ring rather than the imidazole nucleus which is characteristic of histamine and cimetidine [Gaginella and Bauman, 1983]. It is a white or pale yellow and crystalline powder. It is freely soluble in water, sparingly soluble or slightly soluble in anhydrous ethanol.

Ranitidine hydrochloride has short biological half-life (~2.5-3 hours), it is absorbed in only the initial part of the small intestine. It has low bioavailability (50% absolute bioavailability). The site-specific absorption from the upper part of the small intestine and the colonic metabolism of the drug could partially contribute to its reduced bioavailability [Basit, 2001]. It is frequently administrated (for example, the effective treatment of erosive esophagitis requires administration of 150 mg of ranitidine 4 times a day [Kiran *et al*., 2010]). These properties make it an ideal candidate for GRDDS.

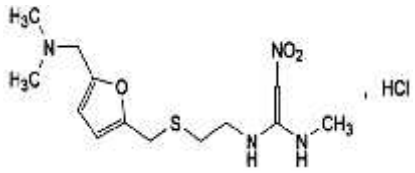


Fig 1.2: Chemical structure of ranitidine hydrochloride [Ph Eur, 2009]

The drug is readily absorbed from the gastrointestinal tract and the main absorption mechanism is paracellular passive diffusion [Kortejarvi *et al.,* 2005]. The apparent volume of the distribution of the drug for terminal phase is about 1.16-1.87 lit/kg. It is weakly bound, about 15% to plasma proteins [Kortejarvi *et al.,* 2005]. A small proportion of ranitidine is metabolized in the liver. In man, N-oxide is the major metabolite but accounts for only about 4-6% of a dose. About 30% of an oral dose and 70% of an intravenous dose is excreted unchanged in the urine in 24 h, primarily by active tubular secretion. Of orally administrated ranitidine, 26% is excreted through the feaces. Renal clearance values amount to some 70% to 80% of total clearance, indicating that renal excretion is the major route of elimination of unchanged ranitidine [Kortejarvi *et al.,* 2005].

This drug is one of the most widely used drugs of all time. This has provided an excellent opportunity to define its safety profile. However, the use of this drug may be associated with some side effects which include headache, skin rashes, tiredness, constipation, nausea, diarrhea, bradycardia, hypersensitivity, contact dermatitis, urticaria etc.

1.5 Optimization studies in gastroretentive drug delivery system

The response surface methodology (RSM) is the most widely used methodology in optimization [Lundstedt et al., 1998]. It determines the exact optimum, and is a good way to graphically illustrate the relation between different experimental variables and the responses. Within the RSM, different statistical designs such as factorial design, central composite design, box–behnken design and simplex lattice design are used for optimization of GRDDS [Rouge et al., 1998]. Central composite design (CCD) is a powerful statistical approach to model and optimize the response of interest influenced by several independent variables. It is efficient for experiments with few numbers of factors ($2 \leq n \leq 6$). The total number of experiments to be performed in this type of design are generally given as sum of the 2n factorial runs, 2n axial runs, and nc center runs (2n + 2n + nc), where n is the number of independent variables. The factorial design portion is used for

estimating main effects (linear terms) and two-factor interactions; 2n axial points for estimating the second-order terms, and nc repeated center points for the curvature and experimental error of the model.

1.6 Rationale of the present study

Because of its short biological half-life, low bioavailability, site specific absorption (absorbed only in the proximal part of small intestine) and its susceptibility to colonic metabolism, ranitidine HCl is an ideal candidate for GRDDS.

Designing the drug as an immediate release dosage form may result bioavailability variation due to many factors such as physiological constraints, pH, gastric transit time, enzymatic activity, surface area, age, gender, posture, disease state, etc. Furthermore, since the drug is frequently administrated in some disease conditions such as erosive esophagitis (which requires administration of 150 mg ranitidine HCl 4 times a day) it poses inconvenience for patients and may lead to noncompliance. Its metabolic degradation in the colon is yet another problem.

Studies have been done on controlled delivery of ranitidine; but most of them focus on sustaining it throughout the GIT [Patel et al., 2015] which may not be optimal strategy due to the inherent characteristics of the drug stated above. In addition to this the conventional controlled drug delivery systems have problems related to gastric emptying.

Floating tablets [Dave *et al*., 2004] and bioadhesive tablets [Adhikary, 2008] of ranitidine HCl have also been prepared. However, as each system has its own inherent limitation (as stated in Table 1.3), these approaches may not also overcome the low bioavailability of the drug and the associated variations among individuals. For example, the floating system doesn't work in the absence of gastric fluid and hence may not be effective for patients in fasting state; the bioadhesive system is associated with the limitation of high mucus turnover; and the swelling system has difficulties of maintaining the matrix integrity. One strategy to overcome these limitations is the use of combination systems (e.g. floating and bioadhesive, floating and swellable, bioadhesive and swelling systems or combination of the three); and this strategy has been effective for many drugs [Zheng *et al.*, 2006].

Most of the designing strategies stated above for the drug involve granulation method which may be time consuming and costly.

The rationale of the present study was therefore to prepare matrix tablets of ranitidine HCl using new approach (a combination of floating, bioadhesive and swelling approaches) so as to increase the mean residence time in the stomach and deliver it to the absorption site, thereby increasing its bioavailability and reducing *in vivo* variability among individuals.

1.7 Research questions

This study attempts to answer the following research questions:

- Is Ranitidine HCl amenable to floating, bioadhesive and swellable matrix tablets?
- What would be the effect of various polymers and other additives on release and other properties of Ranitidine HCl?
- What are the critical factors in the optimization of ranitidine HCl matrix tablets as per RSM using CCD?

1.8 Objectives

1.8.1 General objective

- To formulate and optimize a sustained release floating, bioadhesive and swelling matrix tablet of ranitidine hydrochloride.

1.8.2 Specific objectives

- To prepare floating, bioadhesive and swellable tablets of ranitidine HCl using HPMC and NaCMC alone and in combination and determine their characteristics.
- To evaluate the effect of viscosity grade of HPMC, concentration of polymer, polymer ratio, concentration of $NaHCO_3$ and hardness on floating, bioadhesion, swelling and release properties of tablets
- To optimize the formulation variables of the tablets using central composite design and to validate the optimized formulation.

2. EXPERIMENTAL

2.1 Materials

Ranitidine hydrochloride (China Associate Co. Ltd, China) was kindly supplied by Cadila Pharmaceutical Factory PLC. HPMC K4M (4000 cp) and HPMC K100M (100,000 cp) (Shin-Etsu Chemicals Ltd, Japan), NaCMC (China Associate Co. Ltd, China), magnesium stearate (BDH Chemicals Ltd Poole, England), talc (BDH Chemicals Ltd Poole, England), MCC (China Associate Co. Ltd, China), $NaHCO_3$ (Newport Industries Ltd, UK), hydrochloric acid (BDH Ltd., England) were used as received.

2.2 Methods

2.2.1 Preparation of powder blends

All the ingredients (Table 2.1) except magnesium stearate and talc were weighed and mixed thoroughly using mortar and pestle using geometric dilution technique. Magnesium stearate and talc were added into the powder blend and mixed in a Turbula mixer (Willy A. Bachofen AG, Turbula 2TF, Basel, Switzerland) for 3 min.

Table 2.1: Composition of ranitidine HCl (150mg) matrix tablets in the preliminary studies.

Formulation code	Composition (mg/tablet)								
	Ranitidine HCl*	HPMC K4M	HPMC K100M	NaCMC	Sodium bicarbonate	MCC	Magnesium stearate	Talc	Total
FH1	168	132			54	98	4	4	460
FH2	168	220			54	10	4	4	460
FH3	168		132		54	98	4	4	460
FH4	168		220		54	10	4	4	460
FS1	168			132	54	98	4	4	460
FS2	168			220	54	10	4	4	460
FM1	168		99	33	54	98	4	4	460
FM2	168		66	66	54	98	4	4	460
FM3	168		33	99	54	98	4	4	460
FM4	168		165	55	54	10	4	4	460
FM5	168		110	110	54	10	4	4	460
FM6	168		55	165	54	10	4	4	460
FSB1	168		165	55	44	20	4	4	460
FSB2	168		165	55	64	0	4	4	460

*168mg Rantidine HCl is equivalent to 150 mg Rantidine.

2.2.2 Characterization of powder blends:

2.2.1.1 Flow rate and angle of repose

Flow rate and angle of repose of the samples were determined with the funnel method. 30 g of powder was placed in a funnel (internal diameter of 10 mm at the bottom and 100 mm at the top) and allowed to flow through it on to a graph paper from a fixed height of 10 cm. Time in second for the duration of flow was recorded; and height (h) as well as the diameter (d) of the pile was measured. Flow rate and angle of repose were calculated as per equations 2.1 and 2.2 respectively. Results were expressed as a mean of triplicate determinations.

$$\text{Flow rate} = \frac{m}{t} \tag{2.1}$$

Where m is mass in gram and t is time in sec.

$$\text{Angle of repose } (\theta) = \tan^{-1}\left(\frac{h}{r}\right) \tag{2.2}$$

Where θ is Angle of repose, h is height, and r is radius

2.2.1.2 Bulk density and tapped density

To calculate bulk density, 30 g of powder was transferred into a 250 ml graduated cylinder and the volume of the powder was read after tapping the powder three times on a horizontal plane. To calculate the tapped density, the volume of the powder was read after tapping the granule 250 times using tap densitometer (ERWEKA, SVM 20, Germany). Bulk density (ρ_b) and tapped density were calculated using equation 2.3 and 2.4 respectively. Each experiment was done in triplicate and mean and standard deviation were calculated.

$$\rho_b = \frac{m}{V_b} \tag{2.3}$$

Where ρ_b is bulk density, m is mass of powder and V_b is bulk volume of powder.

$$\rho_t = \frac{m}{V_t} \tag{2.4}$$

Where ρ_t is bulk density, m is mass of powder and V_t is bulk volume of powder.

2.2.1.3 Compressibility index and Hausner ratio:

The Carr's index (compressibility) and the Hausner ratio were calculated from the bulk and tapped densities of the powders using Equations 2.5 and 2.6, respectively. Carr's index and Hausner ratio calculated are averages of three determinations.

$$Carr's\ index\ (\%) = \frac{\rho_t - \rho_b}{\rho_t} x\,100 \qquad (2.5)$$

$$\text{Hausner Ratio (H)} = \frac{\rho_t}{\rho_b} \qquad (2.6)$$

2.2.3 Preparation of floating, bioadhesive and swellable matrix tablets

The blend prepared in section 2.2.1 was compressed into tablets, adjusting the hardness to be between 60 N to 70 N, on eccentric tablet machine (EK0 Korsch, 8410- 68, Berlin, Germany) which was fitted with 10 mm diameter flat-faced punches. The tablets were kept for 24 h at room temperature in glass containers before their properties were evaluated.

2.2.4 Evaluation of the matrix tablets

2.2.4.1 Thickness

Ten tablets were taken and thickness was measured using sliding caliper scale (Nippon Sokutei, Japan). Results were expressed as a mean and standard deviation.

2.2.4.2 Hardness

Ten tablets were taken from each batch and the crushing strengths of the tablets were determinedusing hardness tester (Schleuniger, 2E/205, Switzerland). Each tablet was placed between two anvils and force was applied to the anvils, and the crushing strength that just caused the tablet tobreak was recorded. Results were expressed as a mean and standard deviation.

2.2.4.3 Friability

The friability of the tablets was determined by placing 20 pre-weighed tablets in a friability tester (ERWEKA, TAR 20, Germany) and rotating them for 4 min at 25 rpm. The loss of tablet weight was calculated as a percentage of the initial weight after dedusting the tablet.

2.2.4.4 Floating lag time and floating duration

The floating behavior of the tablets was visually determined, in triplicate, according to the floating lag time method described by Rosa et al. [1994]. Briefly, a tablet was placed in a glass beaker, containing 100 ml of 0.1 N HCl, maintained at 37 ± 0.5 ^{0}C. The floating lag time (the time between tablet introduction and its buoyancy) and total floating duration (the time during which tablet remains buoyant) were recorded. Results are expressed as a mean and standard deviation.

2.2.4.5 Matrix integrity

Matrix integrity was observed throughout *in vitro* dissolution studies and whether or not the swollen mass of the tablets remain intact was checked [Shinde et al., 2010].

2.2.4.6 Bioadhesive strength

Bioadhesive strength of tablets was measured using a modified two-arm balance (Singh et al., 2006). One holder was used to suspend the water-collecting beaker to the balance and another to suspend a glass vial to the other side of the balance as shown in Fig. 2.1. A piece of sheep stomach mucosa, 3×3 cm, obtained from a local slaughter house was used as the mucosal membrane. The mucosal membrane was separated by removing the underlying fat and loose tissues. The experiments were performed within 3 h of procurement of the mucosa. The sheep gastric mucosa was tied to an inverted 100-ml beaker and placed in a large one (250 ml). Then, 0.1 N HCl was added into the large beaker up to the upper surface of the gastric mucosa to simulate the gastric environment. Each tablet was attached to the glass vial with adhesive, and then the beaker was raised slowly until contact between sheep mucosa and the tablet preload time were kept constant for all the formulations. A preload of 50 g was placed on the vial for 5 min (preload time) to establish adhesion bonding between tablet and sheep stomach mucosa. After completion of the preload time, preload was removed from the vial and water was then added into the beaker from the burette in the other side. The addition of water was stopped when the tablet was detached from the sheep mucosa. The weight of water required to detach the tablet from the mucosa was noted as mucoadhesive strength. The experiment was done in triplicate and mean and standard deviation were calculated.

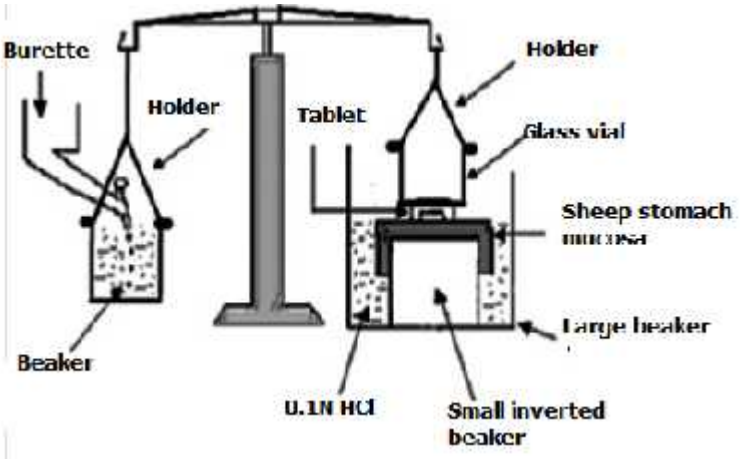


Fig. 2.1. The experimental setup for the determination of bioadhesive strength [adapted from Singh et al., 2006]

2.2.4.7 Tablet adhesion retention period (ex vivo mucoadhesion time)

The *ex vivo* adhesion retention time of the tablets was determined using a locally modified USP tablet disintegration test apparatus (2T 504, Erweka, Germany), based on the method reported by Nakamura et al. [1996]. The medium was composed of 800 ml 0.1N HCl (pH 1.2) in 1 L glass beaker maintained at 37 ± 1 ^{0}C. A segment of sheep gastric mucosa, 2.5 × 2.5 cm, obtained from a local slaughter house, was cut and glued (by cyanoacrylate adhesive) to the surface of a glass slide. One side of the tablet was wetted with 50 µL of 0.1 N HCl and attached to the center of the sheep stomach mucosa by applying a light force with a fingertip for 20 s [Perioli et al., 2009]. 5 min later, the glass was vertically fixed to the apparatus and allowed to move up and down (25 times per min) so that the tablet was completely immersed in the solution at the lowest point and was out at the highest point (Fig 2.2). The time required for the tablet to detach from the gastric mucosa was recorded as the mucoadhesion time. The experiment was repeated thrice and the average was taken.



Fig. 2.2: Modified tablet disintegration tester for ex vivo mucoadhesion time measurement (photo by Birhanu N)

2.2.4.8 Swelling index and determination of diameter of swollen tablets

The swelling behavior of the tablets was determined, in triplicate, according to the method described by Dorozynski *et al*. [2004]. The tablets were weighed individually (designated as W_0) and placed separately in glass beaker containing 200 ml of 0.1 N HCl maintained at 37 ^{0}C ± 0.5 ^{0}C. At regular time intervals, until 12 h, the tablets were removed from beaker, and the excess surface liquid was removed carefully using the tissue paper. The swollen tablets were then re-weighed (W_t), and % swelling index (SI) was calculated using Equation 2.7. The experiment was done in triplicate and mean and standard deviation were calculated.

$$SI\ (\%) = \frac{W_t - W_0}{W_0} x\,100 \qquad (2.7)$$

Where, SI is swelling index, W_t is weight of swollen tablet at time t, W_0 is initial weight of tablet
The diameter of swollen tablets was measured at 1 h and 12 h, in triplicate, using ruler. The mean and standard deviation were calculated.

2.2.4.9 Construction of calibration curve

112 mg of Ranitidine HCl working standard, equivalent to 100 mg ranitidine, was weighed and transferred to 100 ml volumetric flask and shaked with about 60 ml of 0.1N HCl. The solution was diluted to volume with 0.1N HCl and filtered. Different concentrations (µg/ml) of ranitidine hydrochloride solution (20, 60, 100 , 140, 180, and 220 µg/ml) were prepared using 0.1 N HCl as diluent. Then, the absorbance of each of these solutions was measured at max wavelength of 314

nm with UV-Visible Spectrophotometer (T92+ Spectrophotometer, PG Instruments limited, UK) using 0.1N HCl as blank. The Beer Lambert calibration curve (Fig 2.3) yielded a linear regression equation of A= 0.0033C - 0.0028 (where A is the absorbance and C is the concentration in µg/ml with 95% confidence interval) and R^2 of 0.9999.

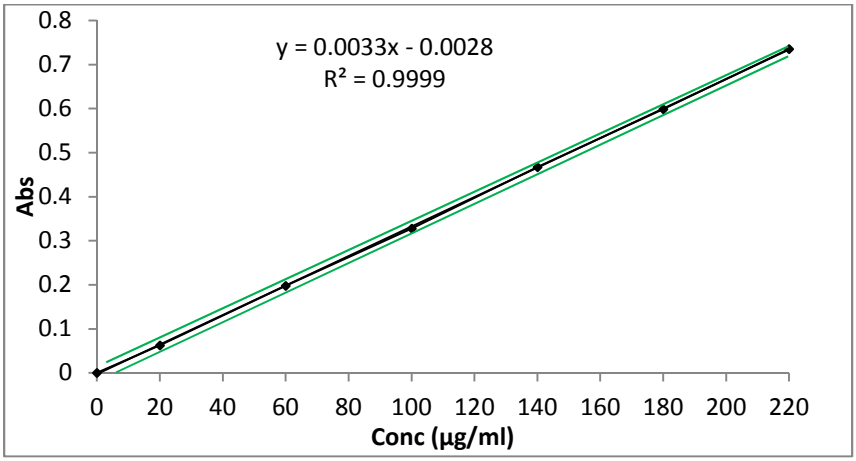


Fig 2.3: UV absorption calibration curve of ranitidine HCl reference standard in 0.1N HCl at 314 nm with 95% confidence interval

2.2.4.10 Drug content analysis

20 tablets were weighed and finely powdered. An accurately weighed powder of ranitidine hydrochloride equivalent to 100 mg of ranitidine was dissolved in about 60 ml of 0.1 N of 0.1N hydrochloric acid. The solution was diluted to 100 ml with 0.1N HCl and filtered. 5 ml of the filtrate was further diluted to 50ml with the same solvent. The absorbance of resultant solution was measured spectrophotometrically (T92+ Spectrophotometer, PG Instruments limited, UK) at 314 nm using 0.1 N HCl as blank and the content was calculated from the absorbance of sample and standard. The experiment was done in triplicate for each batch and mean and standard deviation were calculated.

2.2.4.11 *In vitro* drug release

The *in vitro* drug release studies were performed using USP type II dissolution apparatus (Pharma test type PTDTT, Germany) at 50 rpm. 900 ml of 0.1 N HCl was used as dissolution media at 37 ± 0.5 °C. 5 ml aliquot samples were withdrawn from each dissolution vessel after pre scheduled time intervals (0.25, 0.50, 1, 2, 3, 4, 6, 8, 10, and 12 h) and replaced with an equal volume of fresh dissolution medium which was kept at 37±0.5 °C to maintain sink condition. The withdrawn

samples were filtered through a filter paper of 0.45 µm size and were then analyzed spectrophotometrically (T92+ Spectrophotometer, PG Instruments limited, UK) at maximum wavelength of 314 nm (USP 36/NF31, 2013).

2.2.5 Analysis of kinetics and mechanism of drug release

The dissolution data were fitted into the following drug release kinetic models to evaluate the rate and mechanism of drug release from prepared matrix tablets [Dash *et al.,* 2010]. The order and mechanism of drug release from the matrix system were determined based on high regression (R^2) values [Meka *et al*., 2016].

A. Zero order release model

$$Q = Q_o - K_o.t \quad (2.8)$$

Where, Q_o is the initial amount of drug, Q is amount of drug remaining at time t, K_0 is zero-order rate constant expressed in units of concentration/time and t is the time.

B. First order release kinetic model

$$\log Q = \log Q_0 - K_1 t / 2.303 \quad (2.9)$$

Where, Q_o is the initial amount of drug, Q is amount of drug released at time t and K_1 is first order release constant.

C. Higuchi square root model

$$Q = K_H.t^{1/2} \quad (2.10)$$

Where, Q is amount of drug released at time t and K_H is the Higuchi constant.

D. Hixson-Crowell cube root model

$$Q_o^{1/3} - Q_t^{1/3} = K_{HC}.\ t \quad (2.11)$$

Where, Q_t is the amount of drug released in time t, Q_0 is the initial amount of the drug in the tablets and K_{HC} is the rate constant for Hixson-Crowell rate equation.

E. Korsmeyer–Peppas model:

In order to find out the mechanism of drug release from the polymeric tablets, the first 60% drug release data were fitted to the Korsmeyer–Peppas model:

$$M_t / M_\infty = Kt^n \quad (2.12)$$

where M_t is the amount of drug released at time t, M_o is the amount of total drug in tablets, M_t/M_o is the fractional drug release at time t, K is a constant incorporating the structural and geometric

characteristics of the matrix tablets and n is a diffusional exponent, indicative of the drug release mechanism.

2.2.6 Formulation optimization by RSM

2.2.6.1 Experimental design

CCD with five coded values was employed in this study. According to this design, the total number of treatment combinations is $2^k + 2k + n$, where k is the number of independent variables and n is the number of repetitions of experiments at the centre point. The amount of HPMC K100M/NaCMC (3:1) (X_1) and $NaHCO_3$ (X_2) were selected as independent variables (k=2). The amount of drug substance, magnesium stearate and talc were kept constant while MCC was taken in sufficient quantity to maintain a constant tablet weight of 470 mg. All other formulation and processing variables were kept invariant throughout the study.

The central point (0, 0) was studied in quintuplicate. For k=2, $2^2 + (2\times2) + 5 = 13$. Hence, a total of 13 experiments were carried out to find the optimum area, at which the desired responses are achieved. Table 2.2 summarizes an account of the 13 experimental runs studied, their factor combinations, and the translation of the coded levels to the experimental units employed during the study and Table 2.3 shows the formulae for preparation of the floating, bioadhesive and swellable tablets of ranitidine hydrochloride.

Floating lag time (Y_1), bioadhesive strength (Y_2), maximum swelling index (Y_3), drug release at 1 h (Y_4), time required for 50% drug release ($t_{50\%}$) (Y_5) and drug release at 12 h (Y_6) were taken as the dependent/response variables. The resulting data were fitted into Design Expert Software (Version 10.0.7.0, Stat- Ease Inc, Minneapolis, MN) and analyzed statistically using analysis of variance (ANOVA). The data were also subjected to 3D response surface methodology to determine the influence of the selected formulation factors on the dependent variables.

2.2.6.2 Validation of the experimental design

To validate the chosen experimental design, the experimental values of formulation responses were quantitatively compared with those of predicted values generated by the software. The percentage relative error was calculated using the following equation [Meka et al., 2016]:

% Relative error = (Predicted value - Experimental Value) x100 (2.15)

Predicted value

Floating lag time, bioadhesive strength, maximum swelling index, drug release at 1 h, time to 50% drug release and drug release at 12 h of the statistically optimized formulation were performed for verification of the theoretical prediction.

Table 2.2: Factor combination for formulation of ranitidine HCl (150mg) tablets as per CCD

Formulation code	Point type	Coded Factor Level	
		X_1	X_2
F1	Factorial	-1	-1
F2	Factorial	+1	-1
F3	Factorial	-1	+1
F4	Factorial	+1	+1
F5	Axial	-α	0
F6	Axial	+α	0
F7	Axial	0	-α
F8	Axial	0	+α
F9	Central point	0	0
F10	Central point	0	0
F11	Central point	0	0
F12	Central point	0	0
F13	Central point	0	0

Translation of coded levels in actual units

Coded level	-α	-1	0	+1	+α
X_1, amount of HPMC/NaCMC (3:1) (mg)	113.775	132	176	220	238.225
X_2, amount of $NaHCO_3$(mg)	39.44	44	55	66	70.556

α=1.41421

Table 2.3: Formulae for the preparation of ranitidine HCl (150mg) matrix tablets as per CCD.

S/N	Ingredient	Formulation code and composition (mg/tab)												
		F1	F2	F3	F4	F5	F6	F7	F8	F9	F10	F11	F12	F13
1	Ranitidine HCl*	168	168	168	168	168	168	168	168	168	168	168	168	168
2	HPMC/NaCMC (3:1)	132	220	132	220	113	238	176	176	176	176	176	176	176
3	$NaHCO_3$	44	44	66	66	55	55	44	66	55	55	55	55	55
4	MCC	118	30	96	8	126	1	74	52	63	63	63	63	63
5	Magnesium Stearate	4	4	4	4	4	4	4	4	4	4	4	4	4
6	Purified Talc	4	4	4	4	4	4	4	4	4	4	4	4	4
	Total	470	470	470	470	470	470	470	470	470	470	470	470	470

*168mg Rantidine HCl is equivalent to 150 mg Rantidine.

2.3 Drug-excipient interaction study

FT-IR spectra for pure ranitidine hydrochloride and optimized ranitidine tablet formulation were acquired at room temperature using FT-IR spectrophotometer (FTIR-8400S, Shimadzu, Japan) in transmittance mode. The samples were first ground in a mortar to reduce the average particle size. About 8 mg of finely ground samples were mixed with liquid paraffin in a mortar and pestle. The sample mixture was then placed onto the face of a potassium bromide (KBr) plate and the second window was placed on top of the first salt plate to form a thin film of the mull by compression between the two plates. The sandwiched plates were placed in the IR spectrometer and the spectra were obtained. Each IR spectrum was collected with 20 scans and spectral resolution of 4 cm^{-1}. Scanning was performed between wave numbers 4000 - 400 cm^{-1}. Background spectrum was collected before running each sample. IR Solution Software was used for data treatment.

2.4 Statistical analysis

Origin 8 Software (OriginLab Corporation, MA, and USA) was used to statistically analyze the results and one way analysis of variance (ANOVA) was applied for comparison of all results. To demonstrate graphically the influence of each factor on responses and to indicate the optimum level of factors, the contour and response surface plots were generated using Design-Expert 10.0.7.0 software (Stat-ease, Corp. Australia). At 95% confidence interval, p-values of < 0.05 were considered statistically significant. All the data measured and reported were averages of a minimum of triplicate measurements and the values are expressed as mean ± standard deviation.

3. RESULTS & DISCUSSION

3.1 Preliminary studies

Before applying the experimental design for optimization, preliminary studies were conducted in order to compare the release characteristics of the polymers used and identify the most critical factor variables. Factors that could possibly have significant effects on the response variables, according to literature, were considered including viscosity grade, polymer concentration, polymers ratio, concentration of effervescent agent and hardness of tablets. The response variables considered in the preliminary studies were matrix integrity, floating lag time, floating duration, bioadhesive strength, swelling index, drug release at 1 h, time to 50% drug release, and drug release rate.

3.1.1 Density and related properties

Density and related properties of the prepared blends are summarized in Table 3.1. The bulk density and tapped density of the prepared powder blend ranged from 0.24 to 0.31 g/ml and 0.27 to 0.35 g.ml, respectively. The formulations exhibited excellent to good flow property. Angle of repose ranged from 26.40 to 30.62^0, Hausner ratio ranged from 1.07 to 1.17 and the compressibility index ranged from 7.12 to 12.44 %.

Table 3.1 Density and related properties of ranitidine HCl (150mg) formulations in the preliminary study (n = 3)*

Formulation code	Bulk density (g/ml)	Tapped density (g/ml)	Carr's index (%CI)	Hausner ratio	Angle of repose (Degree)
FH1	0.25 ± 0.01	0.28 ± 0.02	12.44±0.10	1.17±0.04	30.62±0.72
FH2	0.24 ± 0.01	0.27 ± 0.01	11.13±0.77	1.16±0.04	29.28±0.87
FH3	0.26 ± 0.00	0.30 ± 0.00	10.71±0.09	1.12±0.01	29.17±0.51
FH4	0.25 ± 0.01	0.31 ± 0.01	11.10±0.57	1.11±0.02	29.24±0.42
FS1	0.31 ± 0.01	0.33 ± 0.01	8.45±0.67	1.09±0.03	26.40±0.63
FS2	0.30 ± 0.02	0.32 ± 0.02	7.12±0.61	1.07±0.07	26.72±0.62
FM1	0.27 ± 0.01	0.29 ± 0.02	10.0±0.85	1.12±0.05	28.08±0.69
FM2	0.28 ± 0.01	0.31 ± 0.01	9.78±0.58	1.12±0.04	28.93±0.39
FM3	0.30 ± 0.02	0.32 ± 0.02	8.28±0.60	1.10±0.04	28.29±0.46
FM4	0.28 ± 0.02	0.31 ± 0.02	9.24±0.67	1.11±0.06	29.55±0.19
FM5	0.29 ± 0.01	0.32 ± 0.01	7.81±0.12	1.09±0.01	28.70±0.39
FM6	0.31 ± 0.02	0.35 ± 0.02	8.19±0.58	1.10±0.04	28.57±0.70
FSB1	0.29 ± 0.01	0.35 ± 0.01	8.66±0.63	1.09±0.05	29.60±0.68
FSB2	0.28 ± 0.02	0.31 ± 0.02	9.73±0.49	1.11±0.06	29.93±0.61

*Values are expressed as Mean ± SD.

3.1.2 Evaluation of prepared tablets in the preliminary studies

3.1.2.1 Physicochemical properties of the tablets

The hardness, friability, thickness and assay results for the different formulations in the preliminary studies are shown in Table 3.2. The hardness of the tablets ranged from 62.50 to 68.56 N and, the friability values were less than 1% indicating appropriate mechanical strength and resistance to abrasion. No sign of capping, spitting, breaking and cracking was noticed after performing the friability test. The thickness ranged from 3.93 to 4.03 mm; and the drug content valued from 98.02 to 102.3%, meeting the standard USP limits (90-110) %.

Table 3.2: Properties of different formulations of ranitidine HCl (150 mg) matrix tablets in the preliminary study

Formulation Code	Hardness (N)*	Friability (%)	Thickness (mm)*	Assay (%)*
FH1	62.67 ± 0.61	0.23	4.03 ± 0.14	99.00 ± 0.01
FH2	64.40 ± 0.53	0.18	3.93 ± 0.14	98.02 ± 0.01
FH3	62.50 ± 0.50	0.15	4.01 ± 0.00	99.08 ± 0.00
FH4	63.70 ± 0.70	0.28	3.97 ± 0.14	101.04 ± 0.00
FS1	64.33 ± 0.58	0.24	4.00 ± 0.07	102.01 ± 0.00
FS2	67.97 ± 0.15	0.28	4.03 ± 0.14	99.89 ± 0.00
FM1	65.03 ± 0.15	0.14	3.93 ± 0.14	101.03 ± 0.01
FM2	63.83 ± 0.58	0.25	4.00 ± 0.07	99.89 ± 0.00
FM3	63.87 ± 0.32	0.27	4.00 ± 0.14	101.20 ± 0.00
FM4	66.00 ± 0.20	0.19	3.97 ± 0.21	102.30 ± 0.01
FM5	68.56 ± 0.60	0.28	4.00 ± 0.00	99.89 ± 0.00
FM6	64.80 ± 0.26	0.16	4.00 ± 0.14	101.23 ± 0.00
FSB1	63.83 ± 0.76	0.24	3.90 ± 0.07	99.87 ± 0.01
FSB2	67.77 ± 0.25	0.26	4.01 ± 0.14	99.46 ± 0.00

*Values are expressed as Mean ± SD.

The effect of different variables on selected response variables are presented in Table 3.3 and discussed in the following sections.

Table 3.3: Summary of effect of formulation variables on selected response variables during the development of ranitidine HCl (150 mg) matrix tablets in the preliminary studies.

Formulation and process factors (Independent variables)		Response variables /Dependent variables										
		Floating lag time (sec)	Floating duration (h)	Matrix integrity	Ex vivo mucoadhesion time (h)	Bioadhesive strength (g)	Diameter of swollen tab at 1hr (mm)	Diameter of swollen tab at 12 hr (mm)	Max swelling index (%)	Drug release at 1h (%)	$t_{50\%}$ (h)	Drug release rate (%/$h^{-1/2}$)
HPMC K4M [11.7% $NaHCO_3$]	28.7% (FH1)	5.66±0.56	> 12	+	6.50	18.48±0.24	13.21±0.02	14.23±0.01	302±0.01	38.48	2.22	34.56
	47.8% (FH2)	3.33±0.06	> 12	++	8.25	21.63±0.12	14.23±0.01	15.15±0.06	324±0.04	32.57	2.67	31.60
HPMC K100M [11.7% $NaHCO_3$]	28.7% (FH3)	8.66±0.61	> 12	++	7.75	21.30±0.26	13.84±0.05	14.84±0.05	316±0.03	36.45	2.40	33.25
	47.8% (FH4)	6.93±0.11	> 12	+++	9.25	24.68±0.18	14.83±0.03	15.27±0.12	333±0.00	30.35	2.87	30.50
NaCMC [11.7% $NaHCO_3$]	28.7% (FS1)	15.20±0.34	> 12	Not intact	Not intact	27.73±0.21	Not intact	Not intact	Not intact	65.28	0.96	52.03
	47.8% (FS2)	13.17±0.23	> 12	Not intact	Not intact	32.32±0.43	Not intact	Not intact	Not intact	56.28	1.26	45.23
HPMC K100M/ NaCMC ratio (28.7%) [11.7% $NaHCO_3$]	(3:1) (FM1)	8.3±0.10	> 12	+++	10.50	23.50±0.10	13.91±0.04	14.84±0.02	312±0.12	29.28	3.80	26.01
	(1:1) (FM2)	8.90±0.10	> 12	++	11.25	24.40±0.26	13.80±0.06	14.66±0.00	307±0.09	32.31	3.34	28.36
	(1:3) (FM3)	9.53±0.06	> 12	+	> 12	25.27±0.15	13.23±0.01	14.20±0.01	292±0.07	36.27	2.73	31.25
HPMC K100M/ NaCMC ratio (47.8%) [11.7% $NaHCO_3$]	(3:1) (FM4)	10.20±0.10	> 12	+++	> 12	26.27±0.61	14.97±0.01	15.45±0.00	324±0.00	25.02	3.74	25.46
	(1:1) (FM5)	11.84±0.02	> 12	++	> 12	27.30±0.10	14.41±0.01	15.33±0.02	311±0.14	28.54	3.66	27.12
	(1:3) (FM6)	12.94±0.06	> 12	+	> 12	30.07±0.15	14.10±0.02	15.11±0.04	302±0.24	29.63	3.63	27.46
$NaHCO_3$ [HPMC K100M/ NaCMC ratio (47.8%)]	9.5% (FSB1)	16.34±0.15	> 12	+++	> 12	26.84±0.04	14.33±0.03	15.29±0.02	314±0.07	24.05	3.95	24.98
	11.7% (FM4)	10.20±0.10	> 12	+++	> 12	26.27±0.61	14.97±0.01	15.45±0.00	324±0.04	25.02	3.74	25.46
	13.9% (FSB2)	5.30±0.10	> 12	++	10.50	23.47±0.06	15.08±0.01	15.64±0.00	325±0.12	27.08	3.22	27.42
Compression force [Formulation FM4]	50 N	6.73±0.21	> 12	+++	>12	27.07±0.06	14.42±0.02	15.34±0.01	322±0.08	29.84	2.85	29.64
	70 N	10.23±0.06	> 12	+++	>12	27.43±0.32	14.41±0.01	15.33±0.02	318±0.14	27.86	3.34	27.35
	90 N	13.67±0.21	> 12	+++	>12	27.60±0.26	14.40±0.03	15.31±0.03	317±0.09	26.74	3.80	25.62

+++ =Best matrix integrity, ++ = Good matrix integrity, + = Poor matrix integrity

3.1.2.2 Effect of viscosity grade of HPMC on different response variables

To investigate the effect of viscosity grade of HPMC, formulations FH_1 and FH_2 using 28.7 % and 47.8 % HPMC K4M respectively; and formulations FH_3 and FH_4 were prepared using 28.7 % and 47.8 % HPMC K100M. The level of $NaHCO_3$ was kept constant at 11.7 % and all other process variables were kept constant. As shown in Table 3.3, the floating lag time increased with increase in viscosity grade of HPMC ($FH_3 > FH_1$, and $FH_4 > FH_2$) ($p < 0.05$). This is attributed to the smaller effective molecular diffusion area at higher viscosity as compared with lower viscosity grades of HPMC. Moreover, there is more polymer entanglement and more gel strength at higher viscosity than at lower viscosity grades of HPMC [Biswas *et al.,* 2013].

There was significant increase in bioadhesive strength as the viscosity of HPMC increases ($FH_3 > FH_1$, and $FH_4 > FH_2$) ($p < 0.05$). Similar results were obtained by Siddam et al. [2016]. The swelling behavior also increased with increase in viscosity of HPMC (Table 3.3 and Fig 3.1). Similar results were obtained by Qazi et al. [2013]. The degree of swelling determines the diffusional path length of a drug; and the thicker the gel layer the slower the rate of drug release from a matrix [Sujja-areevath et al., 1998].

The results also indicated that the higher the viscosity grade of HPMC, the slower the drug release (Table 3.3 and Fig 3.2). Similar results were obtained by Kumar et al., [2005]. Higher viscosity grades have a higher gel viscosity, which will both slow drug diffusion in the gel layer and also render it more resistant to erosion.

3.1.2.3 Effect of HPMC/NaCMC ratio on different response variables

Different formulations were prepared using combination of HPMC K100M and NaCMC to investigate the effect of the ration of the polymer blend. Among the two viscosity grades of HPMC, the higher viscosity grade (HPMC K100M) was selected because it had better matrix integrity, bioadhesive character and swelling behavior than the lower viscosity grade (HPMC K4M). The results indicate that the floating lag time was shorter for formulations containing higher concentrations of HPMC in comparison to the formulations having higher amounts of NaCMC. For example, the floating lag time of FM_3 (28.7% HPMC K100M / NaCMC (1:3) was 9.53 sec while that of FM_1 (28.7% HPMC K100M / NaCMC (3:1) was 8.30 sec ($p < 0.05$). This could be due to the rapid formation of thick gel by HPMC around the tablets causing rapid entrapment of generated CO_2 compared to NaCMC.

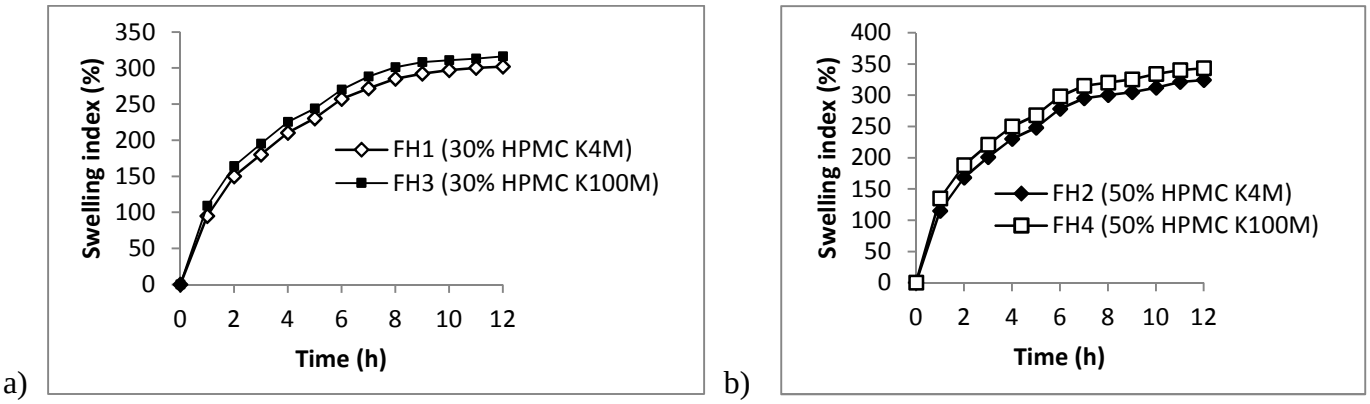


Fig. 3.1. Effect of viscosity grade of HPMC on swelling index of ranitidine HCl (150 mg) matrix tablets at (a) 28.7% and (b) 47.8% polymer concentration.

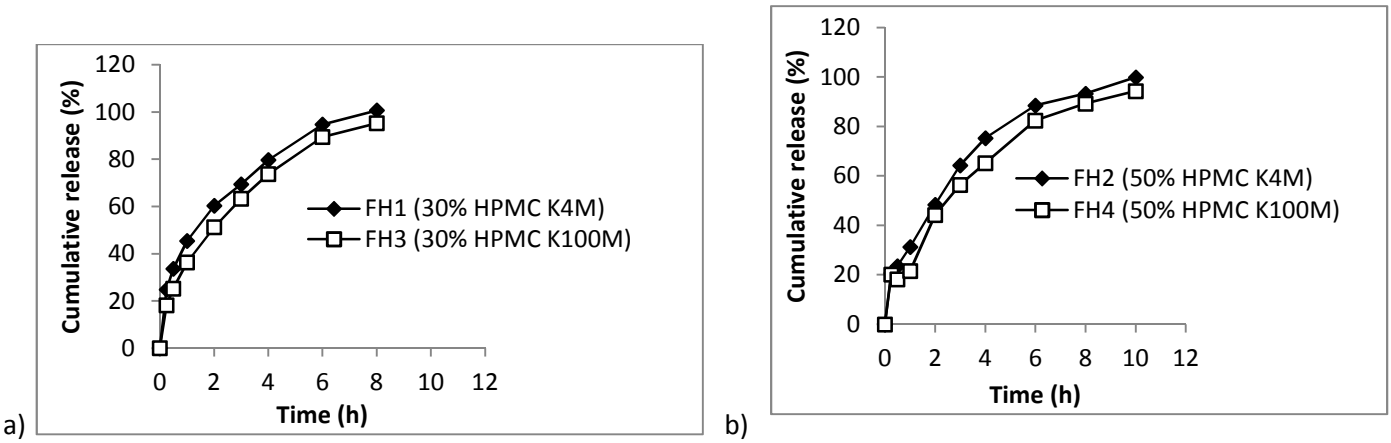


Fig. 3.2. Effect of viscosity grade of HPMC on drug release profile of ranitidine HCl (150 mg) matrix tablets at a) 28.7 % and b) 47.8% polymer concentration

Bioadhesive strength was higher for formulations containing higher concentrations of NaCMC in comparison to the formulations having higher amounts of HPMC K100M. Literature also reveals that non-ionic polymer undergo lesser degree of mucoadhesion when compared to anionic polymers [Roy and Prabhakar, 2010]. NaCMC is an anionic polymer and contains proton donating carboxyl groups responsible for its higher mucoadhesive strength.

Formulations having higher concentrations of HPMC K100M depicted more swelling than those with higher concentrations of NaCMC (Table 3.3 and Fig 3.3). Similar results were obtained by Sant et al. [2011]. This is attributed to the presence of highly hydrophilic hydoxypropyl groups in HPMC. The hydration of these functional groups results in rapid ingress of medium in polymer network, ultimately causing swelling and ordering of polymer chains [Bertram & Bodmeier, 2012].

In contrast, the less swelling of NaCMC could be linked to erosion in parallel to swelling, thus, compromising the matrix integrity.

Matrixes having higher concentration of NaCMC showed rapid dissolution as compared to matrixes having higher concentration of HPMC K100M (Fig. 3.4). This might be due to the high aqueous solubility (because of the presence of ionized carboxylic acid groups within the polymer structure) and hygroscopic nature of NaCMC. The latter may possibly lead to an increase in rate and extent of water uptake due to ion-pair repulsion, stretch in the gel network and break of the bonds responsible for the gel structure [Palmer et al., 2011].

The drug release was slower when binary mixture of the two polymers was used as compared to use of single polymer (Table 3.3 and Fig 3.4). This could be due to the synergistic increase in solution viscosity either as a result of direct interaction between the polymer chains or coil expansion of the anionic polymer in the mixed environment [Walker and Wells, 1982].

3.1.2.4 Effect of polymer concentration on different response variables

As shown in Table 3.3, an increase in the concentration of any of the polymers resulted in a decrease in floating lag time. This might be due to the faster swelling rate and rapid formation of thick gel around the tablets at higher polymer concentration causing rapid entrapment of generated CO_2 (Kotreka & Adeyeye, 2011; Gunjal et al, 2015). The gas generated is trapped and protected within the gel formed by hydration of the polymer, thus lowering the density of the tablet below that of gastric contents, causing buoyancy or floatation. The bioadhesive strength was also increased with increase in concentration of polymer, this is in agreement with literature [Singh and Ahuja, 2002; Singh et al., 2006]. The increase in bioadhesive strength with increase polymer concentration is attributed to the rapid swelling of hydrogels when in contact with hydrated mucous membrane, resulting in reduced glass transition temperature and increased uncoiling along with an increased mobility of polymer chains [Singh et al., 2006]. This tends to increase the adhesive surface for maximum contact with mucin and flexibility for interpenetration with mucin.

The degree of swelling increased as the polymer concentration increased (Fig.3.5). The swelling index of the prepared tablets increased with time because of the increase in hydration rate of polymers with time.

The results also indicated that the drug release was slower at higher polymer concentration (Table 3.3 and Fig. 3.6). The concentration of polymer affects the tortuosity of the gel, and it is likely that formation of a strong gel layer occurs in matrices with high polymer contents. Furthermore, the diffusion layer becomes stronger and more resistant to diffusion and erosion as the polymer concentration is increased [Xu and Sunada, 1995].

3.1.2.5 Effect of concentration of sodium bicarbonate on different response variables

The effect of concentration of $NaHCO_3$ on different response variables was investigated and is summarized in Table 3.3. There was a decrease in floating lag time with increase in sodium bicarbonate. The amount of carbon dioxide produced is exclusively proportional to the quantity of $NaHCO_3$ in the tablet [Chen et al., 2002]. Hence, decrease in floating lag time can be attributed to the availability of an increased amount of carbon dioxide as the concentration of $NaHCO_3$ was increased, and the gas is entrapped in the formed gel to give rapid buoyancy [Hu, et al., 2011].

There was a decrease in bioadhesive strength as the concentration of $NaHCO_3$ is increased. This might be attributed to the formation of higher CO_2 bubbles on the tablet surface in formulations having higher amount of sodium bicarbonate.

The swelling index was slightly increased with increasing amount of effervescent agent (Table 3.3 and Fig. 3.7). This could be explained by the disintegration effect of the effervescent agent, which increases the volume of the tablets and construct porous channels on the surface and inside of tablets. The porous channels increases the area of contacting between polymer particles and water so that the polymers could be hydrated more easily.

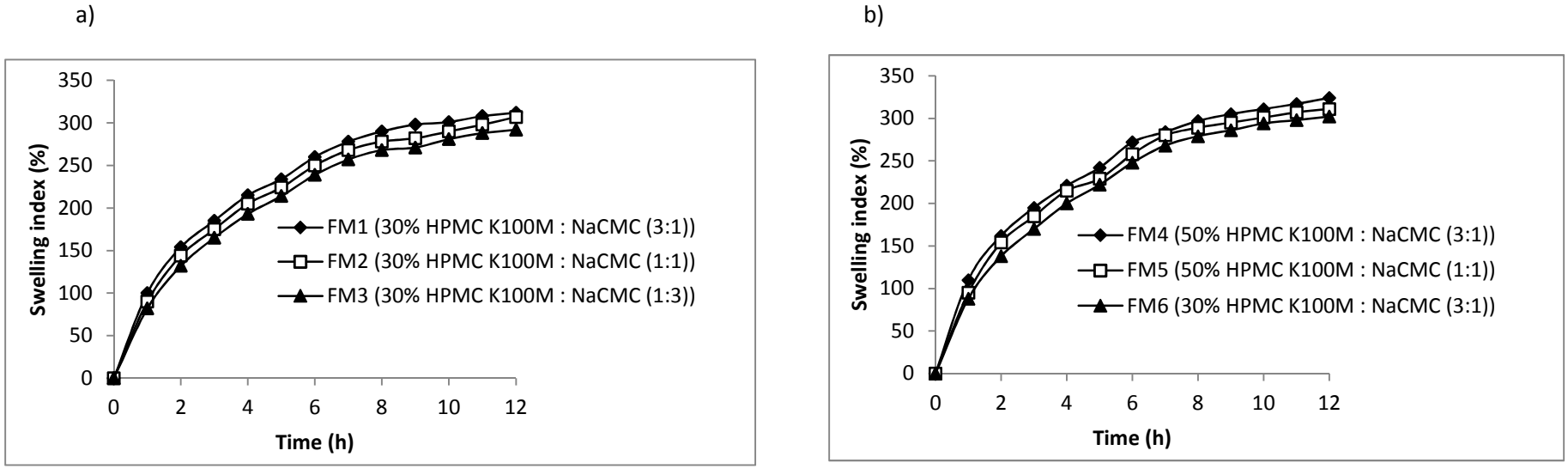


Fig. 3.3: Effect of HPMC/NaCMC ratio at (a) 28.7 % (b) 47.8 % polymer concentration on swelling index of ranitidine (150 mg) matrix tablet

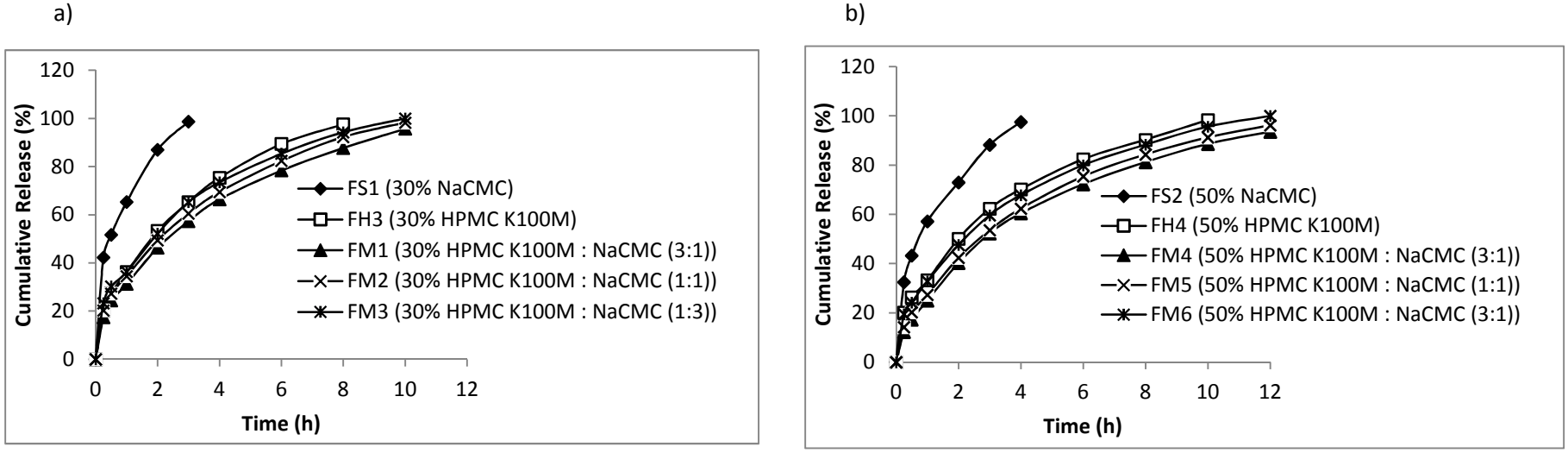


Fig. 3.4: Effect of HPMC/NaCMC ratio at a) 28.7% and b) 47.8% polymer conc on drug release profile of ranitidine (150 mg) matrix tablet

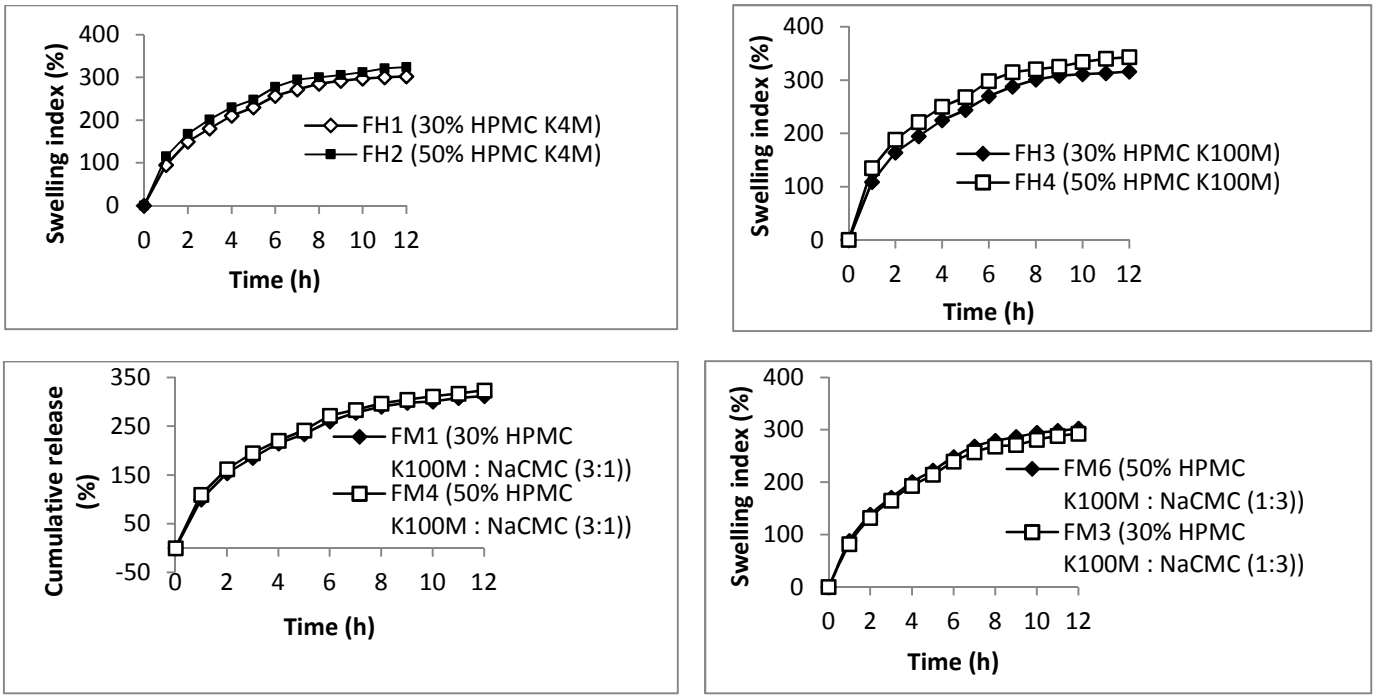


Fig. 3.5: Effect of polymer concentration on swelling index of ranitidine HCl (150 mg) matrix tablet.

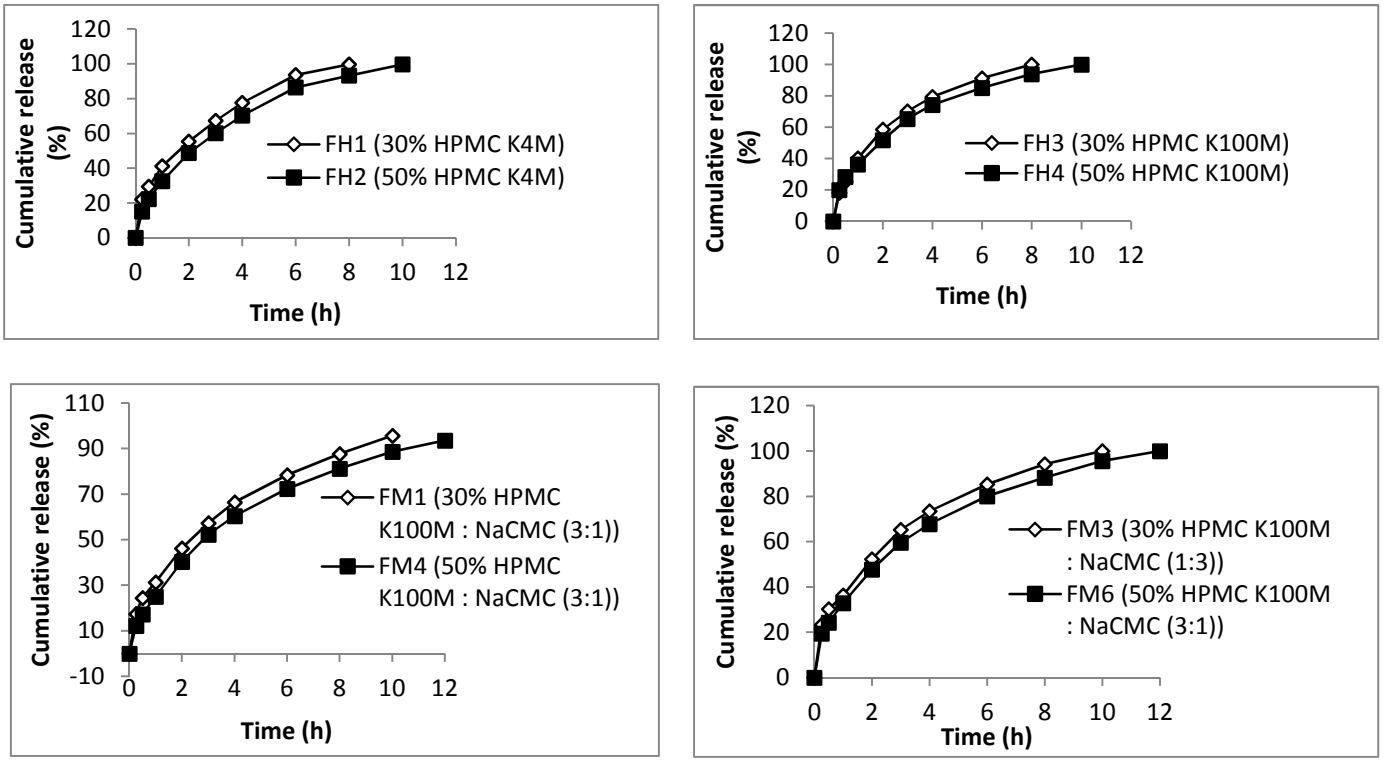


Fig. 3.6: Effect of polymer concentration on release profile of ranitidine from ranitidine HCl (150 mg) matrix tablet.

The results also indicated that the drug release was faster at higher effervescent concentration (Table 3.3 and Fig. 3.8). This could be due to the higher porosity in the tablets promoting ingress of medium, consequently, rapid dissolution of drug. Moreover, the rapid gas formation erodes the matrices surface area, resulting in faster release.

3.1.2.6 Effect of hardness on different response variables

To investigate the effect of hardness on different response variables, tablets of formulation FM_4 with different hardness (50, 70 and 90 N) were compared. As shown in Table 3.3, there was an increase in floating lag time with increase in hardness ($p < 0.05$). This could be due to the lesser porosity in formulations prepared at higher hardness. There was no significant difference in the bioadhesive strength and swelling index (Fig 3.9).

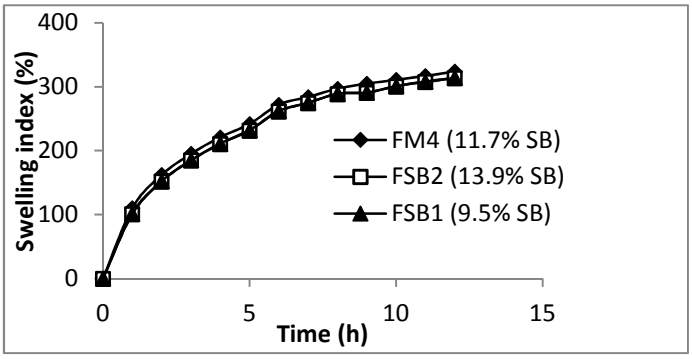


Fig. 3.7: Effect of concentration of $NaHCO_3$ on swelling index of ranitidine HCl (150 mg) matrix tablet.

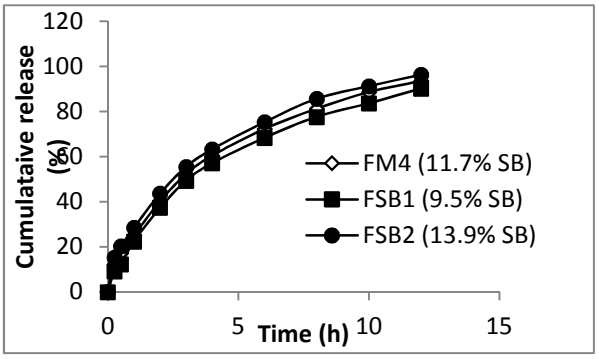


Fig. 3.8: Effect of concentration of $NaHCO_3$ on drug release profile of ranitidine from ranitidine HCl (150 mg) matrix tablet.

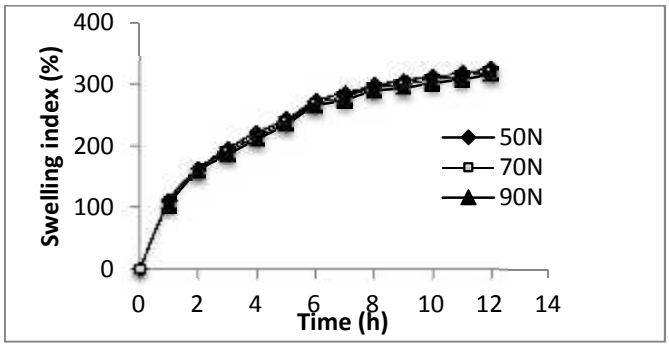


Fig. 3.9: Effect of hardness on swelling index of ranitidine HCl (150 mg) matrix tablets.

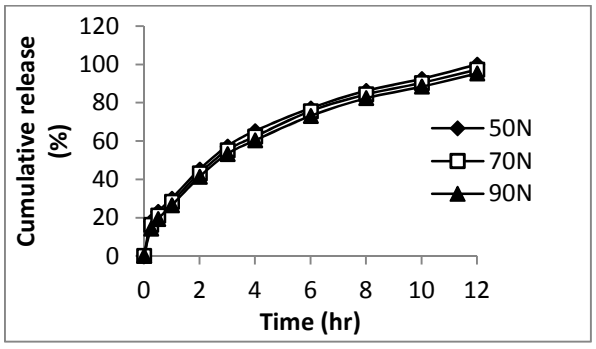


Fig. 3.10: Effect of hardness on release profile of ranitidine from ranitidine HCl (150 mg) matrix tablets.

There was no significant difference on the release properties (Table 3.3 and Fig 3.10) ($p > 0.05$). Variation in compression force is closely related to a change in porosity of tablets. However, since the porosity of hydrated matrix is independent of the initial porosity, the compression force seemed to have little influence on drug release [Kumar et al., 2005].

3.2 Optimization

3.2.1 Powder characteristics

The physical properties of the powder (bulk density, tapped density, compressibility index, Hausner ratio, and angle of repose) of all the 13 formulations prepared as per CCD are presented in Table 3.4. The bulk density of the formulations ranged from 0.24 to 0.30 and the tapped density ranged from 0.27 to 0.34. The blend indicated excellent to good flow properties for all formulations with the angle of repose values ranging from 28.54^{o} to 32.46^{0} according to fixed funnel method. The powder flow rate was between 2.67 and 7.59 g/sec. Moreover, the values of compressibility index ranged between 10.34 and 13.79, and the Hausner's ratios were between 1.01 and 1.16; indicating good flow properties.

Table 3.4: Powder characteristics of the 13 formulations of ranitidine HCl prepared as per CCD.

Formulation Code	Flow rate (g/sec)	Bulk density(g/ml)	Tapped Density (g/ml)	Carr's index (%)	Hausner ratio (h)	Angle of repose(^{0})
F1	5.89 ± 0.28	0.28 ± 0.28	0.32 ± 0.07	12.51 ± 0.38	1.14 ± 0.06	28.59 ± 0.72
F2	3.58 ± 0.82	0.24 ± 0.24	0.27 ± 0.01	11.12 ± 0.77	1.12 ± 0.04	31.28 ± 0.86
F3	7.59 ± 0.75	0.27 ± 0.27	0.31 ± 0.00	12.9 ± 0.09	1.14 ± 0.01	27.89 ± 0.51
F4	4.28 ± 0.62	0.25 ± 0.25	0.29 ± 0.01	13.79 ± 0.57	1.16 ± 0.02	32.01 ± 0.42
F5	3.08 ± 0.54	0.29 ± 0.29	0.33 ± 0.01	12.12 ± 0.42	1.14 ± 0.03	31.05 ± 0.61
F6	2.67 ± 0.28	0.30 ± 0.43	0.34 ± 0.02	11.76 ± 0.7	1.14 ± 0.06	32.46 ± 0.64
F7	6.97 ± 0.19	0.27 ± 0.27	0.31 ± 0.01	12.9 ± 0.67	1.01 ± 0.03	28.97 ± 0.63
F8	5.87 ± 0.65	0.28 ± 0.28	0.32 ± 0.02	12.51 ± 0.6	1.14 ± 0.07	29.87 ± 0.62
F9	7.28 ± 0.48	0.26 ± 0.26	0.29 ± 0.02	10.34 ± 0.69	1.11 ± 0.05	29.78 ± 0.61
F10	5.68 ± 0.53	0.28 ± 0.28	0.32 ± 0.06	12.5 ± 0.08	1.14 ± 0.05	29.25 ± 0.69
F11	6.97 ± 0.75	0.25 ± 0.25	0.29 ± 0.03	13.73 ± 0.58	1.16 ± 0.04	28.97 ± 0.39
F12	7.29 ± 0.91	0.27 ± 0.27	0.31 ± 0.07	12.9 ± 0.6	1.15 ± 0.03	29.05 ± 0.46
F13	7.09 ± 0.37	0.26 ± 0.26	0.3 ± 0.02	13.3 ± 0.37	1.15 ± 0.06	28.54 ± 0.19

* Values are expressed as Mean ±SD

3.2.2 Characteristics of tablets

3.2.2.1 Physicochemical properties of the tablets

The tablets of 13 different batches were evaluated for different physicochemcial tests and the results are summarized in Table 3.5. The tablets mean thickness values ranged from 3.89 mm to 4.02 mm. The hardness of the tablets ranged between 60.40 to 67.80 N. The friability was in a range of 0.18 to 0.50% and this was within the pharmacopeia limit (< 1%). The drug content of tablets was 98.25% to 102.50% and this was also within the limit of (90-110) %.

The prepared tablets exhibited excellent floating duration which was > 12 h in all cases; and the floating lag time ranged from 4.10 sec to 13.54 sec. An increase in the concentration of polymer showed decrease in floating lag time. For example the floating lag time of formulations F_5 (24.21% polymer), F_{12} (37.40% polymer) and F_6 (50.69% polymer) were 8.60, 7.50 and 6.44 sec, respectively ($p < 0.05$). On the other hand, the floating lag time decreased with increasing amount of sodium bicarbonate. For example, the floating lag time of formulations F_7 (8.40% $NaHCO_3$), F_9 (11.70% $NaHCO_3$), and F_8 (15.01% $NaHCO_3$) were 13.54, 6.20, and 4.10 sec ($p < 0.05$), respectively. The matrix integrity of all the tablets was maintained up to 12 h except for formulation F_5 (the matrix of this formulation was not intact due to low amount of polymer).

All formulations showed sufficiently high bioadhesion strength (> 20 g). The bioadhesive strength ranged from 20.23 to 32.50 g. The tablets showed *ex vivo* mucoadhesion time of more than 12 h except for formulation F_1, F_3 and F_5. A distinct increase in the bioadhesive strength was observed with an increase in the amount of polymer. For example formulations F_5 (24.21% polymer), F_{10} (37.40% polymer) and F_6 (50.69% polymer) have bioadhesive strength of 20.23, 26.57 and 32.50 g respectively ($p < .00001$). There was a decrease in bioadhesive strength with an increase in concentration of sodium bicarbonate. For example, formulations F_7 (8.40% $NaHCO_3$), F_9 (11.70% $NaHCO_3$), and F_8 (15.01% $NaHCO_3$) showed bioadhesive strength of 27.24, 26.43 and 24.40g, respectively ($p < 0.05$).

Table 3.5: Tablet characteristics of the 13 formulations of ranitidine HCl (150) matrix tables prepared as per CCD*

Formulation Code	Hardness (N)	Friability (%)	Thickness (mm)	Assay (%)	Floating lag time (Sec)	Floating Duration (h)	Matrix integrity	Bioadhesive strength (g)	*Ex vivo* mucoadhesion time (h)	Average diameter at 1h (mm)	Average diameter at 12 h (mm)
F1	62.20 ± 0.01	0.31	3.89 ± 0.00	98.25 ± 0.04	12.25 ± 0.01	> 24	+	23.80 ± 0.01	10.50	14.08 ± 0.01	14.56 ± 0.01
F2	65.40 ± 0.01	0.41	3.95 ± 0.01	101.01 ± 0.01	11.28 ± 0.01	> 24	+	30.35 ± 0.50	>12	14.14 ± 0.03	14.78 ± 0.01
F3	62.10 ± 0.08	0.32	3.95 ± 0.04	102.50 ± 0.01	5.80 ± 0.02	> 24	+	23.30 ± 0.08	10.05	14.06 ± 0.01	14.63 ± 0.01
F4	63.10 ± 0.01	0.42	3.91 ± 0.04	100.01 ± 0.00	5.10 ± 0.08	> 24	+	29.47 ± 0.04	>12	14.52 ± 0.01	14.86 ± 0.01
F5	64.40 ± 0.08	0.50	3.95 ± 0.00	99.56 ± 0.04	8.60 ± 0.00	> 24	Not intact	20.23 ± 0.00	6.25	13.32 ± 0.04	13.95 ± 0.01
F6	61.50 ± 0.04	0.41	4.01 ± 0.05	98.87 ± 0.09	6.44 ± 0.00	> 24	+	32.50 ± 0.08	>12	14.73 ± 0.01	15.02 ± 0.01
F7	67.80 ± 0.04	0.41	3.98 ± 0.01	100.01 ± 0.04	13.54 ± 0.00	> 24	+	27.24 ± 0.03	>12	14.19 ± 0.01	14.61 ± 0.00
F8	66.40 ± 0.05	0.42	4.01 ± 0.01	101.04 ± 0.00	4.10 ± 0.05	> 24	+	24.43 ± 0.12	>12	14.36 ± 0.01	14.73 ± 0.01
F9	60.40 ± 0.01	0.31	4.00 ± 0.04	102.00 ± 0.00	6.20 ± 0.01	> 24	+	26.47 ± 0.05	>12	14.24 ± 0.02	14.91 ± 0.01
F10	64.10 ± 0.00	0.51	3.98 ± 0.00	98.68 ± 0.04	6.5 ± 0.01	> 24	+	26.57 ± 0.07	>12	14.20 ± 0.01	14.86 ± 0.04
F11	65.40 ± 0.03	0.21	3.97 ± 0.01	99.76 ± 0.05	7.00 ± 0.04	> 24	+	27.10 ± 0.08	>12	14.27 ± 0.01	14.85 ± 0.05
F12	61.50 ± 0.02	0.18	4.02 ± 0.03	100.21 ± 0.02	7.50 ± 0.01	> 24	+	25.50 ± 0.08	>12	14.31 ± 0.01	14.87 ± 0.04
F13	63.70 ± 0.00	0.24	4.00 ± 0.01	99.27 ± 0.01	6.60 ± 0.01	> 24	+	26.57 ± 0.09	>12	14.29 ± 0.10	14.78 ± 0.03

*Values are expressed as Mean ± SD.

The *in vitro* swelling study showed that all batches had good swelling properties. The average diameter after 1 h and 12 h were above 14 mm (greater than the average diameter of the pylorus sphincter, 12.8 mm) for all the formulations except for formulation F_5. The results of the swelling index (Figure 3.11) indicates that swelling index of the tablets increased with increase in polymer concentration and effervescent agent. For example, the swelling index was highest for formulation F_6 (50.69% polymer) and least for F_5 (24.21% polymer). In the same manner, comparing formulations F_7 (8.40% $NaHCO_3$), F_{12} (11.70% $NaHCO_3$), and F_8 (15.01% $NaHCO_3$), F_8 had the highest swelling index.

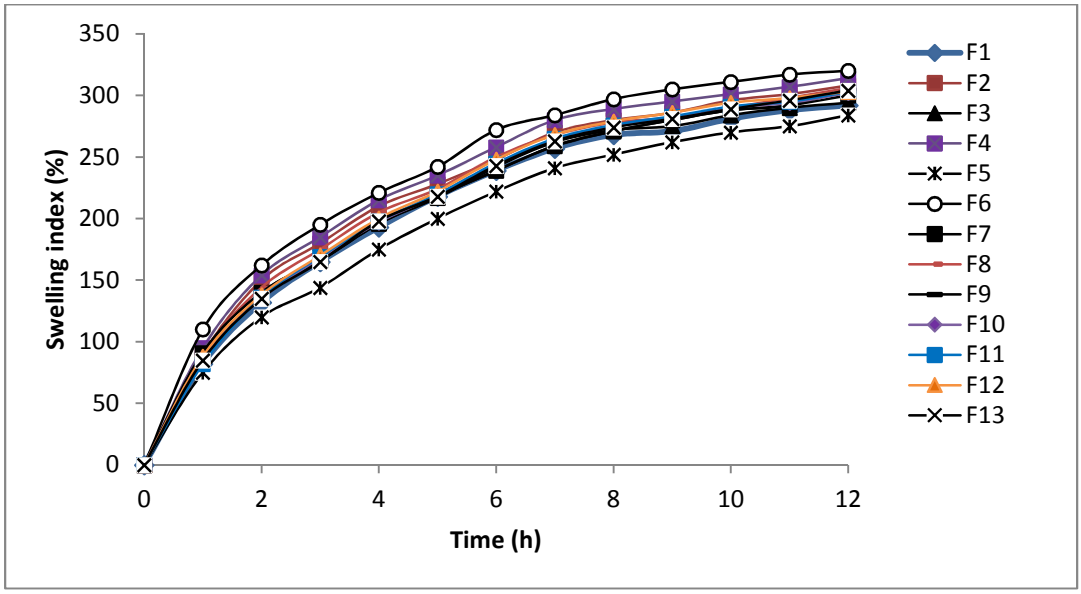


Fig 3.11: Swelling index of the 13 formulations of ranitidine HCl (150mg) matrix tablets prepared as per CCD

3.2.2.2 *In vitro* drug release

Results of the dissolution parameters (% release at 1 h, $t_{50\%}$ and % release at 12 h) for the 13 formulations are shown in Table 3.6. The initial release in 1 h ranged from 21.10 – 31.50%. At the end of 12 h, the figure was between 87.60 and 100 %. The $t_{50\%}$ varied between 3.15 and 3.98 h. Sustained release up to 12 h was achieved in all formulations except F_5 in which about 100 % of the drug release was observed within 8 h (Fig 3.12). Complete release from F5 within short time was due to less polymer concentration (24.21%). For the majority of formulations, the rate of drug release was found to be higher during the first 2 h followed by a gradual release phase for more than 10 h. The initial faster release may be due to surface erosion and shorter diffusion path. The

release rate then decreases because the external layers of the tablet become depleted and drug must travel longer path through the gel layer to reach the surface.

Table 3.6: Drug release properties for the 13 formulations of ranitidine HCl (150mg) matrix tablets prepared as per CCD.

.

Formulation Code	Drug release at 1h (%)	Time to 50% drug release	Drug release at 12 h (%)
F1	30.08	3.45	98.50
F2	22.40	3.91	87.60
F3	30.50	3.23	98.00
F4	23.10	3.84	88.90
F5	31.50	3.15	100.00
F6	21.10	3.98	87.85
F7	24.10	3.83	92.30
F8	28.31	3.50	95.30
F9	26.35	3.85	94.80
F10	27.04	3.75	94.30
F11	25.50	3.84	93.65
F12	26.21	3.75	93.50
F13	27.04	3.79	93.54

The release profile revealed that F_1, F_3 and F_5 showed more than 30 % drug release at 1st hour. It is reported in literature that more than 30% drug release in the first hour of dissolution indicates the chance for dose dumping. This indicates formulations with lower levels of polymer exhibited initial burst drug release. The results also indicate that drug release was faster with an increase in concentration of sodium bicarbonate. For example, the drug release after 12 h for formulations F7 (8.40% $NaHCO_3$), F12 (11.70% $NaHCO_3$), and F8 (15.01% $NaHCO_3$) were 92.30%, 93.50% and 95.30% respectively (p value < 0.005).

In general, results from ANOVA indicated the presence of significant difference ($p < 0.05$) among the formulations in their release profiles. These differences evidenced that changes in values of the investigated formulation variables had significant influence on pattern of release and thus optimization was required to have an optimum release over a fixed period of time.

3.2.3 Drug release kinetics

The results of the curve fitting into the different mathematical models are given in Table 3.7. The determination coefficient (R^2) was used as an indicator of the best fitting for each of the models considered. Among the different models studied, the dissolution data best fitted to Higuchi model. Hence, the drug release was proportional to the square root of time.

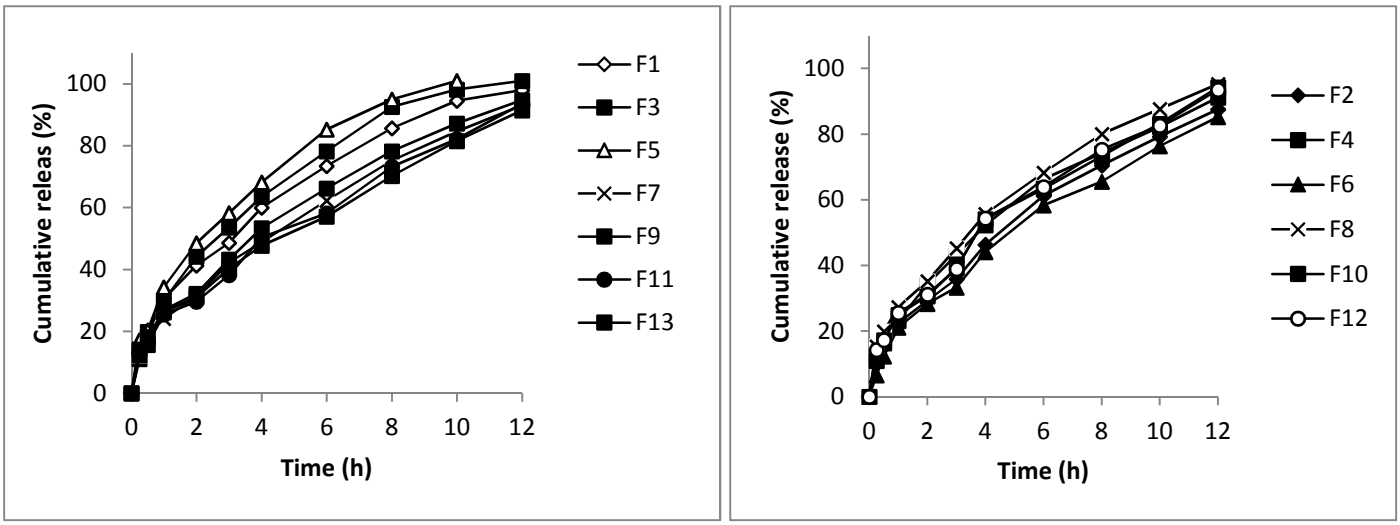


Fig 3.12: *In vitro* release profiles of the 13 formulations of ranitidine HCl (150mg) matrix tablets prepared as per CCD.

The drug release mechanism was determined by fitting the data from the first 60% drug release to the Korsmeyer-Peppas model**.** In this model, the value of the diffusion constant (n) illustrates the type of release mechanism. For cylindrical tablets; $n \leq 0.45$ corresponds to a Fickian diffusion mechanism, $0.45 < n < 0.89$ to non-Fickian transport, $n = 0.89$ to Case II (relaxational) transport, and $n > 0.89$ to super case II transport [Shoaib et al., 2006; Ali et al., 2007; Sinha et al., 2011]. As shown in Table 3.7, the value of diffusion exponent (n) ranged from 0.4722 to 0.6045 indicating an anomalous diffusion ($0.45<n<0.89$) mechanism. Anomalous diffusion of drug release mechanism signifies a coupling of both diffusion and erosion mechanisms which indicate that the drug release is controlled by more than one process during the entire period of drug release (Dash et al., 2010).

Table 3.7: Rate constants and correlation coefficient fits of different kinetic equations for the 13 formulations of ranitidine HCl (150mg) matrix tablets prepared as per CCD.

Formulation code	Model										
	Zero order release		First order release		Higuchi square root		Hixson-Crowell cubic root		Korsmeyer-Peppas		
	K_o	R^2	K_1	R^2	K_H	R^2	K_{HC}	R^2	K	R^2	n
F1	7.58	0.9206	-0.12	0.9474	28.98	0.9981	0.26	0.9922	0.38	0.9961	0.5128
F2	6.57	0.9346	-0.07	0.9765	24.92	0.9974	0.17	0.9828	0.31	0.9885	0.5495
F3	7.97	0.9047	-0.15	0.9516	30.64	0.9927	0.30	0.9858	0.37	0.9889	0.6045
F4	6.73	0.9379	-0.07	0.9756	25.50	0.9978	0.18	0.9850	0.31	0.9981	0.5432
F5	7.92	0.8657	-0.21	0.9155	30.96	0.9817	0.34	0.9946	0.41	0.9867	0.5201
F6	7.11	0.9781	-0.07	0.9663	26.09	0.9780	0.19	0.9883	0.25	0.9840	0.5586
F7	7.23	0.9552	-0.08	0.9711	27.08	0.9954	0.21	0.9933	0.33	0.9930	0.5065
F8	7.21	0.9514	-0.09	0.9472	27.05	0.9934	0.22	0.9863	0.36	0.9863	0.4760
F9	7.25	0.9587	-0.09	0.9473	27.04	0.9934	0.21	0.9860	0.34	0.9842	0.4914
F10	7.23	0.9605	-0.08	0.9405	26.91	0.9885	0.21	0.9821	0.32	0.9797	0.4914
F11	7.14	0.9618	-0.08	0.9441	26.54	0.9858	0.20	0.9819	0.32	0.9670	0.4732
F12	7.09	0.9590	-0.08	0.9440	26.38	0.9858	0.20	0.9811	0.33	0.9610	0.4722
F13	7.18	0.9591	-0.08	0.9485	26.74	0.988	0.21	0.9837	0.31	0.9776	0.5129

3.2.4 Selection of response variables

Based on preliminary studies, the response variables selected for optimization were floating lag time (Y_1), bioadhesive strength (Y_2), maximum swelling index (Y_3), % cumulative drug release at 1 h (Y_4), $t_{50\%}$ (Y_5) and % cumulative drug release after 12 h (Y_6). The summary of these experimental responses in the CCD are as summarized in Table 3.8. These results were input into the Design-Expert (version 10.0.7.0) software for optimization.

Table 3.8: Summary of experimental responses of the 13 formulations of ranitidine HCl (150mg) matrix tablets prepared as per CCD

Formulation	Response					
	Floating lag time (sec) (Y_1)	Bioadhesive strength (g) (Y_2)	Max swelling index (%) (Y_3)	Cumulative release at 1 h (%) (Y_4)	$t_{50\%}$ (Y_5)	Cumulative release at 12 h (%) (Y_6)
F1	12.25	23.80	292	30.08	3.40	98.50
F2	11.28	30.35	308	22.40	3.91	87.60
F3	6.20	23.30	294	30.50	3.23	98.00
F4	5.10	29.47	314	23.10	3.84	88.90
F5	8.50	20.23	284	31.50	3.15	100.00
F6	6.40	32.20	320	21.10	3.98	87.85
F7	13.54	27.24	300	24.10	3.83	92.30
F8	4.00	24.43	306	28.31	3.50	95.30
F9	6.20	26.47	305	26.35	3.85	94.80
F10	6.50	26.57	302	25.02	3.75	94.30
F11	7.00	27.10	303	25.50	3.84	93.65
F12	7.50	25.50	303	26.21	3.75	93.50
F13	6.60	26.57	304	27.04	3.79	93.50

3.2.5 Selection of mathematical model

The relationship between the two independent variables (HPMC K100M/NaCMC and Sodium bicarbonate) and the six response variables (floating lag time (Y_1), bioadhesive strength (Y_2), swelling index (Y_3), % drug release at 1 h (Y_4), $t_{50\%}$ (Y_5) and % drug release at 12 h (Y_6)) were analyzed using response surface methodology. Polynomial models including linear, interaction and quadratic terms were generated for all the response variables using Design Expert software. The best fitting mathematical model was selected based on the comparisons of several statistical

parameters including the coefficient of variation (CV), the multiple correlation coefficient (R^2), adjusted multiple correlation coefficient (adjusted R^2) and the predicted residual sum of square (PRESS) provided by the Design Expert software (Table 3.9).

Table 3.9: Fit summary statistics for response variables of the 13 formulations of ranitidine HCl (150mg) matrix tablets prepared as per CCD

Response	Source	SD	R-Squared	Adjusted R-Squared	Predicted R-Squared	PRESS	
Floating lag time (sec)	Linear	1.10	0.8762	0.8514	0.7916	20.42	
	2FI	1.16	0.8762	0.8349	0.6665	32.69	
	Quadratic	0.54	0.9793	0.9646	0.9103	8.79	Suggested
	Cubic	0.59	0.9824	0.9577	0.5176	47.28	Aliased
Bioadhesive strength (g)	Linear	0.75	0.9530	0.9436	0.9081	10.94	Suggested
	2FI	0.79	0.9533	0.9377	0.8532	17.48	
	Quadratic	0.88	0.9546	0.9222	0.7404	30.91	
	Cubic	0.69	0.9803	0.9527	0.4479	65.73	Aliased
Swelling index (%)	Linear	2.06	0.9583	0.9499	0.9157	86.05	Suggested
	2FI	2.07	0.9622	0.9496	0.8719	130.72	
	Quadratic	2.19	0.9672	0.9437	0.7947	209.54	
	Cubic	1.07	0.9944	0.9866	0.9607	40.12	Aliased
Release at 1h (%)	Linear	0.77	0.9515	0.9418	0.9157	10.38	Suggested
	2FI	0.81	0.9517	0.9356	0.8675	16.31	
	Quadratic	0.89	0.9550	0.9229	0.7909	25.75	
	Cubic	0.72	0.9789	0.9493	0.8945	13.00	Aliased
T 50% (h)	Linear	0.12	0.8358	0.8030	0.7314	0.23	
	2FI	0.12	0.8387	0.7850	0.6152	0.33	
	Quadratic	0.049	0.9806	0.9668	0.9209	0.068	Suggested
	Cubic	0.045	0.9885	0.9724	0.9240	0.065	Aliased
Release at 12 hr (%)	Linear	0.77	0.9672	0.9606	0.9370	11.38	Suggested
	2FI	0.75	0.9717	0.9622	0.9076	16.68	
	Quadratic	0.81	0.9745	0.9563	0.8598	25.32	
	Cubic	0.64	0.9888	0.9730	0.7438	46.27	Aliased

The fit of the model was evaluated through R^2-values. As observed from Table 3.9, R^2 was high (> 0.90) for all responses, which indicates a high degree of correlation between the experimental and predicted responses. In addition, the 'Predicted R^2' value was in good agreement with the 'Adjusted R^2' value (the difference is less than 0.2), indicating reliable models. Table 3.9 also shows that the selected models have smaller PRESS values compared to other models; again indicating the models fit the data.

Based on the fit summary shown in Table 3.9, linear model was selected as best fit for bioadhesive strength, swelling index, drug release at 1 h and 12 h; and the quadratic model was selected as best fit for floating lag time and $t_{50\%}$, as suggested by the software. In this study, the fit summary output was analyzed without performing any transformation (logarithmic, power, inverse, etc.) on the response data.

3.2.6 Model adequacy checking

The information about the model reliability was verified by using the analysis of variance (ANOVA). ANOVA was used to analyze the data to obtain the interaction between process of independent variables and responses. At 5% level of significance, a model is considered significant if the p-value is less than 0.05. The results of ANOVA (Table 3.10) indicated that models X_2, X_1^2 and X_2^2 for Y_1; X_1 and X_2 for Y_2; X_1 and X_2 for Y_3; X_1 and X_2 for Y_4; X_1, X_2, X_1^2 and X_2^2 for Y_5; X_1 and X_2 for Y_6 were significant model terms ($p < 0.05$).

As can be seen from Table 3.10, the p-values of lack of fit (LOF) were greater than 0.05 for all the response variables, which further strengthened the reliability of the models (for a model to be successfully used for prediction, the LOF, which is a special diagnostic test for adequacy of a model that compares the pure error and describes the variation of data around the fitted model, should be insignificant).

Adequate precision (signal to noise ratio) values higher than 4 for all the responses (Table 3.11) confirmed that all proposed models can be used to navigate the design space. For all the models % CV were not greater than 10%; indicating the reproducibility of the models.

Table 3.10: Summary of ANOVA results for dependent variables of the 13 formulations of ranitidine HCl (150mg) matrix tablets prepared as per CCD

Response	Source	Sum of Squares	df	Mean Square	F Value	p-value Prob > F	
Floating lag time	Model	95.99	5	19.20	66.32	< 0.0001	significant
	A-X1	*3.18*	*1*	*3.18*	*10.97*	*0.0129*	
	B-X2	*82.70*	*1*	*82.70*	*285.71*	*< 0.0001*	
	AB	*4.225E-003*	*1*	*4.225E-003*	*0.015*	*0.9072*	
	A^2	*1.70*	*1*	*1.70*	*5.87*	*0.0458*	
	B^2	*9.27*	*1*	*9.27*	*32.03*	*0.0008*	
	Residual	2.03	7	0.29			
	Lack of Fit	*1.01*	*3*	*0.34*	*1.34*	*0.3806*	*not significant*
	Pure Error	*1.01*	*4*	*0.25*			
	Cor Total	98.01	12				
Bioadhesive strength	Model	113.46	2	56.73	101.38	< 0.0001	significant
	A-X1	*109.88*	*1*	*109.88*	*196.35*	*< 0.0001*	
	B-X2	*3.58*	*1*	*3.58*	*6.40*	*0.0298*	
	Residual	5.60	10	0.56			
	Lack of Fit	*4.24*	*6*	*0.71*	*2.09*	*0.2482*	*not significant*
	Pure Error	*1.35*	*4*	*0.34*			
	Cor Total	119.06	12				
Swelling index	Model	978.18	2	489.09	114.83	< 0.0001	significant
	A-X1	*944.21*	*1*	*944.21*	*221.68*	*< 0.0001*	
	B-X2	*33.97*	*1*	*33.97*	*7.98*	*0.0180*	
	Residual	42.59	10	4.26			
	Lack of Fit	*37.39*	*6*	*6.23*	*4.79*	*0.0755*	*not significant*
	Pure Error	*5.20*	*4*	*1.30*			
	Cor Total	1020.77	12				
Release at 1hr	Model	117.17	2	58.58	98.14	< 0.0001	significant
	A-X1	*110.91*	*1*	*110.91*	*185.81*	*< 0.0001*	
	B-X2	*6.25*	*1*	*6.25*	*10.48*	*0.0089*	
	Residual	5.97	10	0.60			
	Lack of Fit	*3.51*	*6*	*0.59*	*0.95*	*0.5444*	*not significant*
	Pure Error	*2.46*	*4*	*0.61*			
	Cor Total	123.14	12				
T 50%	Model	0.84	5	0.17	70.80	< 0.0001	significant
	A-X1	*0.66*	*1*	*0.66*	*275.59*	*< 0.0001*	
	B-X2	*0.062*	*1*	*0.062*	*26.16*	*0.0014*	
	AB	*2.500E-003*	*1*	*2.500E-003*	*1.05*	*0.3401*	
	A^2	*0.10*	*1*	*0.10*	*42.33*	*0.0003*	
	B^2	*0.035*	*1*	*0.035*	*14.49*	*0.0067*	
	Residual	0.017	7	2.386E-003			
	Lack of Fit	*7.585E-003*	*3*	*2.528E-003*	*1.11*	*0.4435*	*not significant*
	Pure Error	*9.120E-003*	*4*	*2.280E-003*			
	Cor Total	0.86	12				
Release at 12 h	Model	174.69	2	87.34	147.30	< 0.0001	significant
	A-X1	*171.51*	*1*	*171.51*	*289.24*	*< 0.0001*	
	B-X2	*3.18*	*1*	*3.18*	*5.36*	*0.0431*	
	Residual	5.93	10	0.59			
	Lack of Fit	*4.59*	*6*	*0.76*	*2.28*	*0.2219*	*not significant*
	Pure Error	*1.34*	*4*	*0.33*			
	Cor Total	180.62	12				

Table 3.11: Numerical test results of model adequacy checking for the 13 formulations of ranitidine HCl (150mg) matrix tablets prepared as per CCD

Response	Source	R-Squared	Adjusted R-Squared	Predicted R-Squared	Adequate precision	% CV
Y1	Quadratic	0.9793	0.9646	0.9103	24.880	6.92
Y2	Linear	0.9530	0.9436	0.9081	29.17	2.83
Y3	Linear	0.9583	0.9499	0.9157	30.99	0.68
Y4	Linear	0.9515	0.9418	0.9157	28.37	2.94
Y5	Quadratic	0.9806	0.9668	0.9209	24.45	1.33
Y6	Linear	0.9672	0.9606	0.9370	35.40	0.82

The adequacy of the models was also confirmed with residual plot tests of regression models. Two plots related to residuals namely the normal probability plot of residuals and the plot of internally studentized residuals versus predicted values were considered as additional tests of model adequacy checking tools. The normal probability plot is a graphical technique for assessing whether or not a data set is approximately normally distributed. The residual is the difference between the observed and the predicted value (or the fitted value) from the regression. If the points on the plot fall fairly close to the straight line then the data are normally distributed.

The normal probability plot of residuals and the plot of residuals versus predicted values of the responses for Y_1, Y_2, Y_3, Y_4, Y_5 and Y_6 are shown in the preceding figures. The results in Fig 3.13a, 14a, 3.15a, 3.16a, 3.17a, and 3.18a show that points or point clusters are placed closely to the diagonal line implying that the errors are distributed normally for the responses. Furthermore the residuals in Fig 3.13b, 2.14b, 3.15b, 3.16b, 3.17b, and 3.18b appear to be randomly scattered about zero. These results again indicate that the models satisfy the assumptions of the ANOVA.

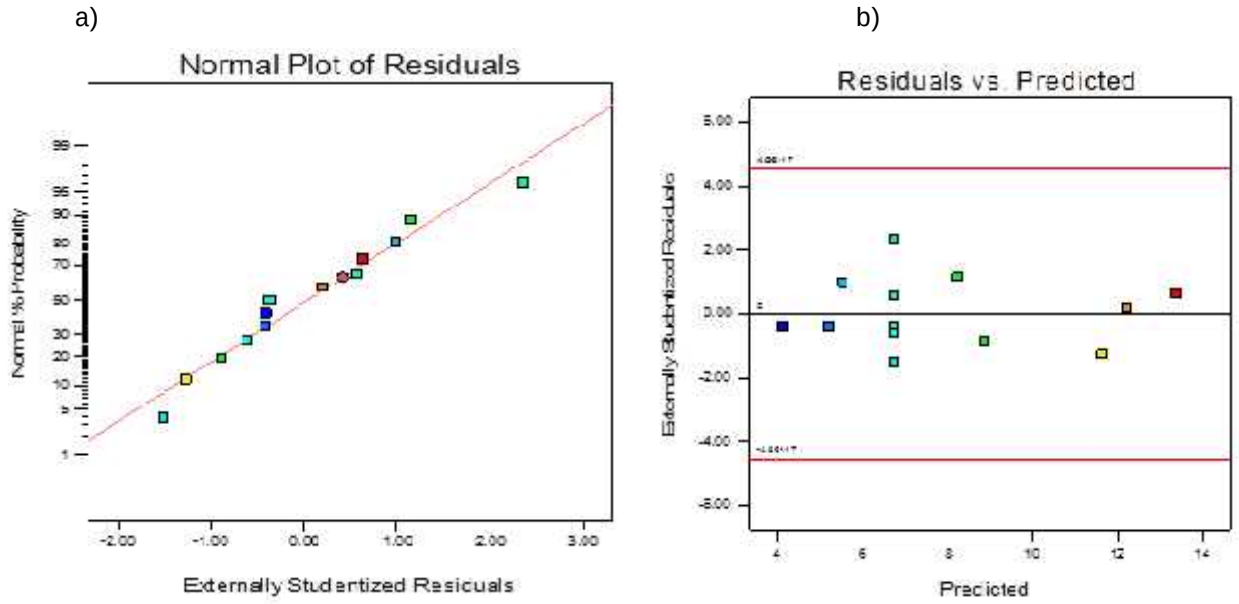


Fig 3.13: a) Normal probability plot of residuals b) plots of the residuals against predicted response for Y_1 (floating lag time) results of the 13 formulations of ranitidine HCl (150mg) prepared as per CCD

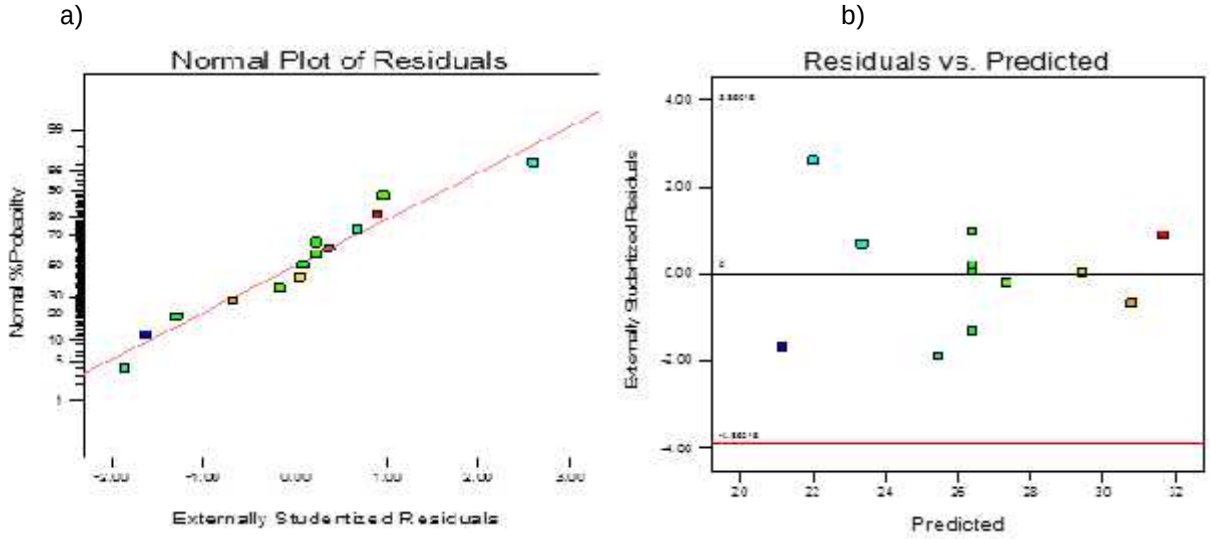


Fig 3.14: a) Normal probability plot of residuals b) plots of the residuals against predicted response for Y_2 (bioadhesive strength) results of the 13 formulations of ranitidine HCl (150mg) prepared as per CCD.

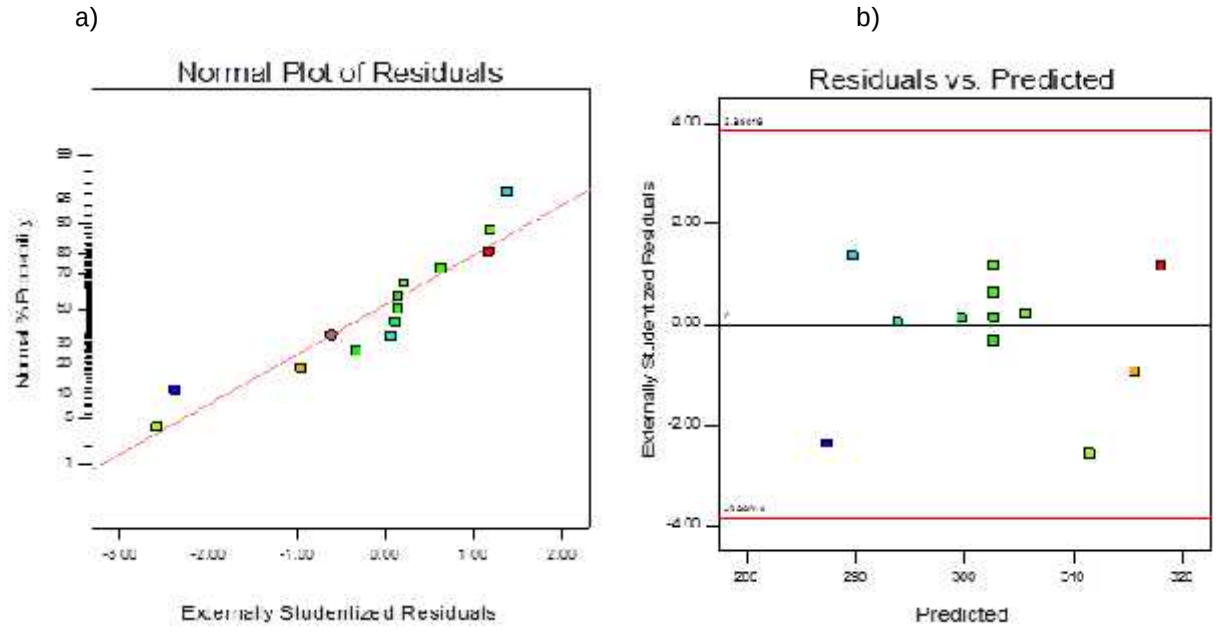


Fig. 3.15: a) Normal probability plot of residuals b) plots of the residuals against predicted response for Y_3 (swelling index) results of the 13 formulations of ranitidine HCl (150mg) prepared as per CCD.

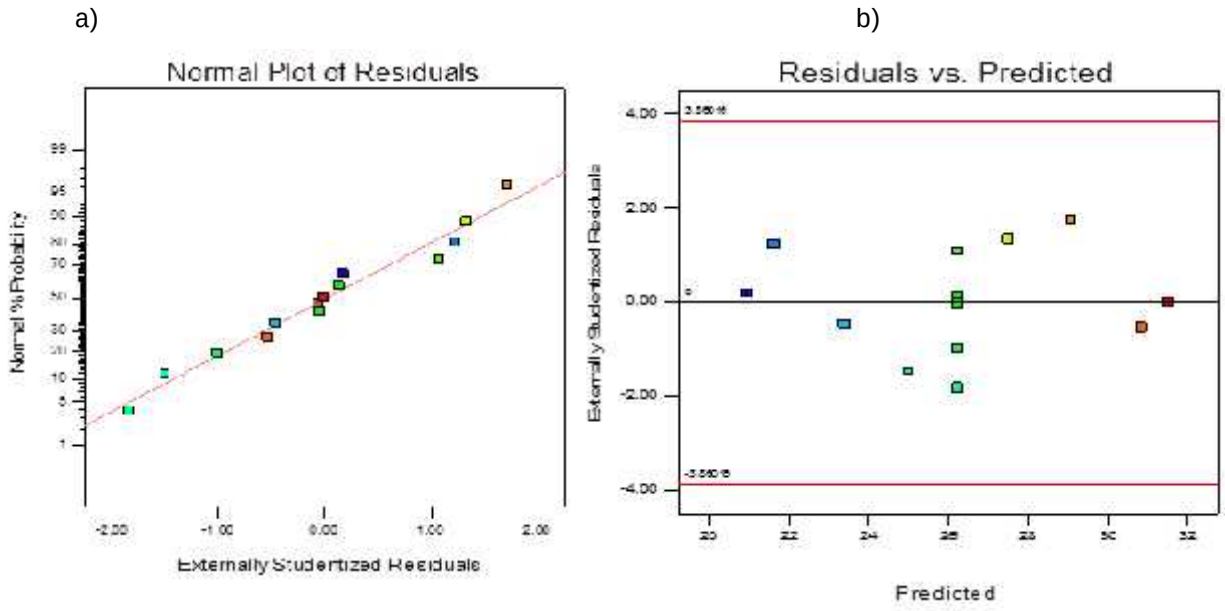


Fig 3.16: a) Normal probability plot of residuals b) plots of the residuals against predicted response for Y_4 (drug release at 1h) results of the 13 formulations of ranitidine HCl (150mg) prepared as per CCD.

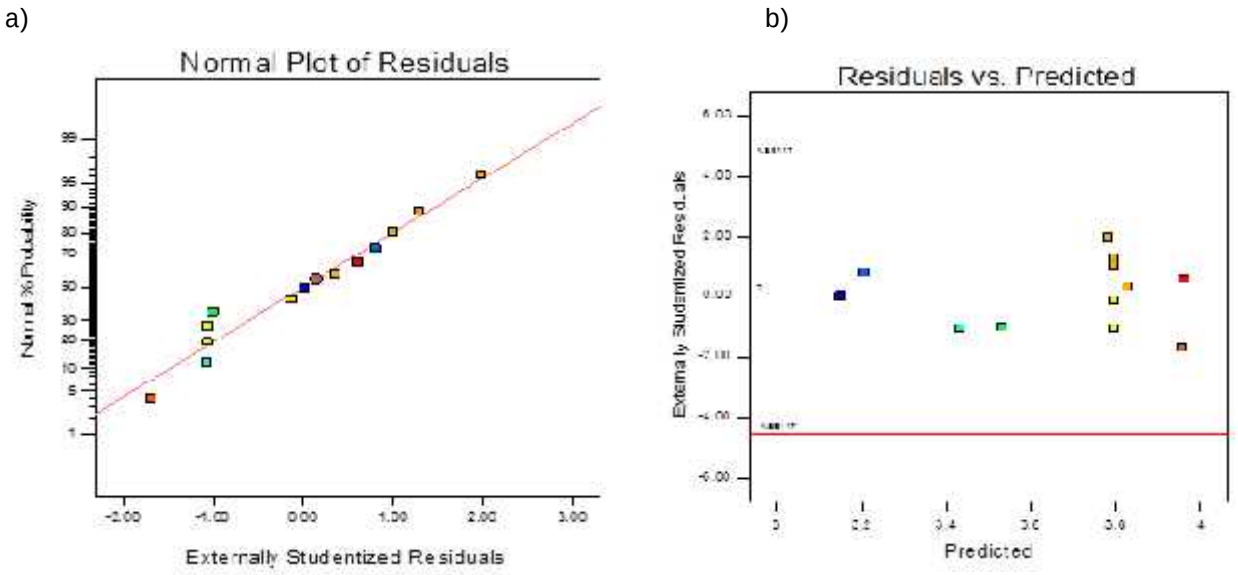


Fig 3.17: a) Normal probability plot of residuals b) plots of the residuals against predicted response for Y_5 (t50%) for results of the 13 formulations of ranitidine HCl (150mg) prepared as per CCD.

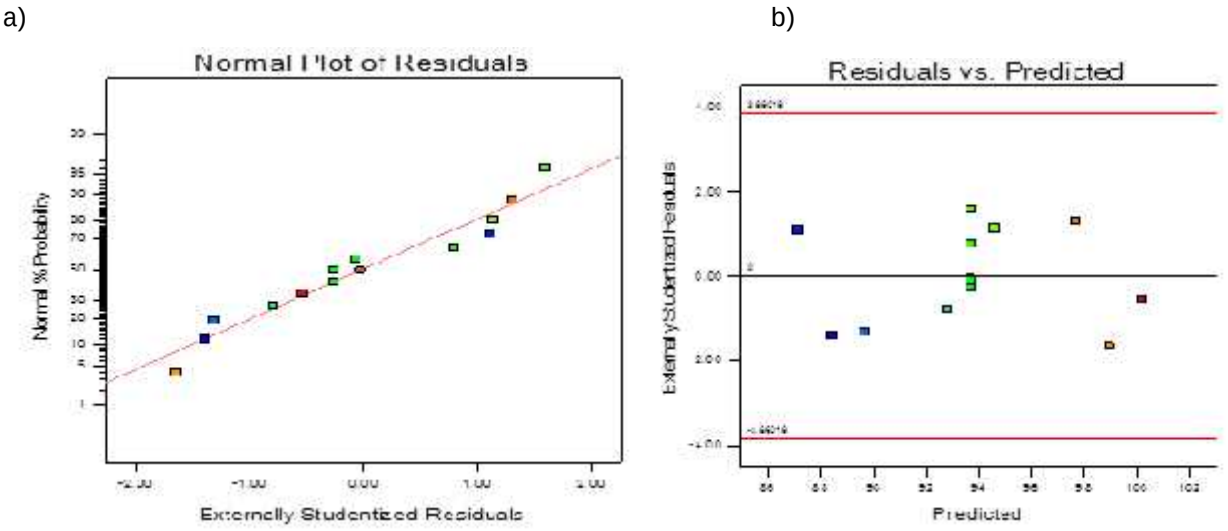


Fig 3.18: a) Normal probability plot of residuals b) plots of the residuals against predicted response for Y_6 (drug release at 12 h) results of the 13 formulations of ranitidine HCl (150mg) prepared as per CCD.

In order to determine the levels of factors which yield optimum responses, mathematical relationships were generated between the dependent and independent variables. The final equations in terms of coded factors (Eq. 3.1 to Eq. 3.6) were developed using model term coefficients shown in Table 3.12.

$$Y_1 = +6.76 - 0.63^* X_1 - 3.21^* X_2 - 0.03^* X_1X_2 + 0.49^* X_1^2 + 1.15^* X_2^2 \quad \text{Eq. 3.1}$$

$$Y_2 = +26.40 + 3.71^* X_1 - 0.67^* X_2 \quad \text{Eq. 3.2}$$

$$Y_3 = +302.69 + 10.86^* X_1 + 2.06^* X_2 \quad \text{Eq. 3.3}$$

$$Y_4 = +26.25 - 3.72^* X_1 + 0.88^* X_2 \quad \text{Eq. 3.4}$$

$$Y_5 = +3.80 + 0.29^* X_1 - 0.088^* X_2 + 0.025^* X_1 X_2 - 0.12^* X_1^2 - 0.071^* X_2^2 \quad \text{Eq. 3.5}$$

$$Y_6 = +93.70 - 4.63^* X_1 + 0.63^* X_2 \quad \text{Eq. 3.6}$$

The p-values were used as a tool to check the significance of each coefficient, which was necessary to understand the pattern of the mutual interactions between the best factors (Chen *et al.*, 2009). The smaller the p-value, the bigger the significance of the corresponding coefficient (Li *et al.*, 2007). A coefficient is the amount the response changes when that term is changed by one unit, while holding the other terms constant. Coefficients of developed models have physical meanings on response variables. Both the magnitude and sign of coefficients are important. The magnitude implies the strength whereas the sign indicates the direction of that factor variable on the corresponding response variable. A positive sign indicates a positive effect whereas a negative sign indicates a negative effect on the response [Singh *et al.*, 2010].

As seen in Eq. 3.1 to 3.6 and Table 3.12, Y_1 (floating lag time) was affected negatively by both the amount of polymer and amount of sodium bicarbonate. The second order interaction effect positively affected the floating lag time. Quadratic effects (X_1^2 and X_2^2) were found to have positive relationship with floating lag time. Response Y_2 (bioadhesive strength) was positively affected by polymer concentration and negatively affected by concentration of sodium bicarbonate; Y3 (swelling index) was affected positively by both the percentage of the polymer and percentage of sodium bicarbonate; Y_4 (drug release at first 1 h) and Y_6 (drug release at 12 h) were affected positively by the percentage of the $NaHCO_3$ and negatively by the percentage of polymer. Response Y_5 ($t_{50\%}$) was positively affected by polymer concentration and negatively

affected by concentration of sodium bicarbonate. The second order interaction positively affects this response while the quadratic effects (X_1^2 and X_2^2) were found to have negative relationship with it. From the coefficients, it is clear that the response Y_1 was strongly affected by the amount of $NaHCO_3$ than that of polymer; while responses Y_2-Y_6 were strongly affected by the amount of polymer than the amount of sodium bicarbonate.

Table 3.12: Estimated model term regression coefficients for the responses of the 13 formulations of ranitidine HCl (150mg) prepared as per CCD.

Response	Intercept	X_1	X_2	X_1X_2	X_1^2	X_2^2
Y1	6.76	-0.629981	-3.2152	-0.0325	0.494375	1.15438
p		0.0129	< 0.0001	0.9072	0.0458	0.0008
Y2	26.4023	3.70602	-0.669243			
p		< 0.0001	0.0298			
Y3	302.692	10.864	2.06066			
p		< 0.0001	0.0180			
Y4	26.2469	-3.72348	0.88423			
p		< 0.0001	0.0089			
Y5	3.796	0.286725	-0.0883363	0.025	-0.1205	-0.0705
p		< 0.0001	0.0014	0.3401	0.0003	0.0067
Y6	93.7	-4.63016	0.63033			
p		< 0.0001	0.0431			

3.2.7 Contour plot and surface response analysis

The 2D contour and 3D response surface plots are the graphical representations of the fitted regression models. These plots, presented on the basis of the model equations, display the interaction between the independent variables and assist in determining the optimum values of the variables within the ranges considered [Chen *et al*., 2009].

Contour plots (Fig 3.19a, 3.20a, 3.21a, 3.22a, 3.23a and 3.24a) and response surface plots (Fig 3.19b, 3.20b, 3.21b, 3.22b, 3.23b and 3.24b) for the obtained responses (Y_1, Y_2, Y_3, Y_4, Y_5 and Y_6) were drawn based on the model polynomial functions to assess the change of the response surface. These plots explain the relationship between the dependent and independent variables.

As can be seen from the plots, the results are in agreement with the ANOVA results indicated in Table 3.10. For example, the contour and response surface plots shown in Fig. 3.19a and 3.19b, respectively indicate the combined effect of X_1 (amount of HPMC/NaCMC polymer) and X_2 (amount of sodium bicarbonate) on the response Y_1 (floating lag time) of the formulations. As can be seen from these plots, the factors have non-linear relationship on Y_1. Both the factors affected the response; however, the effect of X_2 appeared to be more pronounced as compared to that of X_1. This was in agreement with the ANOVA results (Table 3.10), where X_2 showed more significant effect ($p < 0.0001$) than X_1 ($p = 0.2117$) on Y_1. The contribution of the second order terms from Eq. 3.1 and Table 3.12 was interpreted as the presence of curvature in the plots.

The contour and response surface plots shown in Fig. 3.20a and 3.20b, respectively, indicate the combined effect of the two factors X_1 and X_2 on the response variable, Y_2 (bioadhesive strength) of the formulations. The series of parallel straight lines of the contour plot and the non-twisted response surface indicate that there was no interaction effect of the two parameters on Y_2. The plots show that the linear model components individually affect Y_2, with comparatively a more significant effect by X_1. The same is indicated in the ANOVA results (Table 3.12), where X_1 showed more significant effect ($p < 0.0001$) than X_2 ($p = 0.0298$) on Y_2. In the same way, the counter and response plots shown in Fig 3.21 to Fig 3.24 for the remaining response variables (Y_3, Y_4, Y_5 and Y_6) were consistent with their ANOVA results indicated in Table 3.10.

a) b)

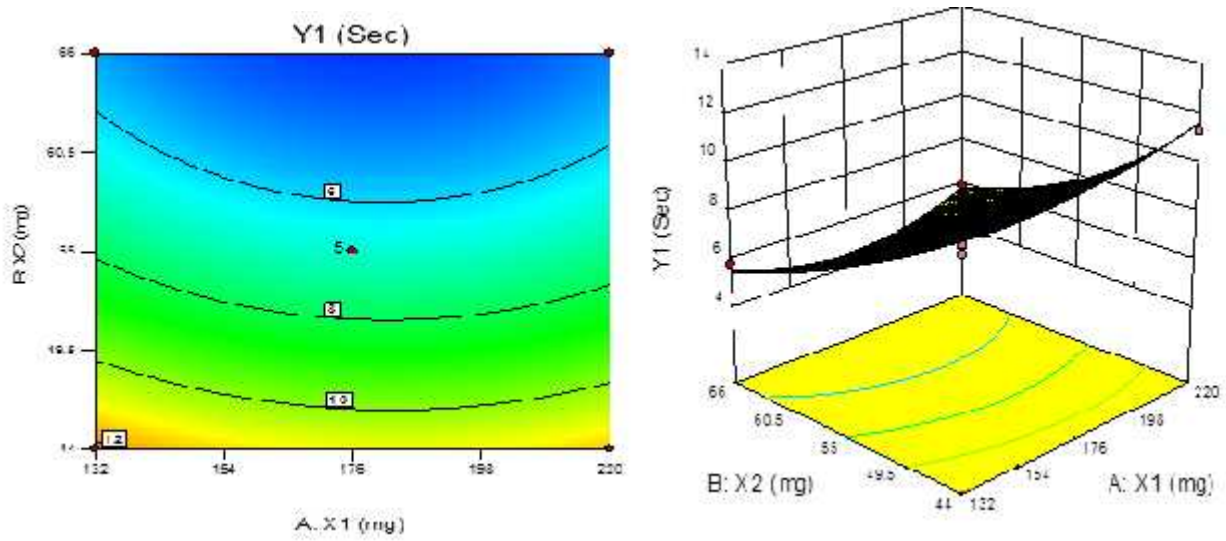


Fig 3.19: a) Contour plot and b) response surface plot showing the effect of X_1 (amount of polymer) and X_2 (amount of sodium bicarbonate) on Y_1 (floating lag time) for the 13 formulations of ranitidine HCl (150mg) prepared as per CCD.

a) b)

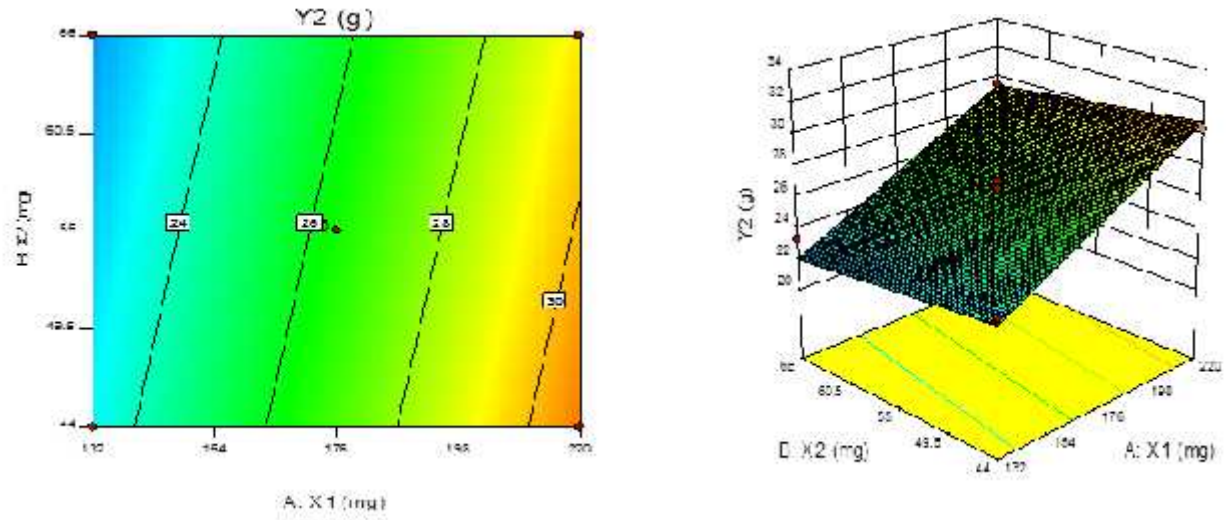


Fig 3.20: a) Contour plot b) response surface plot showing the effect of X_1 (amount of polymer) and X_2 (amount of sodium bicarbonate) on Y_2 (bioadhesive strength) for the 13 formulations of ranitidine HCl (150mg) prepared as per CCD.

a) b)

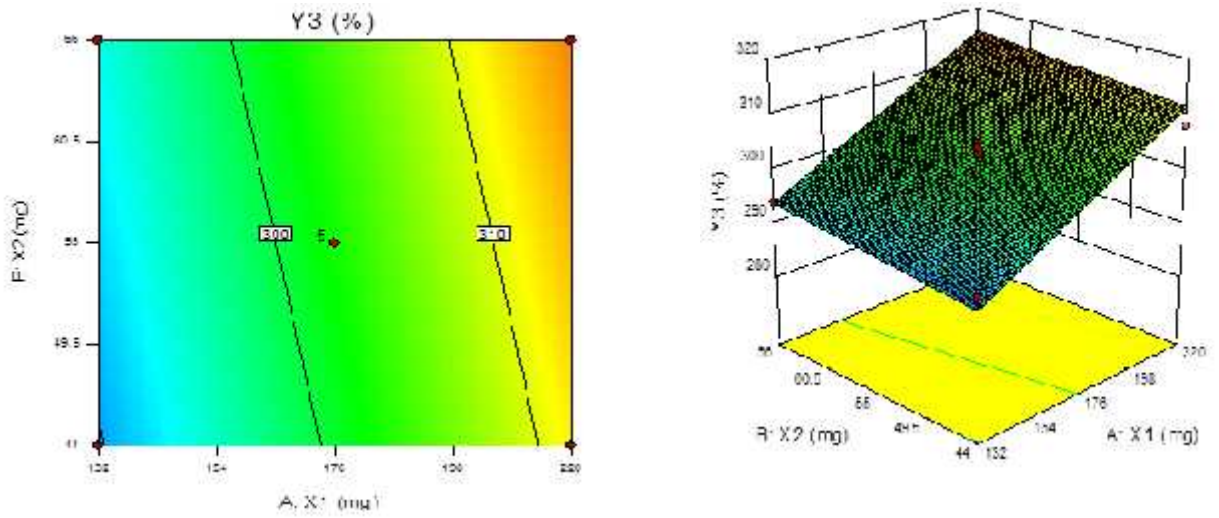


Fig 3.21: a) Contour plot b) response surface plot showing the effect of X_1 (amount of polymer) and X_2 (amount of sodium bicarbonate) on Y_3 (maximum swelling index) for the 13 formulations of ranitidine HCl (150mg) prepared as per CCD.

a) b)

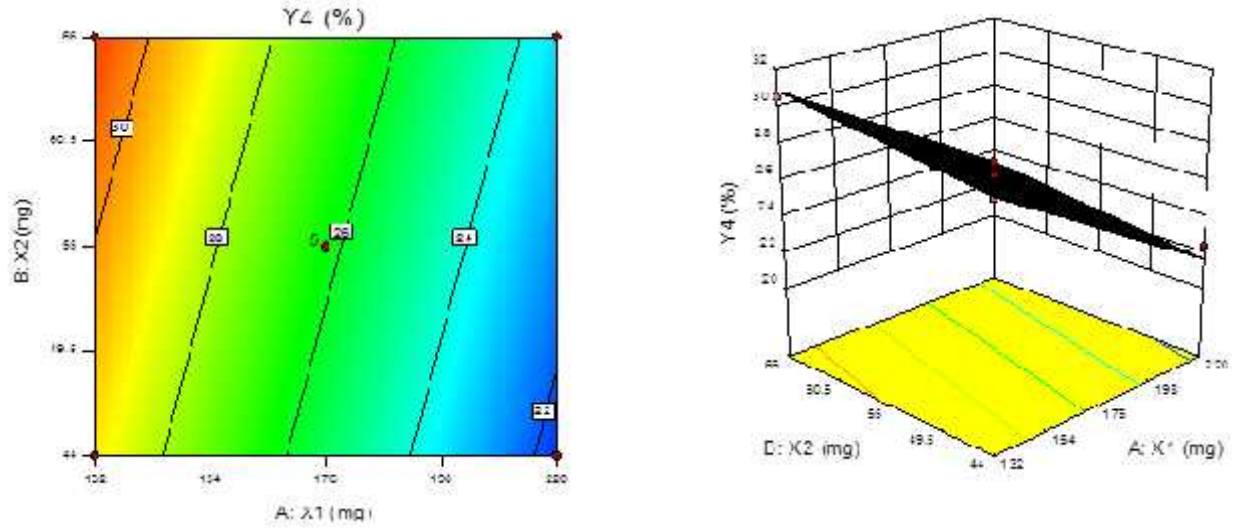
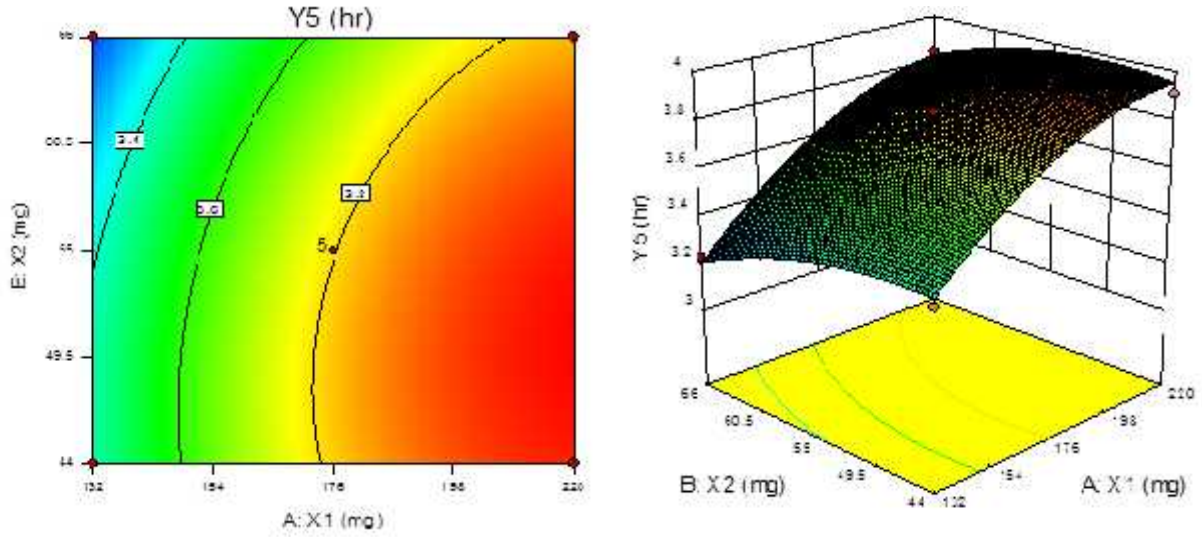


Fig 3.22: a) Contour plot b) response surface plot showing the effect of X_1 (amount of polymer) and X_2 (amount of sodium bicarbonate) on Y_4 (drug release at 1 h*)* for the 13 formulations of ranitidine HCl (150mg) prepared as per CCD.

a) b)



.

Fig 3.23: a) Contour plot b) response surface plot showing the effect of X_1 (amount of polymer) and X_2 (amount of sodium bicarbonate) on Y_5 (time to 50% drug release) for the 13 formulations of ranitidine HCl (150mg) prepared as per CCD.

a) b)

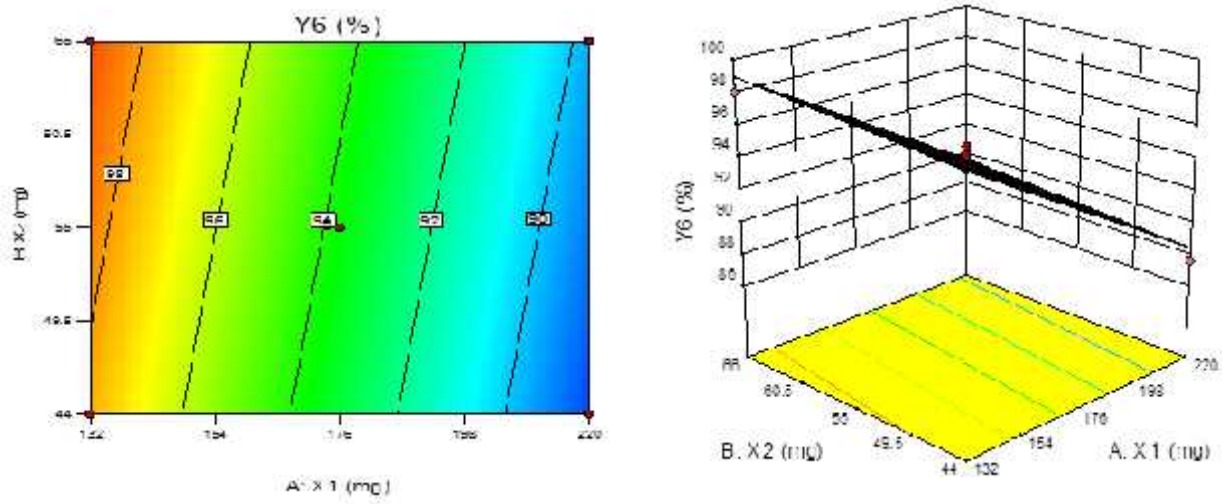


Fig 3.24: a) Contour plot b) response surface plot showing the effect of X_1 (amount of polymer) and X_2 (amount of sodium bicarbonate) on Y_6 (drug release at 12 h) for the 13 formulations of ranitidine HCl (150mg) prepared as per CCD.

3.2.8 Simultaneous optimization of response variables

After generating the model polynomial equations to relate the dependent and independent variables, the formulation was optimized for the six responses (floating lag time, bioadhesive sterngth, swelling index, drug release at 1 h, $t_{50\%}$ and drug release at 12 h) simultaneously. The final optimal experimental parameters were obtained using both numerical and graphical optimization techniques of Design-Expert 10.0.7.0 software, which allows compromise among various responses and searches for a combination of factor levels that jointly optimize a set of responses by satisfying the requirements for each response in the set. Table 3.13 presents the criteria defined for factors and responses during optimization with both numerical and graphical techniques.

Table 3.13: Constraints for factors and responses used during numerical and graphical optimization for the 13 formulations of ranitidine HCl (150mg) prepared as per CCD.

Factor constraints				
Factor	Low	High		
HPMC/NaCMC (3:1) (mg)	132	220		
$NaHCO_3$ (mg)	44	66		
Response constraints				
Response	Goal	Lowe limit	Upper limit	Importance
Floating lag time (sec)	Minimize	4	13.4	3
Bioadhesive strength (g)	Maximize	23	30	3
Swelling index (%)	In range	284	320	3
Drug release at 1h (%)	Minimize	21.1	31.5	3
Time to 50% release (h)	Maximize	3.15	3.98	3
Drug release at 12 h (%)	In range	90	100	5

3.2.8.1 Numerical optimization

The desirability function approach is one of the most widely used methods for optimization of multiple responses. Overall desirability function is a measure of how well the combined goals for all responses are satisfied. Desirability function ranges from 0 to 1, with value closer to one indicating a higher satisfaction of response goal(s). Table 3.14 shows the predicted optimum values according to the set goals. In this study, a total of 9 results were obtained and among these one with the overall desirability of 0.856 was selected by the software. The 3D plot of the overall desirability function is shown in Fig 3.25.

Table 3.14: Numerical optimization results of predicted optimum values for the 13 formulations of ranitidine HCl (150mg) prepared as per CCD.

Number	X_1	X_2	Y_1	Y_2	Y_3	Y_4	Y_5	Y_6	Desirability	
1	214.546	61.216	5.123	29.271	313.374	23.485	3.895	90.000	0.856	Selected
2	214.499	61.131	5.138	29.272	313.347	23.482	3.896	90.000	0.856	
3	214.592	61.301	5.108	29.269	313.401	23.488	3.894	90.000	0.856	
4	214.693	61.487	5.077	29.267	313.461	23.494	3.891	90.000	0.856	
5	214.331	60.821	5.193	29.277	313.247	23.471	3.899	90.000	0.856	
6	214.842	61.761	5.031	29.263	313.549	23.503	3.888	90.000	0.856	
7	213.830	59.902	5.368	29.290	312.951	23.440	3.910	90.000	0.855	
8	213.559	59.405	5.469	29.298	312.791	23.423	3.915	90.000	0.854	
9	215.765	63.456	4.782	29.237	314.095	23.562	3.865	90.000	0.853	

3.2.8.2 Graphical optimization

The region of optimized formulation was also ratified using overlay plot. Based on the criteria indicated in Table 3.13, the overlay plot (Fig 3.26) was drawn in which the yellow area represents the area satisfying the imposed criteria. The point identified by the flag was one of the solutions given by the software (same solution shown in Table 3.14).

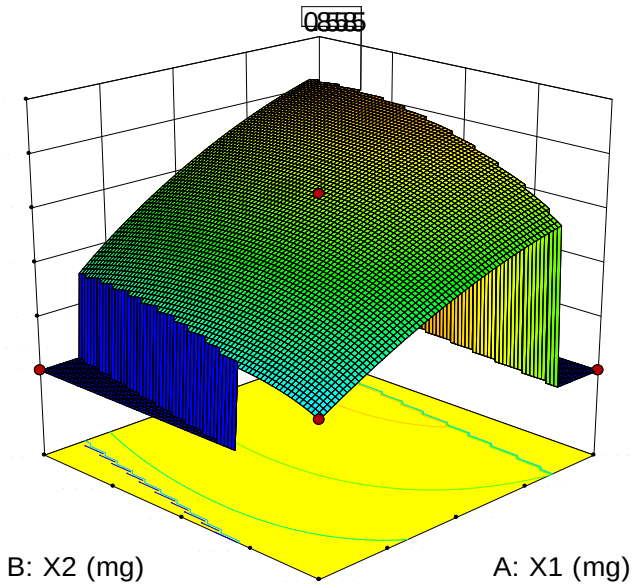


Fig 3.25: 3D plot of the overall desirability function**.**

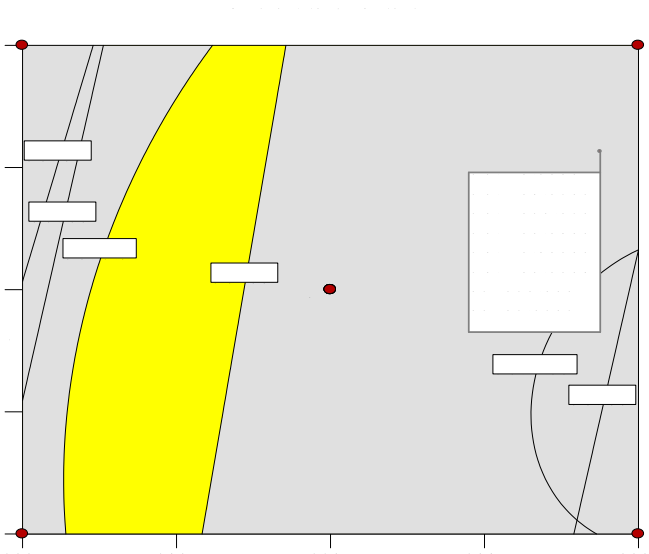


Fig 3.26: Overlay plot of the six responses as functions of dependent variables for the 13 formulations of ranitidine HCl (150mg) prepared as per CCD.

3.2.9 Evaluation and validation of the optimized formulation

3.2.9.1 Evaluation of optimized formulation

The optimized formulation was evaluated for its powder and tablet properties. The results are presented in Table 3.15. As shown in the table, the angle of repose, Hausner ratio and Carr's index values were 29.35 ± 0.63^0, 1.09 ± 0.03 and $10.04 \pm 0.02\%$, respectively, indicating that the powder blend of the optimized formulation has excellent flow property. The tablets showed low friability (0.25%), acceptable drug content value (99.06 ± 0.00) and were intact and floated for more than 12 h with floating lag time of 5.09 ± 0.04 sec. The bioadhesive strength was 29.69 ± 0.05 g and the maximum swelling index was $315.04 \pm 0.12\%$.

Table 3.15: Density and related properties of the optimized powder blend and tablet formulation of Ranitidine HCl (15 mg).

Parameters	**Experimental results**
Powder properties	
Bulk density (g/cm3)	0.29 ± 0.01
Tapped density (g/cm3)	0.33 ± 0.00
Flow rate (g/sec)	3.62 ± 0.12
Carr's Index (%)	10.04 ± 0.02
Hausner ratio	1.09 ± 0.03
Angle of repose (^{0})	29.35 ± 0.63
Tablet properties	
Hardness (N)	65.32 ± 0.04
Thickness (mm)	3.95 ± 0.02
Friability (%)	0.25
Assay (%)	99.06 ± 0.00
Matrix integrity	Intact
Floating lag time (sec)	5.09 ± 0.04
Floating duration (h)	> 12
Bioadhesive strength (g)	29.69 ± 0.05
Ex vivo mucoadhesion time (h)	> 12 h
Maximum swelling index (%)	315.04 ± 0.12

In vitro dissolution study was carried out on the optimized formulation using three different batches (Figure 3.27). The results indicate that there was no significant difference in the release properties among the three batches; leading to the conclusion that the optimal formulation had reproducible results.

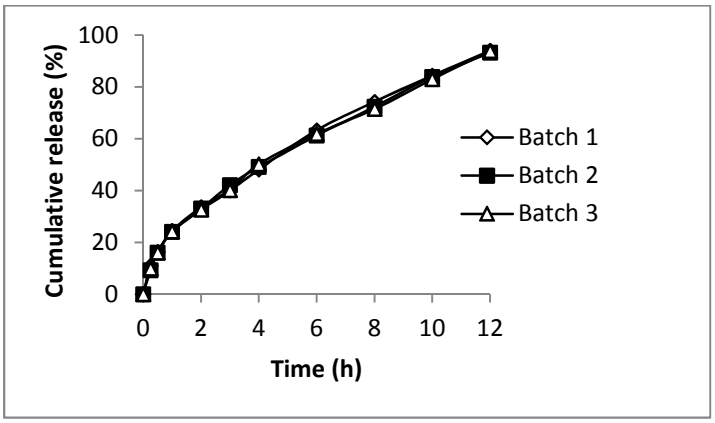


Fig 3.27: Release profile of optimized formulation of ranitidine HCl (150mg) matrix tablets

Table 3.16 shows the release kinetics and release mechanisms for the optimized formulation. Release kinetics study revealed that Higuchi square root model was the best fit model with R^2 > 0.996. The drug release mechanism from the optimized formulation was also evaluated using the Korsmeyer-Peppas model at 60% release and the results showed that n value ranges from 0.55 to 0.58 indicating drug release from the optimized formulation follows non-Fickian diffusion release mechanism.

Table 3.16: Release kinetics and release mechanism results for the optimized formulation of ranitidine HCl (150) mg matrix tablets**.**

Formulation code	Model										
	Zero order		First order		Higuchi		Hixson-Crowell		Korsmeyer-Peppas		
	K_o	R^2	K_1	R^2	K_H	R^2	K_{HC}	R^2	K_o	R^2	n
Batch 1	7.09	0.9555	-0.08	0.9751	26.57	0.9963	0.20	0.9925	0.562	0.9953	0.55
Batch 2	7.15	0.9528	-0.08	0.9755	26.83	0.9966	0.20	0.9922	0.575	0.9969	0.58
Batch 3	7.14	0.9528	-0.07	0.9755	26.65	0.9965	0.19	0.9922	0.574	0.9945	0.58

3.2.9.2 Validation of the optimized formulation

To experimentally confirm the validity of obtained optimal formulation, confirmation experiments were carried out in triplicate at the optimal combinations of the factors (X_1 = 214.55 mg, X_2 =61.22 mg). Table 3.17 provides the predicted values, experimental results and the percentage error values obtained at optimal levels of the factors. As seen in the table, the values of percentage errors had fallen within about 5% and this confirmed that the experimental values of the optimized formulations agreed well with the predicted values.

Table 3.17: Response values of predicted, experimental and percentage error obtained at optimal levels of the factors.

Response	Predicted value	Experimental value	% Error
FLT (Y_1)	5.12	5.09	-0.59
Bioadhesive strength (Y_2)	29.27	29.69	1.30
Max Swelling index (Y_3)	313.37	315.04	0.53
Rel 1h (Y_4)	23.48	24.21	3.11
t50% (Y_5)	3.89	3.86	-0.77
Rel 12 h (Y_6)	90.00	93.65	4.06

3.3 Drug-excipient compatibility studies

Fig. 3.28, 3.29, 3.30 and 3.31 depict the IR spectra of excipients, pure ranitidine HCl, optimized formulation and overlay of ranitidine HCl and the optimized formulation respectively. The characteristic peaks of ranitidine HCl are observed at the same wavenumber in both the pure ranitidine HCl and the optimized formulation, indicating that there was no interaction between the drug and excipients. The bands around 3247 and 3180 cm^{-1} are assigned to the symmetric stretching peaks of NH and those around 3066 cm^{-1} are due to the C-H stretching in the furan ring. The bands around 1304 and 1263 cm^{-1} are due to the C-N stretching. The bands at around 1618 are due to NH bending. The bands at around 1589 cm^{-1} correspond to the C=C stretching vibrations and those at around 1045, 1022 cm^{-1} are assigned to the C-C in plane bending vibrations. The peaks around 1163 cm^{-1} are due to C-O stretching vibrations. The bands at around 760, 692, 640 cm^{-1} are assigned due to C-S stretching modes of vibration. Furthermore, the bands at around 1560 cm^{-1} are due to the N–O asymmetric stretch [Ramesh et al., 2015].

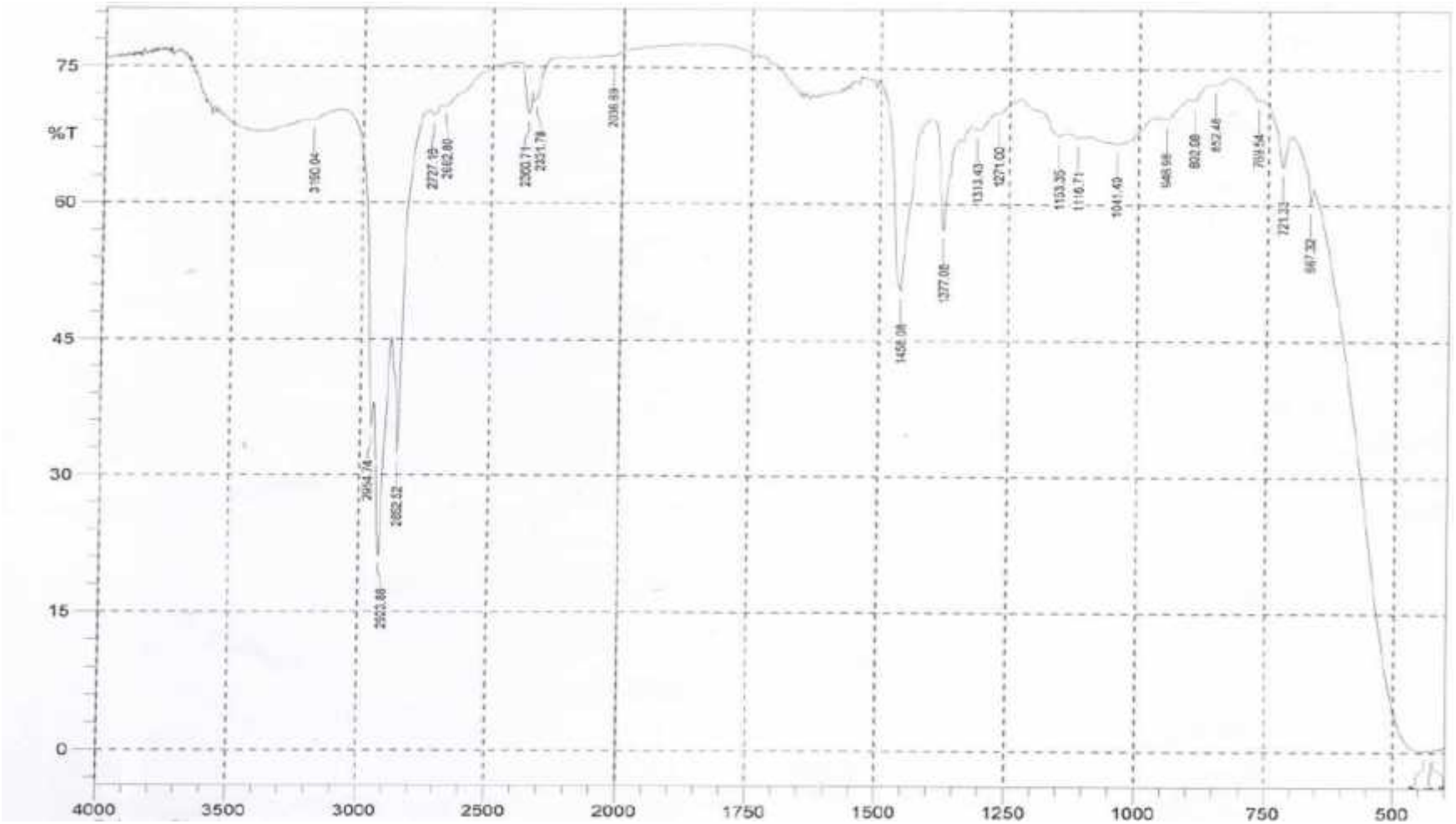


Fig 3.28: FTIR spectrum of excipients used in the optimized formulation.

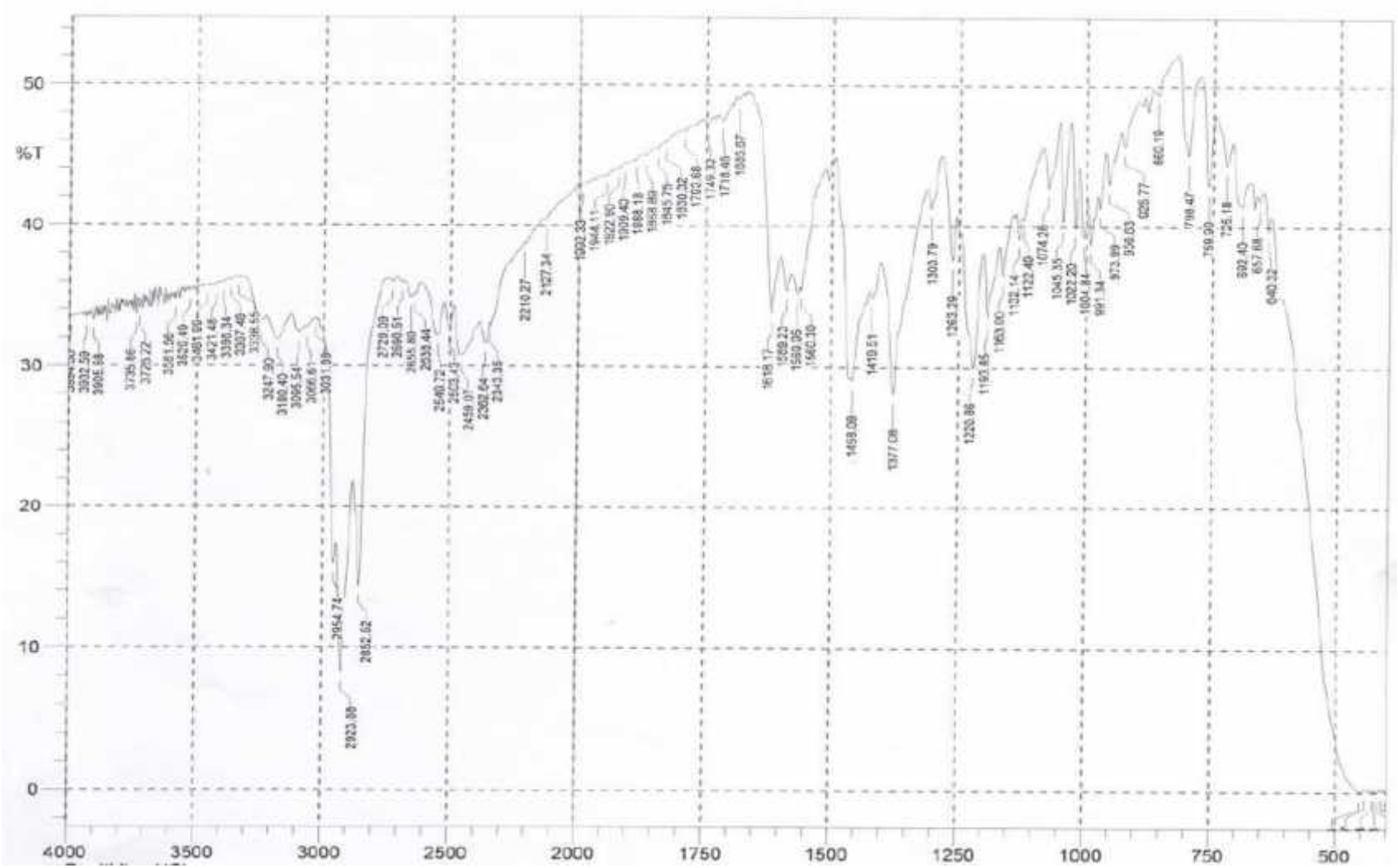


Fig 3.29: FTIR spectrum of pure ranitidine hydrochloride.

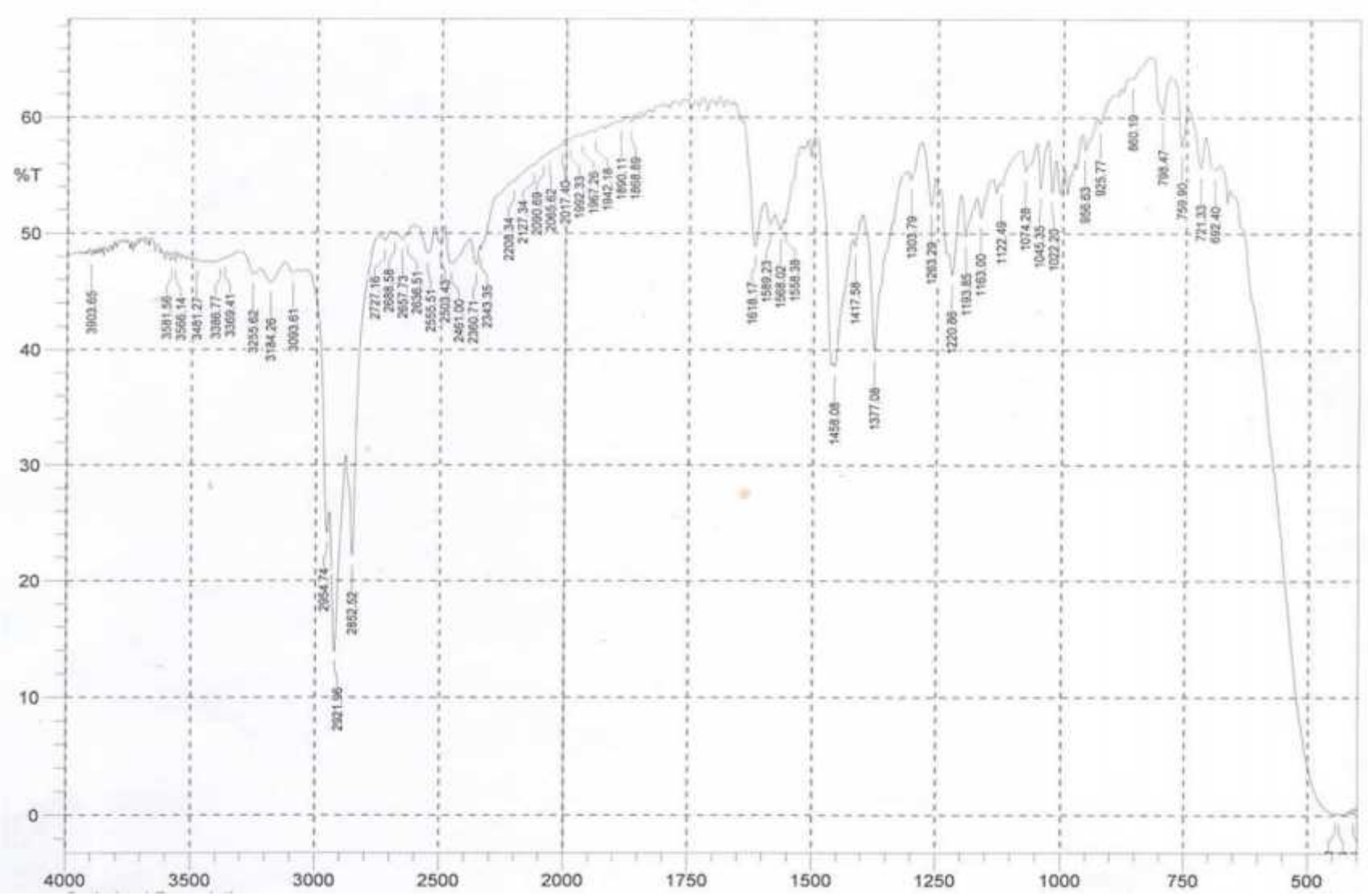


Fig 3.30: FTIR spectrum of optimized formulation of ranitidine HCl (150mg) matrix tablets.

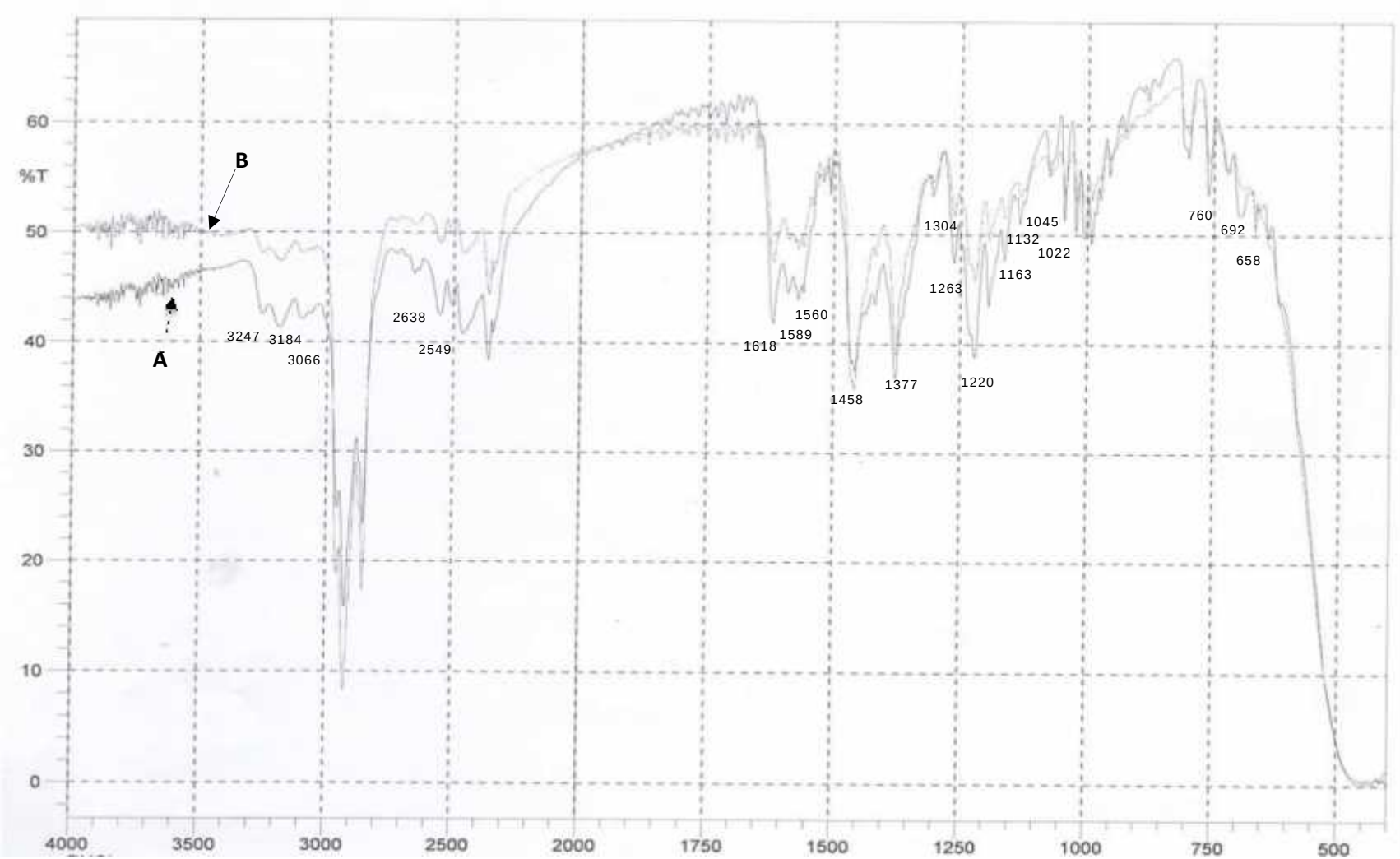


Fig 3.31: FTIR spectrum overlay plot of (A) ranitidine HCl and B) optimized formulation of ranitidine HCl (150mg) matrix tablets showing characteristic bands of ranitidine HCl at the same wavenumber.

4. CONCLUSION

From the foregoing, it is apparent that floating, bioadhesive and swellable matrix tablets of ranitidine HCl, prepared by direct compression using HPMC and NaCMC (as release retarding polymers) and $NaHCO_3$ (as gas generating agent), exhibited *in vitro* sustained drug release profile over the study period of 12 h.

The preliminary studies indicated that factors such as viscosity grade of HPMC, concentration of polymer, HPMC/NaCMC ratio, and concentration of $NaHCO_3$ affect the floating, bioadhesive, swelling and *in vitro* release properties of the matrix tablets. The two polymers (HPMC and NaCMC) exhibited synergistic effect in sustaining drug release from the matrix.

The concentration of polymer and $NaHCO_3$ were found to be the critical factors for floating, bioadhesive, swelling and drug release properties of the matrix tablets. The RSM based on CCD provided the optimum concentration of polymer blend HPMC/NaCMC (3:1) at 214.55mg (46.64%) and $NaHCO_3$ at 61.22mg (13.31%) with respect to floating lag time, bioadhesive strength, maximum swelling index, cumulative drug release at 1 h, $t_{50\%}$ and cumulative drug release at 12 h. The experimental values of the matrix tablets under the optimum concentrations were close to the predicted values.

The drug release profile of the optimized formulation followed Higuchi square root kinetic model with non-Fickian diffusion release mechanism. The FT-IR spectra showed no incompatibility between ranitidine HCl and the excipients.

Therefore, based on the *in vitro* studies, the optimized matrix tablet formulation may improve the bioavailability of oral ranitidine HCl and overcome the associated variability among individuals.

5. SUGGESTIONS FOR FURTHER WORK

As a follow up of the current work, the following studies are suggested:

- Accelerated and long term stability studies of the matrix tablets, and
- *In vivo* performance of the matrix tablets in animal models and humans.

REFERENCES

Adhikary A., Vavia R. P., 2008. Bioadhesive Ranitidine Hydrochloride for Gastroretention with Controlled Microenvironmental pH. Drug Development and Industrial Pharmacy. **34**: 860-869

Ali, J., Arora, S., Ahuja, A., Babbar, A.K., Sharma, R.K., Khar, R.K., Baboota, S., 2007. Formulation and development of hydrodynamically balanced system for metformin: *in vitro* and *in vivo* evaluation. Eur. J. Pharm. Biopharm. **67**: 196–201

Aouam K., Bouida W., Fredj B.N; Chaabane A.; Boubaker H.; Boukef R.; Boughattas N.A; Nouira S., 2011. Case Report: Severe ranitidine-induced anaphylaxis: a case report and literature review J. Clin. Pharm. Ther. **37**: 494-496.

Babu, V.B., and Khar, R.K., 1990. *In vitro* and *in vivo* studies of sustained-release floating dosage forms containing salbutamol sulfate. Pharmazie **45**: 268-270.

Bardonnet, P. L., Faivre, V., Pugh, W. J., Piffaretti, J. C., and Falson, F., 2006. *Gastroretentive dosage forms: overview and special case of Helicobacter pylori*, J Control Release **111:** 1–18.

Basit, A. 2001. Colonic metabolism of ranitidine: implications for its delivery and absorption. Int. J. Pharm. **227**: 157-165.

Bennink, R., Peeters, M., Maegdenbergh, V. V., Geypens, B., Rutgeerts, P., Roo, D. M., and Mortelmans, L., 1998. Comparison of total and compartmental gastric emptying and antral motility between healthy men and women, Eur J Nucl Med. **25:** 1293–1299.

Bertram U. and Bodmeier R., 2012. Effect of polymer molecular weight and of polymer blends on the properties of rapidly gelling nasal inserts. Drug Development and Industrial Pharmacy. **38**: 659–669.

Biswas M., Gupta N.R., Parhi R, Sethi K.K., Sahoo K.S., 2013. Formulation and *in vitro* evaluation of gastroretentive floating drug delivery system of ritonavir. Turk J Pharm Sci. **10**: 69-86.

Boyle, R., Behan, P. O., and Sutton, J. A., 1990. A correlation between severity of migraine and delayed gastric emptying measured by an epigastric impedance method, Br J Clin Pharmacol. **30:** 405–409.

Brennan, I. M., Feltrin, K. L., Nair, N. S., Hausken, T., Little, T. J., Gentilcore, D., Wishart, J. M., Jones, K. L., Horowitz, M., and Feinle-Bisset, C., 2009. Effects of the phases of the menstrual cycle on gastric emptying, glycemia, plasma GLP-1 and insulin, and energy intake in healthy lean women, Am J Physiol - Gastroint Liver Physiol. **297:** G602–G610.

Camilleri, M., Malagelada, J. R., Brown, M. L., Becker, G., and Zinsmeister, A. R., 1985. Relation between antral motility and gastric emptying of solids and liquids in humans, Am J Physiol. **249**: G580–G585.

Charman, W. N., Porter, C. J. H., Mithani, S., and Dressman, J. B., 1997. Physicochemical and physiological mechanisms for the effects of food on drug absorption: the role of lipids and pH, J Pharm Sci, **86**: 269–282.

Chavanpatil, M.D., Jain, P., Chaudhari, S., Shear, R., Vavia, P.R., 2006. Novel sustained release, swellable and bioadhesive gastroretentive drug delivery system for ofloxacin. Int. J. Pharm. **316**: 86–92.

Chen C.X., Bai J.X., Cao J.M., Li Z.J., Xiong J., Zhang L., Hong Y., Ying H.J., 2009. Medium optimization for the production of cyclic adenosine 30 ,50 -monophosphate by Microbacterium sp. no. 205 using response surface methodology. Bioresource Technology **100**: 919–924.

Chen Y.H, Yaung J.F., 2002. Alka Seltzer fizzing- determination of percent by mass of $NaHCO_3$ in alka seltzer tablets. J Chem Ed. **79**:848–50.

Choi, B.Y., Park, H.J., Hwang, S.J., Park, J.B., 2002. Preparation of alginate beads for floating drug delivery system: effects of CO(2) gas-forming agents. Int. J. Pharm. **239:** 81–91.

Chopra D., Arora P., Khan S., Dwivedi S., 2014. Anaphylaxis following intravenous ranitidine: A rare adverse reaction of a common drug. **46**: 234-236.

Clarke, G.M., Newton, J.M., Short, M.D., 1993. Gastrointestinal transit of pellets of differing size and density. Int. J. Pharm. **100:** 81-92.

Colombo P., Bettini R., Peppas N.A., 1999. Observation of swelling process and diffusion front position during swelling in hydroxypropyl methyl cellulose (HPMC) matrices containing a soluble drug. Journal of Controlled Release **61:** 83–91

Datz, F. L., Christian, P. E., and Moore, J., 1987. Gender-related differences in gastric emptying, J Nucl Med, **28:** 1204–1207.

Dash S., Murthy N.P., Nath L. And Chowdhury P., 2010. Kinetic modeling on drug release from controlled drug delivery systems. Acta Poloniae Pharmaceutica - Drug Research, Vol. **67:** 217-223.

Desai, S., Bolton, S., 1993. A Floating Controlled-Release Drug Delivery System: In Vitro-*in Vivo* Evaluation. Pharm. Res. **10:**1321-1325.

Dave B. S., Amin A. F., and Patel M. M., 2004. Gastroretentive drug delivery system of ranitidine hydrochloride: formulation and *in vitro* evaluation, AAPS Pharm Sci Tech, **5:** 77–82.

Davis, S. S., Hardy, J. G., and Fara, J. W., 1986. Transit of pharmaceutical dosage forms through the small intestine, Gut, **27:** 886–892.

Davies, W. T., Kirkpatrick, J. R., Owen, G. M., and Shields, R., 1971. Gastric emptying in atrophic gastritis and carcinoma of the stomach, Scan J Gastroentero, **6:**297–301.

Deshpande, A.A., Rhodes, C.T., Shah, N.H., Malick, A.W., 1996. Controlled-Release Drug Delivery Systems for Prolonged Gastric Residence: An Overview. Drug Dev. Ind. Pharm. **22**: 531-539.

Devereux J. E., Newton J. M., and Short M. B., 1990. The influence of density on the gastrointestinal transit of pellets, J Pharm Pharmacol, **42:**500–501.

Devlin, M. J., Kissileff, H. R., Zimmerli, E. J., Samuels, F., Chen, B. E., Brown, A. J., Geliebter, A., and Walsh, B. T., 2012. Gastric emptying and symptoms of bulimia nervosa: effect of a prokinetic agent, Physiol Behav, **106:**238–242.

Dooley, C. P., Lorenzo, C. D., and Valenzuela, J. E., 1992. Variability of migrating motor complex in humans, Dis Dis sci, **37:** 723–728.

Dorozynski, P., Jachowicz, R., Kulinowski, P., Kwiecinski, S., Szybinski, K., Skorka, T., Jasinski, A., 2004. The polymers for the preparation of hydrodynamically balanced systems – methods of evaluation, Drug Dev. Ind. Pharm. **30** : 947–957.

Dressman, J. B., Berardi, R. R., Dermentzoglou, L. C., Russell, T. L., Schmaltz, S. P., Barnett, J. L., and Jarvenpaa, K. M., 1990. Upper gastrointestinal (GI) pH in young, healthy men and women, Pharmaceut Res, **7**: 756–761.

Eberle, V. A., Schoelkopf, J., Gane, P. A. C., Alles, R., Huwyler, J., and Puchkov, M., 2014. Floating gastroretentive drug delivery systems: comparison of experimental and simulated dissolution profiles and floatation behavior, Eur J Pharm Sci, **58**: 34–43.

Feldman M., Smith H. J., and Simon T. R., 1984. Gastric emptying of solid radiopaque markers: studies in healthy subjects and diabetic patients, Gastroenterology, **87:** 895–902.

Fell J. T., 1996. Targeting of drugs and delivery systems to specific sites in the gastrointestinal tract, J Anat, 189; p. 517.

Fujimori, J., Machida, Y., Tanaka, S., and Nagai, T., 1995. Effect of magnetically controlled gastric residence of sustained release tablets on bioavailability of acetaminophen, Int J Pharm, **119:** 47–55.

Gaginella S.T.; Bauman H.J, 1983.Ranitidine hydrochloride; Drug Intell. Clin. Pharm., **17:** 873-885.

Goole J., Vanderbist F., Amighi K., 2007. Development and evaluation of new multiple-unit levodopa sustained-release floating dosage forms. International Journal of Pharmaceutics **334:** 35–41

Goo R. H., Moore J. G., Greenberg E., and Alazraki N. P., 1987. Circadian variation in gastric emptying of meals in humans, Gastroenterology, **93:** 515–518.

Gröning R. and Berntgen M., 1996. Estimation of the gastric residence time of magnetic dosage forms using the Heidelberg capsule, Pharmazie, **51:** 328–331.

Gröning R., Berntgen M., and Georgarakis M., 1998. Acyclovir serum concentrations following peroral administration of magnetic depot tablets and the influence of extracorporal magnets to control gastrointestinal transit, Eur J Pharm Biopharm, **46:** 285–291.

Gröning, R., Cloer, C., Georgarakis, M., Müller, R.S., 2007. Compressed collagen sponges as gastroretentive dosage forms: *In vitro* and *in vivo* studies. Eur. J. Pharm. Sci. **30:** 1-6.

Gunjal T. P., Shinde B. M., Gharge S.V., Pimple V.S., Gurjar K.M and Shah N.M., 2015. Design, Development and Optimization of S (-) Atenolol Floating Sustained Release Matrix Tablets Using Surface Response Methodology. Indian J Pharm Sci.; **77**: 563–572.

Horowitz M., Donovan D. O, Jones K. L., Feinle C., Rayner C. K., and Samsom M., 2002. Gastric emptying in diabetes: clinical significance and treatment, Diabetic Med, **19**; 177–194

Houghton L. A., Hickson F., and Read N. W., 1987. Effect of food consistency on gastric emptying in man, Gut, **28:** 1584–1588.

Hwang S.J., Park H., Park K., 1998. Gastric retentive drug-delivery systems. Ther Drug carrier Syst **15:**243-84

Ishak, R.A.H., Awad, G.A.S., Mortada, N.D., Nour, S.A.K., 2007. Preparation, *in vitro* and *in vivo* evaluation of stomach-specific metronidazole-loaded alginate beads as local anti-Helicobacter pylori therapy. J. Control. Release **119:** 207–214.

Jiménez-Castellanos, M. R., Zia, H., and Rhodes, C. T., 1994. Design and testing *in vitro* of a bioadhesive and floating drug delivery system for oral application, Int J Pharm, **105:** 65–70.

Jiménez-Martínez, I., Quirino-Barreda, T., Villafuerte-Robles, L., 2008. Sustained delivery of captopril from floating matrix tablets. Int. J. Pharm. **362:** 37–43

Johansson C. and Ekelund K., 1976. Relation between body weight and the gastric and intestinal handling of an oral caloric load, Gut, **17**: 456–462.

Kedzierewicz, F., Thouvenot, P., Lemut, J., Etienne, A., Hoffman, M., Maincent, P., 1999. Evaluation of peroral silicone dosage forms in humans by gamma-scintigraphy. J. Control. Rel. **58:** 195-205.

Keinke, O., and Ehrlein, H. J., 1983. Effect of oleic acid on canine gastroduodenal motility, pyloric diameter and gastric emptying. Experimental Physiology **68:** 675-686.

Kellow J. E., Borody T. J., Phillips S. F., Tucker R. L., and Haddad A. C., 1986. Human interdigestive motility: variations in patterns from esophagus to colon, Gastroenterology, **91:** 386–395.

Khattar, D., Ahuja, A., Khar, R.K., 1990. Hydrodynamically balanced systems as sustained release dosage forms for propranolol hydrochloride. Pharmazie **45:**356-358.

Klausner, E.A., Lavy, E., Stepensky, D., Friedman, M., Hoffman, A., 2002. Novel Gastroretentive Dosage Forms: Evaluation of Gastroretentivity and Its Effect on Riboflavin Absorption in Dogs. Pharm. Res. **19**: 1516-1523.

Klausner, E.A., Lavy, E., Friedman, M., Hoffman, A., 2003a. Expandable gastroretentive dosage forms. J. Control. Release. **90**:143-162.

Klausner E. A., Lavy E., Barta M., Cserepes E., Friedman M., and Hoffman A., (2003b). Novel gastroretentive dosage forms: evaluation of gastroretentivity and its effect on levodopa absorption in humans, Pharmaceut Res, **20**: 1466–1473.

Kong, F. and Singh, R. P., 2008. Disintegration of solid foods in human stomach, J Food Sci, **73**:R67–R80.

Kortejarvi H., Yliperttula M., Dressman J.B., Junginger H.E., Midha K.K., Shah V.P., Barends D.M., 2005. Biowaiver Monographs for Immediate Release Solid Oral Dosage Forms: Ranitidine Hydrochloride. Journal of Pharmaceutical Sciences, **94:** 1617-1625.

Kotreka K. U. & Adeyeye C. M., 2011. Gastroretentive Floating Drug-Delivery Systems: A Critical Review. Critical Reviews™ in Therapeutic Drug Carrier Systems, **28:** 47–99.

Kumar T., Srinivas. G., Jalasubaramaniam J., and Pandit J.K., 2005. HPMC-based matrix tablets of atenolol and cisapride: Effect of viscosity of polymer and drug solubility on *in vitro* release. Indian J. Pharm.Sci., **64:**414:421

Lahner E. and Annibale B., 2009. Pernicious anemia: new insights from a gastroenterological point of view, World J Gastroenterol, **15:**5121.

Lam S. K., Isenberg J. I., Grossman M. I., Lane W. H., and Hogan D. L., 1982. Rapid gastric emptying in duodenal ulcer patients, Dig Dis Sci, **27**: 598–604.

Li, Y., Liu, Z., Zhao, H., 2007. Statistical optimization of xylanase production from new isolated *Penicillium oxalicum* ZH-30 in submerged fermentation. Biochem.Eng. J. **34**, 82–86

Longo W. E. and Vernava A. M., 1993. Prokinetic agents for lower gastrointestinal motility disorders, Dis Colon Rectum, **36:** 696–708.

Lopes, C. M., Bettencourta, C., Rossi, A., Buttinib, F., Barata, P., 2016. Review: Overview on gastroretentive drug delivery systems for improving drug bioavailability. International Journal of Pharmaceutics **510**: 144–158

Luiking Y. C., Reijden van der A. C., Henegouwen G. P. van Berge, and Akkermans L. M. A., 1998. Migrating motor complex cycle duration is determined by gastric or duodenal origin of phase III, A J Physiol - Gastroint Liver Physiol, **27:** G1246–G1251.

Lundstedt T., Seifert E., Abramo L., Thelin B, Nystrom A., Pettersen J., Bergman R., 1998. Experimental design and optimization. Chemometrics and Intelligent Laboratory Systems. **42**: 3–40

Mangoni A. A. and Jackson S. H. D., 2004. Age-related changes in pharmacokinetics and pharmacodynamics: basic principles and practical applications, Br J Clin Pharmacol, **57**: 6–14.

McCallum R. W., Berkowitz D. M., and Lerner E., 1981. Gastric emptying in patients with gastroesophageal reflux, Gastroenterology, **80**: 285–291.

Mcintyre A. S., Thompson D. G., Day S., Burnham W. R., and Walker E. R., 1992. Modulation of human upper intestinal nutrient transit by a beta adrenoreceptor mediated pathway, Gut, **33:** 1062–1070.

Meka S.V, Li E.C, and Sheshala R.I, 2016. Design and statistical optimization of an effervescent floating drug delivery system of theophylline using response surface methodology. Acta Pharm. **66**: 35–51.

Michaels AS, Bashwa JD, Zaffaroni A., 1975. Integrated device for administering beneficial drug at programmed rate. US patent 3 901 232.

Michaels AS., 1974. Drug delivery device with self actuated mechanism for retaining device in selected area. US patent 3 786 813..

Miller L. J., Malagelada J.R., Longstreth G. F., and Go V. W., 1980. Dysfunctions of the stomach with gastric ulceration, Dig Dis Sci, **25**:857–864.

Moore J. G., Datz F. L., Christian P. E., Greenberg E., and Alazraki N., 1988. Effect of body posture on radionuclide measurements of gastric emptying, Dig Dis Sci, **33**: 1592–1595.

Murata, Y., Sasaki, N., Miyamoto, E., Kawashima, S., 2000. Use of floating alginate gel beads for stomach-specific drug delivery. Eur. J. Pharm. Biopharm. **50**:221-226.

Murphy D. B., Sutton J. A., Prescott L. F., and Murphy M. B., 1997. Opioid-induced delay in gastric emptying: a peripheral mechanism in humans, Anesthesiology, **87**:765–770.

Nakamura F., Ohta R., Machida Y., Nagai T., 1996. *In vitro* and *in vivo* nasal mucoadhesion of some water-soluble polymers, Int. J. Pharm. **134**: 173– 181

Nama, M., Gonugunta, C.S., Reddy Veerareddy, P., 2008. Formulation and evaluation of gastroretentive dosage forms of clarithromycin. AAPS PharmSciTech **9**: 231– 237.

Nóbrega A. C. M., Ferreira B. R. S., Oliveira G. J., Sales K. M. O., Santos A. A., Souza M. Â. N., Braga L. L. B. C., Troncon A., and Souza M. H. L. P., 2012. Dyspeptic symptoms and delayed gastric emptying of solids in patients with inactive crohn's disease, BMC Gastroenterol, **12**: 175.

Omidian, H., Rocca, J. G., and Park, K., 2005. Advances in superporous hydrogels, J Control Release, **102:**3–12.

Ozdemir N, Ordu S, Ozkan Y., 2000. Studies of floating dosage forms of furosemide: *in vitro* and *in vivo* evaluation of bilayer tablet formulation. Drug Dev Ind Pharm., **26**:857-866.

Pahwa R., Sharma S., Kumar V. and Kohli K., 2016. Ranitidine hydrochloride: An update on analytical, clinical and pharmacological aspects. J. Chem. Pharm. Res., **8:**70-78.

Palmer D., Levina M., Nokhodchi A., Douroumis D., Farrell T. and Rajabi-Siahboomi A., 2011. The Influence of Sodium Carboxymethylcellulose on Drug Release from Polyethylene Oxide Extended Release Matrices. AAPS PharmSciTech, **12**: 862-871.

Patel P. , Dave A., Vasava A., and Patel P., 2015. Formulation and characterization of sustained release dosage form of moisture sensitive drug. Int J Pharm Investig. **5**: 92–100.

Pawar, V. K., Kansal, S., Garg, G., Awasthi, R., Singodia, D., and Kulkarni, G. T., 2011. Gastroretentive dosage forms: a review with special emphasis on floating drug delivery systems, Drug Deliv, **18**: 97–110.

Pawar, V.K., Kansal, S., Asthana, S., Chourasia, M.K., 2012. Industrial perspective of gastroretentive drug delivery systems: physicochemical, biopharmaceutical, technological and regulatory consideration. Exp. Opin. Drug Deliv. **9**:551–565.

Perioli L., Ambrogi V., Paganoa C., Scuota S., Rossi C., 2009. FG90 chitosan as a new polymer for metronidazole mucoadhesive tablets for vaginal administration, Int. J. Pharm. **377**:120–127.

Prajapati V. D., Jani G. K., Khutliwala T. A., and Zala B. S., 2013. Raft forming system - an upcoming approach of gastroretentive drug delivery system, J Control Release, **168:**151–165.

Prinderre, P., Sauzet, C., and Fuxen, C., 2011. Advances in gastro retentive drug-delivery systems, Expert Opin Drug Deliv, **8**:1189–1203.

Qazi F., Shoaib H.M., Yousuf I.R, Qazi M.T, Mehmood A.Z. and Hasan F.M.S., 2013. Formulation development and evaluation of Diltiazem HCl sustained release matrix tablets using HPMC K4M and K100M. Pak. J. Pharm. Sci. **26:**653-663.

Quigley, E.M., 1996. Gastric and small intestinal motility in health and disease. Gastroenterol. Clin. North. Am. **25**:113-145.

Rajinikanth, P.S., Balasubramaniam, J., Mishra, B., 2007. Development and evaluation of a novel floating in situ gelling system of amoxicillin for eradication of Helicobacter pylori. Int. J. Pharm. **335**:114–122.

Ramesh P., Gunasekaran1 S. and Ramkumar G. R., 2015. Molecular Structure, Vibrational Spectra, UV-Visible and NMR Spectral Analysis on Ranitidine Hydrochloride using AB Initio and DFT Methods. Int.J.Curr.Res.Aca.Rev. **11**: 117-138

Rashid M. U. and Bateman D. N., 1990. Effect of intravenous atropine on gastric emptying, paracetamol absorption, salivary flow and heart rate in young and fit elderly volunteers, Br J Clin Pharmacol, **30**: 25–34.

Robertson D. R., Renwick A. G., Wood N. D., Cross N., Macklin B. S., Fleming J. S., Waller D. G., and George C. F., 1990. The influence of levodopa on gastric emptying in man, Br J Clin Pharmacol, **29**:47–53.

Rohith, G., Sridhar, B.K., Srinatha, A., 2009. Floating drug delivery of a locally acting H2-antagonist: an approach using an in situ gelling liquid formulation. Acta Pharm. **59**:345–354

Rosa, M., Zia H., Rhodes, T., 1994. Dosing and testing in-vitro of a bioadhesive and floating drug delivery system for oral application, Int. J. Pharm. **105** : 65–70.

Rouge, N., Allémann, E., Gex-Fabry, M., Balant, L., Cole, E.T., Buri, P., Doelker, E., 1998. Comparative pharmacokinetic study of a floating multiple-unit capsule, a high-density multiple-unit capsule and an immediate-release tablet containing 25 mg atenolol. Pharm. Acta Helv. **73**: 81-87.

Rouge, N., Buri, P., Doelker, E., 1996. Drug absorption sites in the gastrointestinal tract and dosage forms for site-specific delivery. Int. J. Pharm. **136**:117-139.

Rouge, N., Leroux, J.-C., Cole, E.T., Doelker, E., Buri, P., 1997. Prevention of the sticking tendency of floating minitablets filled into hard gelatin capsules. Eur. J. Pharm. Biopharm. **43**: 165-171.

Roy K.S. and Prabhakar B., 2010. Bioadhesive Polymeric Platforms for Transmucosal Drug Delivery Systems – a Review. Trop J Pharm Res. **9**:91–104.

Russell, J. and Bass, P., 1985. Canine gastric emptying of fiber meals: influence of meal viscosity and antroduodenal motility. Am J Physiol Gastrointest Liver Physiol **249**: G662-667.

Russell, T. L., Berardi, R. R., Barnett, J. L., Dermentzoglou, L. C., Jarvenpaa, K. M., Schmaltz, S. P., and Dressman, J. B., 1993. Upper gastrointestinal pH in seventy-nine healthy, elderly, north american men and women, Pharmaceut Res, **10**: 187–196.

Saeio K., Pongpaibul Y., Veirnstein H., Okonogi S., 2007. Factors influencing drug dissolution characteristic from hydrophilic polymer matrix tablet. Sci. Pharm. **75**:147-163.

Sant S , Swati S , Awadhesh K , Sajid MA , Pattnaik GD , Tahir MA , Farheen S., 2011. Hydrophilic polymers as release modifiers for primaquine phosphate: Effect of polymeric dispersion. Ars Pharm. **52:** 2.

Sawicki, W., 2002. Pharmacokinetics of verapamil and norverapamil from controlled release floating pellets in humans. Eur. J. Pharm. Biopharm. **53**:29– 35

Sheth, P.R., Tossounian, J., 1984. The Hydrodynamically Balanced System (HBS): A Novel Drug Delivery System for Oral Use. Drug Dev. Ind. Pharm. **10**:313 - 339.

Singh B., Ahuja N., 2002. Development of controlled-release buccoadhesive hydrophilic matrices of diltiazem hydrochloride: Optimization of bioadhesion, dissolution, and diffusion parameters. Drug Dev Ind Pharm.; **28**:431–442

Singh B., Chakkal SK, Ahuja N., 2006. Formulation and optimization of controlled release mucoadhesive tablets of atenolol using response surface methodology. AAPS PharmSciTech.**7**:E1–E10

Singh B. N. and Kim K. H., 2000. Floating drug delivery systems: an approach to oral controlled drug delivery via gastric retention, J Control Release, **63:**235–259.

Smekhova E. I., Moldaver L.B., and Perova M.Y., 2009. Equivalence of ranitidine generic tablets studied using the *in vitro* dissolution test. Pharmaceutical Chemistry Journal **43:** 632-636.

Spickett, R. G. W., Vidal, J. L. F., and Escoi, J. C., 1994. Antacid compositions with prolonged gastric residence time. US Patent 5,288,506

Srikanth M V, Ram B.J., Sunil S.A, Rao N. S, and Murthy K.V.R., 2011. Gastroretentive Drug Delivery Systems: Novel Approaches And Its Evaluation- A Review. International Journal of Pharmaceutical Sciences Review and Research. **10:** Article-034.

Sriamornsak, P., Thirawong, N., Korkerd, K., 2007. Swelling, erosion and release behavior of alginate-based matrix tablets. Eur. J. Pharm. Biopharm. **66**:435–450.

Streubel, A., Siepmann, J., Bodmeier, R., 2002. Floating microparticles based on low density foam powder. Int. J. Pharm. **241**:279-292.

Streubel, A., Siepmann J., and Bodmeier R., 2006. Drug delivery to the upper small intestine window using gastroretentive technologies. Current Opinion in Pharmacology, **6**: 501-508.

Sujja-areevath, J.; Munday, D.L.; Cox, P.J.; Khan, K.A., 1998. Relationship between swelling, erosion and drug release in hydrophilic natural gum mini-matrix formulations. Eur. J. Pharm. Sci. **6:** 207–217.

Tack J., 2008. Prokinetics and fundic relaxants in upper functional GI disorders, Curr Opin Pharmacol, **8:** 690–696.

Talukder, R., and Fassihi, R., 2004. Gastroretentive delivery systems: a mini review. Drug Dev. Ind. Pharm. **30**:1019–1028.

Varshosaz, J., Tavakoli, N., and Roozbahani, F., 2006. Formulation and *in vitro* characterization of ciprofloxacin floating and bioadhesive extended-release tablets, Drug Deliv, **13**: 277–285.

Velchik M. G., Reynolds J. C., and Alavi A., 1989. The effect of meal energy content on gastric emptying, J Nucl Med, **30**: 1106–1110.

Verdich C., Madsen J. L., Toubro S., Buemann B., Holst J. J., and Astrup A., 2000. Effect of obesity and major weight reduction on gastric emptying, Int J Obes Relat Metab Disord, **24:** 899–905.

Walker C.V., Wells J.I., 1982. Rheological synergism between ionic and non-ionic cellulose gums. Int J Pharm. **11**: 309–22

Whitehead, L., Fell, J.T., Collett, J.H., Sharma, H.L., Smith, A.M., 1998. Floating dosage forms: an *in vivo* study demonstrating prolonged gastric retention. J. Control. Rel. **55**: 3-12.

Xu G. and Sunada H., 1995. Influence of formulation change on drug release kinetics from hydroxypropylmethylcellulose matrix tablets. Chem Pharm Bull.**43**:483–7.

Zhang, W.-Q., Chen, L.-B., Zhe, A., Liu, G.-H., Zhang, L., Wang, Y.-H., et al., 2016. Gastroretentive floating microspheres of carvedilol: preparation, *in vitro* and *in vivo* characterization. J. Biomater. Tissue Eng. **6** : 74–78.

Zheng, J., Liu, C., Bao, D., Zhao, Y., and Ma, X., 2006. Preparation and evaluation of floating-bioadhesive microparticles containing clarithromycin for the eradication of Helicobacter pylori, J Appl Polym Sci, **102**: 2226–2232.

ADDIS ABABA UNIVERSITY

COLLEGE OF HEALTH SCIENCES, SCHOOL OF PHARMACY

DEPARTMENT OF PHARMACEUTICS AND SOCIAL PHARMACY

Declaration

I declare that the thesis for the MSc Degree at Addis Ababa University, hereby submitted by me, is my original work and has not been submitted for a degree at this university or any other university, and that all reference materials contained therein have been duly acknowledged.

Declared by

Name: Birhanu Nigusse

Signature: _ _ _ _ _ _ _ _ _

Date: 08 March 2018

Advisors

Name	Signature	Date
Prof. Tsige Gebre-Mariam	.....	08 March 2018
Dr. Anteneh Belete	.....	08 March 2018